INFLUENZA HEMAGGLUTININ 1 (HA1) SURFACE-DISPLAYED ON LACTOCOCCUS LACTIS IN THE INDUCTION OF PROTECTIVE MUCOSAL IMMUNITY AGAINST INFLUENZA VIRUS

JEE PUI FONG

FACULTY OF MEDICINE
UNIVERSITY OF MALAYA
KUALA LUMPUR

2018

INFLUENZA HEMAGGLUTININ 1 (HA1) SURFACE-DISPLAYED ON LACTOCOCCUS LACTIS IN THE INDUCTION OF PROTECTIVE MUCOSAL IMMUNITY AGAINST INFLUENZA VIRUS

JEE PUI FONG

**THESIS SUBMITTED IN FULFILMENT
OF THE REQUIREMENTS FOR THE DEGREE OF
DOCTOR OF PHILOSOPHY**

**FACULTY OF MEDICINE
UNIVERSITY OF MALAYA
KUALA LUMPUR**

2018

UNIVERSITY OF MALAYA
ORIGINAL LITERARY WORK DECLARATION

Name of Candidate: **Jee Pui Fong**

Matric No: **MHA110046**

Name of Degree: **Doctor of Philosophy**

Title of Project Paper/Research Report/Dissertation/Thesis ("this Work"): **Influenza hemagglutinin 1 (HA1) surface-displayed on *Lactococcus lactis* in the induction of protective mucosal immunity against influenza virus**

Field of Study: **Medicine (Medical Microbiology)**

I do solemnly and sincerely declare that:

(1) I am the sole author/writer of this Work;
(2) This Work is original;
(3) Any use of any work in which copyright exists was done by way of fair dealing and for permitted purposes and any excerpt or extract from, or reference to or reproduction of any copyright work has been disclosed expressly and sufficiently and the title of the Work and its authorship have been acknowledged in this Work;
(4) I do not have any actual knowledge nor do I ought reasonably to know that the making of this work constitutes an infringement of any copyright work;
(5) I hereby assign all and every rights in the copyright to this Work to the University of Malaya ("UM"), who henceforth shall be owner of the copyright in this Work and that any reproduction or use in any form or by any means whatsoever is prohibited without the written consent of UM having been first had and obtained;
(6) I am fully aware that if in the course of making this Work I have infringed any copyright whether intentionally or otherwise, I may be subject to legal action or any other action as may be determined by UM.

Candidate's Signature Date:

Subscribed and solemnly declared before,

Witness's Signature Date:

Name:

Designation:

ABSTRACT

Influenza virus infection can result in respiratory illnesses and may contribute to high rate of morbidity and mortality. In addition to the pandemic influenza, seasonal influenza remains a major health concern worldwide. To date, vaccination is still the most effective approach for the prevention and control of influenza. Vaccines are usually delivered by intramuscular (IM) injection using needle, which causes pain and possibility of blood transmissible infections. Side effects associated with conventional vaccines, such as local reactions at the injection site, are among the issues necessitating alternative modes of vaccine delivery. Currently, there is great interest in developing mucosal vaccine as an alternative over the conventional IM route. It is suggested that administration of mucosal vaccines will eliminate the need for needles and skilled personnel, and these would be a more favorable approach to mass vaccination, especially of children. One of the current mucosal vaccine strategies is by oral administration of antigen displayed on *Lactococcus lactis*. In the present study, influenza A (H1N1) hemagglutinin 1 (HA1) was surface-displayed on non-recombinant *L. lactis*. The objective of the study was to evaluate the non-recombinant *L. lactis* ability to induce mucosal immune response and to accord protection against influenza virus infection in mice. The HA1/L/AcmA recombinant protein was constructed by fusing HA1 with N-acetylmuramidase (AcmA) binding domain using a single-chain variable fragment (scFv) peptide linker comprising $(Gly_4Ser)_3$. The inclusion of this peptide linker in the recombinant protein was investigated for its ability to improve the surface display on *L. lactis*. Flow cytometry and immunoblotting analysis suggested that the amount of HA1 bound on *L. lactis* was improved in the presence of this peptide linker. The recombinant protein completely agglutinated red blood cells (RBCs), suggesting that insertion of the scFv peptide linker between HA1 and AcmA binding

domain did not affect the biological function of HA. The non-recombinant *L. lactis* displaying HA1/L/AcmA recombinant protein, LL-HA1/L/AcmA, was administered into mice orally to evaluate the host immune responses. Mice immunized with LL-HA1/L/AcmA developed detectable specific sIgA in faecal extract, small intestine wash, BAL fluid and nasal fluid. The results obtained suggested that oral immunization of mice with LL-HA1/L/AcmA elicited mucosal immunity in both the gastrointestinal tract and the respiratory tract. The protective efficacy of LL-HA1/L/AcmA in immunized mice against a lethal dose challenge with A/TN/1-560/2009-MA2(H1N1) influenza virus was also assessed. Upon challenge, the PBS-treated group (control) of mice showed total body weight loss up to 20%, suggesting high susceptibility to influenza virus infection. In contrast, 7/8 of mice immunized with LL-HA1/L/AcmA and 6/8 of mice immunized with HA1/L/AcmA recombinant protein survived. The latter group however, had severe sickness and total body weight loss when compared to the former group, suggesting that oral immunization with LL-HA1/L/AcmA resulted in less morbidity and better survival upon challenge with influenza virus. In conclusion, oral administration of LL-HA1/L/AcmA in mice induced mucosal immunity and provided protection against lethal challenge with influenza virus. These results highlight the potential application of *L. lactis* as a platform for delivery of influenza virus vaccine.

ABSTRAK

Jangkitan virus influenza mengakibatkan penyakit pernafasan dan menyumbang kepada mobiditi dan kadar kematian yang tinggi. Selain influenza pandemik, influenza bermusim juga kekal sebagai masalah kesihatan utama yang membimbangkan di seluruh dunia. Setakat ini, vaksin merupakan strategi yang paling berkesan dalam mencegah dan mengawal penularan virus influenza. Vaksin kebiasaannya diberikan melalui suntikan intramuskular (IM) dengan menggunakan jarum, di mana ini mengakibatkan kesakitan dan kemungkinan jangkitan penyakit bawaan darah. Kesan sampingan yang dikaitkan dengan vaksin konvensional seperti reaksi di bahagian suntikan adalah antara isu-isu yang memerlukan kaedah alternatif bagi pemberian vaksin. Pada masa ini, perhatian yang tinggi diberikan terhadap pembangunan vaksin mukosa sebagai alternaif bagi vaksin konvensional jenis suntikan. Adalah dicadangkan bahawa, aplikasi vaksin mukosa yang tidak memerlukan pelalian menggunakan jarum serta kakitangan terlatih untuk proses vaksinasi merupakan pendekatan yang baik bagi tujuan vaksinasi secara besar-besaran terutamanya bagi kanak-kanak. Salah satu strategi vaksinasi secara mukosa terkini adalah pemberian antigen yang dipaparkan di atas *Lactococcus lactis* secara oral. Dalam kajian ini, influenza A (H1N1) hemagglutinin 1 (HA1) telah dipaparkan pada permukaan *L. lactis* secara bukan-rekombinan. Objektif kajian ini adalah untuk menilai kebolehupayaan HA1 yang terpapar pada permukaan *L. lactis* secara bukan-rekombinan dalam merangsang tindak balas imun mukosa dan potensi perlindungannya daripada jangkitan influenza virus di dalam tikus. Protein rekombinan HA1/L/AcmA telah dihasilkan dengan menggabungkan HA1 dengan domain pengikatan N-acetylmuramidase (AcmA) menggunakan pemaut peptida *single-chain variable fragment* (scFv) yang terdiri daripada $(Gly_4Ser)_3$. Keupayaan kewujudan pemaut peptida bagi meningkatkan paparan

protein rekombinan di permukaan *L. lactis* telah diselidik. Analisis sitometri aliran dan imunoblot mencadangkan bahawa kewujudan pemaut peptida telah mempertingkatkan jumlah HA1 yang terpapar pada *L. lactis.* Kebolehupayaan protein rekombinan yang terhasil mengaglutinasi sel darah merah (RBCs) dengan sepenuhnya mencadangkan bahawa kewujudan pemaut peptide scFv di antara HA1 dan domain pengikatan AcmA tidak menjejaskan fungsi biologi HA. *L. lactis* bukan-rekombinan memaparkan protein rekombinan HA1/L/AcmA, LL-HA1/L/AcmA, telah diberikan kepada tikus secara oral untuk menilai tindak balas imun perumah. Tikus yang menerima imunisasi LL-HA1/L/AcmA menunjukkan penghasilan sIgA spesifik yang dikesan di dalam ekstrak najis, usus kecil, cecair BAL dan cecair hidung. Keputusan yang diperolehi mencadangkan bahawa pemberian LL-HA1/L/AcmA secara oral merangsang imuniti mukosa di dalam gastrousus dan saluran penafasan tikus. Keberkesanan perlindungan yang diperoleh dari imunisasi LL-HA1/L/AcmA di dalam tikus turut dinilai dengan cabaran terhadap dos maut virus influenza A/TN/1-560/2009-MA2(H1N1). Selepas cabaran, kumpulan dirawat-PBS (kawalan) menunjukkan pengurangan jumlah berat badan sehingga 20% yang mana mancadangkan kecenderungan tinggi dijangkiti oleh virus influenza bagi kumpulan ini. Sebaliknya, 7/8 tikus yang diimunisasi dengan LL-HA1/L/AcmA dan 6/8 tikus yang diimunisasi dengan HA1/L/AcmA protein rekombinan kekal hidup. Walaubagaimanapun, tikus yang diimunisasi dengan HA1/L/AcmA mengalami simptom penyakit dan pengurangan berat badan yang lebih teruk berbanding dengan tikus yang diimunisasi dengan LL-HA1/L/AcmA. Ini mencadangkan bahawa imunisasi LL-HA1/L/AcmA secara oral mengurangkan morbiditi dan meningkatkan kadar hidup selepas cabaran terhadap virus influenza. Kesimpulannya, imunisasi LL-HA1/L/AcmA secara oral pada tikus merangsang imuniti mukosa dan memberi perlindungan terhadap dos maut virus influenza. Hasil kajian ini

menunjukkan potensi *L. lactis* bagi digunakan sebagai platform untuk penghantaran vaksin virus influenza.

ACKNOWLEDGEMENTS

The journey of this study has been a truly life-challenging experience and it could not have been completed without the great support from many people over the years.

Foremost, I would like to extend my gratitude and appreciation to all my supervisors, Prof. Sazaly AbuBakar, Prof. Raha Abdul Rahim, Assoc. Prof. Chang Li Yen and Dr. Wong Won Fen. They have been exceptional mentors for their dedication to the research. Their guidance and advice throughout the completion of this study have been priceless. I would also like to thank the rest of my thesis committee for their insightful comments and helpful advice.

In addition, I would like to extend my appreciation to Dr. Richard J. Webby and Dr. Wong Sook San from St. Jude Children's Research Hospital, USA, for kindly providing us with the mouse adapted viral isolate to make the animal challenge study possible. I would also like to thank Dr. Haryanti Azura Mohamad Wali and Dr. Syahar Amir A. Gani for their assistance and help in animal handling and care. A special thanks to all SABLAB members: Eva, Christina, Jing Jing, Sam, Boon Teong, Fezshin, Fang Shiang, kak Aziyah, Kak Ju, Firdaus, Connie, Wai Hong, Kim Kee, Hasliana, Yani, Hafiza, for insightful discussions and suggestions, as well as for being helpful and caring friends. I was glad to work with them together over the years.

I also truly grateful for the MyBrain15 scholarship (MyPhD) offered by the Ministry of Higher Education of Malaysia (MOHE), which help me in achieving educational goal without much financial constraint.

Last but not least, I would like to thank my family members for their encouragement and care, especially to my fiancé, Bryan Lin, for the unconditional love during my good and bad times. They have been very understanding, while I have been focusing on this study and have not spent much time with them.

TABLE OF CONTENT

LIST OF FIGURES

LIST OF TABLES

LIST OF SYMBOLS AND ABBREVIATIONS

AcmA	N-acetylmuramidase
ACN	acetonitrile
ANOVA	one-way analysis of variance
APCs	antigen presenting cells
APRIL	A Proliferation-Inducing Ligand
ASC	antibody secreting cell
ATCC	American Type Culture Collection
BAL	bronchoalveolar lavage
BALT	bronchus-associated lymphoid tissue
BLPs	bacterium-like particles
bp	base pairs
BSA	bovine serum albumin
°C	degree celsius
$CaCl_2$	calcium chloride
CAN	acetonitrile
cDNA	complementary DNA
CFA	complete Freund adjuvant
CFU	colony forming unit
CMC	carboxymethyl-cellulose sodium salt
CO_2	carbon dioxide
CPE	cytopathic effect
CPSs	capsular polysaccharides
cRNAs	complementary RNAs
CTB	cholera toxin subunit B

CV	column volume
DCs	dendritic cells
DMEM	Dulbecco's modified Eagle's medium
dNTP	deoxyribonucleotide triphosphate
ELISA	enzyme-linked immunosorbent assay
EPSs	exopolysaccharides
FACS	fluorescence-activated cell sorting
FAE	follicle associated epithelium
FBS	fetal bovine serum
FoDCs	follicular dendritic cells
FS	forward angle light scatter
GALT	gut-associated lymphoid tissue
GlcNAc	N-acetylglucosamine
GM17	M17 broth supplemented with glucose
GRAS	generally recognized as safe
HA	hemagglutinin
HA1	hemagglutinin 1
HPV 16	human papillomavirus type 16
HRP	horseradish peroxide
IELs	intraepithelial lymphocytes
IFA	incomplete Freund adjuvant
Ig	immunoglobulin
IIV	inactivated influenza virus vaccine
IL-2	interleukin 2
IL-6	interleukin 6
IOD	Integrated Optical Density

IPTG	isopropyl β-D thiogalactosidase
kb	kilobase
kDa	kiloDalton
LAB	lactic acid bacteria
LAIV	live attenuated influenza virus vaccine
LB	Luria-Bertani
LPXTG	cell wall anchoring motif
LTA	lipoteichoic acid
LysM	lysine motif
M1	matrix protein 1
M2	matrix protein 2
M2e	matrix protein 2 extracellular domain
M	molar
MADCAM1	mucosal addressin cell-adhesion molecule 1
MALT	mucosal surfaces lymphoid tissues
M cells	microfold cells
MDCK	Madin-Darby canine kidney
MFI	mean fluorescence intensity
MHC	major histocompatibility complex
ml	mililiter
MLD_{50}	fifty percent mouse lethal dose
mM	milimolar
MMPs	matrix metalloproteinase
mRNAs	messenger RNAs
MS/MS	mass spectrometry/mass spectrometry
MurNAc	N-acetylmuramic acid

NA	neuraminidase
NALT	nasopharynx-associated lymphoid tissue
NEP	nuclear export protein
NICE	nisin-controlled expression
nm	nanometer
NP	nucleoprotein
NS1	non-structural protein 1
NS2	non-structural protein 2
OD	optical density
p.i.	post-infection
PA	acidic polymerase protein
PB1	basic polymerase protein 1
PB1-F2	basic polymerase protein 1-frame 2
PB2	basic polymerase protein 2
PBS	phosphate buffered saline
PDB	Protein Data Bank
PFU	plaque forming unit
pH	power of hydrogen
pI	isoelectric point
pIgA	polymeric IgA
pIgR	polymeric immunoglobulin receptor
PLN	peripheral lymph nodes
PMF	peptide mass fingerprinting
PMSF	phenylmethanesulfonyl fluoride
PPs	Peyer’s patches
RBCs	red blood cells

RE	restriction endonuclease
RT-PCR	reverse transcription-polymerase chain reaction
SC	secretory component
scFv	single-chain variable fragment
SDS-PAGE	sodium dodecyl sulphate-polyacrylamide gel electrophoresis
sIgA	secretory IgA
SP	signal peptide
SS	side angle light scatter
TCA	trichloroacetic acid
TFA	trifluoroacetic acid
TTFC	tetanus toxin fragment C
V_H	variable region of heavy chain of immunoglobulin
V_L	variable region of light chain of immunoglobulin
VLPs	virus-like particles
VP1	capsid protein
vRNPs	ribonucleoproteins
WHO	World Health Organization
WPSs	cell wall polysaccharides
WTA	wall teichoic acid
w/v	weight per volume
µl	microliter
µM	micromolar

LIST OF APPENDICES

CHAPTER 1: INTRODUCTION

Influenza virus infection results in respiratory illnesses and contributes to a high rate of morbidity and mortality in humans, particularly children, the elderly and immunocompromised individuals. Three influenza pandemics have occurred in the 20th century: 1918 Spanish flu, 1957-1958 Asian influenza and 1968 Hong Kong influenza, while one has occurred in the 21st century: 2009 pandemic H1N1 (Zhang *et al.*, 2015). Mortality rates varied in these pandemics, with the 1918 Spanish flu being the most severe pandemic, causing approximately 50 million deaths globally (Johnson & Mueller, 2002; Zhang *et al.*, 2015). In addition to the pandemic influenza, seasonal epidemics of influenza are also of great concern, as they cause approximately 3-5 million cases of severe illness and 250,000-500,000 deaths annually worldwide (WHO, 2014). Controlling the spread of influenza remains a major challenge. It is undeniable that a vaccine which can confer protection against influenza will be beneficial.

Currently, there are three types of influenza vaccine available in the market: an inactivated influenza virus vaccine (IIV), a live attenuated influenza virus vaccine (LAIV) and a recombinant vaccine. While these vaccines are effective, they are not without limitations. The IIV is a good inducer of systemic immune response but it is ineffective at stimulating mucosal immune response (Cox *et al.*, 2004). LAIV on the other hand, induces both systemic and mucosal immune responses. It induces cell-mediated immune response and mucosal IgA, specifically in the upper and lower respiratory tract (Carter & Curran, 2011). However, there is an associated risk of the attenuated virus reverting back to its highly virulent form and thus causing an infection (Cox *et al.*, 2004). A case of LAIV transmission to a recipient was previously reported (Carter & Curran, 2011). In addition, a study had shown that LAIV increased risk of wheezing within 42 days after vaccination in children <12-months-old (Belshe *et al.*,

2007). LAIV was also reported to result in higher wheezing in vaccine-naïve children <24-months-old as compared to IIV, therefore it is not approved for use in children <24-months-old (Carter & Curran, 2011). The recombinant vaccine is potentially of advantage especially in the event of a pandemic due to quick production potential. This vaccine is administered intramuscularly and therefore, it induces immune response similar to the IIV (Dunkle *et al.*, 2015). However, a few serious adverse events associated with this vaccine such as vasovagal syncope, pericardial effusion and Bell's palsy were previously reported (Cox & Hashimoto, *et al.*, 2014). Taken together, influenza vaccines that are currently available present several drawbacks, including their limited ability at stimulating mucosal immunity without compromising safety issues. As influenza virus initiates infection at the respiratory tract mucosal surface, it would be advantageous to have a vaccine that is able to induce the mucosal immune response, mainly the secretory IgA (sIgA). The sIgA plays an important role as the first line of defense, where viruses are eliminated before initiation of an infection (Taylor & Dimmock, 1985; Asahi-Ozaki *et al.*, 2004; Renegar *et al.*, 2004; van Riet *et al.*, 2012). sIgA has also been shown to confer heterosubtypic immunity (Liew *et al.*, 1984; Tamura *et al.*, 1990; Tamura *et al.*, 1991; Asahi-Ozaki *et al.*, 2004), which is an important aspect in developing an ideal influenza virus vaccine given that influenza viruses continuously undergo unpredictable antigenic evolution.

One of the current strategies in mucosal vaccine research targeting the stimulation of the mucosal immunity is by means of oral administration of antigen using *Lactococcus lactis* as a delivery platform. *L. lactis* is a generally recognized as safe (GRAS) bacterium. It has become a promising candidate in mucosal vaccine research due to its non-pathogenic and non-colonizing properties. It is being extensively explored as an effective oral-based vaccine vehicle to deliver antigen of several parasites (Ramasamy *et al.*, 2006), bacteria (Robinson *et al.*, 1997; Lee *et al.*, 2001; Buccato *et al.*, 2006;

Audouy *et al.*, 2007) and viruses (Xin *et al.*, 2003; Pei *et al.*, 2005; Sim *et al.*, 2008; Lei *et al.*, 2011; Marelli *et al.*, 2011; Zhang *et al.*, 2011; Varma *et al.*, 2013). Studies have shown that *L. lactis* expressing and displaying antigens were capable of inducing strong systemic as well as mucosal immune responses (Xin *et al.*, 2003; Ramasamy *et al.*, 2006; Lei *et al.*, 2011; Marelli *et al.*, 2011; Zhang *et al.*, 2011; Gao *et al.*, 2015; Lei *et al.*, 2015a; Lei *et al.*, 2015b). Considering the role of mucosal immunity in protection against influenza, the present study, therefore, aimed to develop a non-recombinant *L. lactis* surface displaying influenza A (H1N1) 2009 hemagglutinin 1 (HA1) to target on the stimulation of the mucosal immunity.

Surface display of antigens on *L. lactis* using the N-acetylmuramidase (AcmA) binding domain has been well described (Buist *et al.*, 1997; Steen *et al.*, 2003; Raha *et al.*, 2005; Varma *et al.*, 2013; Visweswaran *et al.*, 2014). AcmA is a major autolysin found on *L. lactis* MG1363. It is responsible for bacterial cell separation and is involved in stationary phase bacterial cell lysis (Buist *et al.*, 1995). AcmA consists of three domains: the N-terminal signal domain, followed by an N-acetyl-glucosaminidase active domain and the C-terminal binding domain which belongs to the lysine motif (LysM) domain (Buist *et al.*, 1995; Buist *et al.*, 1997). The AcmA C-terminal binding domain binds strongly to peptidoglycan of lactococcal cells, specifically around the pores and septum of the cell (Steen *et al.*, 2003). To date, this binding domain has been used for surface display of parasitic protozoan, viral and bacterial antigens (Buist *et al.*, 2008; Visweswaran *et al.*, 2014), such as *Plasmodium berghei* circumspozoite protein (Bosma *et al.*, 2006), human enterovirus 71 viral capsid protein (Raha *et al.*, 2005), respiratory syncytial virus glycoproteins (Lim *et al.*, 2010), and pneumococcal proteins, particularly IgA1 protease, putative proteinase mature protein A and streptococcal lipoprotein rotamase A (Audouy *et al.*, 2007).

Surface display of antigens, however, can be hindered by the presence of lipoteichoic acid (LTA) or surface layer protein on the *L. lactis* cell surface (Steen *et al.*, 2003; Andre *et al.*, 2008; Buist *et al.*, 2008; Visweswaran *et al.*, 2014). Such hindrance limits the amount of antigens that can be displayed on the surface of a single *L. lactis* cell. It has been shown that bacterial species containing more LTA on the cell surface had lower LysM-mediated binding ability (Zadravec *et al.*, 2015). Trichloroacetic acid (TCA) treatment of lactococcal cells was shown to be able to remove LTA, and thus, increase the binding of AcmA all over the cell surface (Steen *et al.*, 2003; Bosma *et al.*, 2006; Van Braeckel-Budimir *et al.*, 2013). Various heterologous proteins including purified influenza hemagglutinin (HA), matrix protein 2 extracellular domain (M2e) and nucleoprotein (NP) that were fused to AcmA were reported to be successfully surface displayed on TCA-treated lactococcal cells (Van Braeckel-Budimir *et al.*, 2013).

In the present study, a single-chain variable fragment (scFv) peptide linker comprising $(Gly_4Ser)_3$ was used to fuse HA1 with AcmA binding domain in the construction of HA1/L/AcmA recombinant protein, as an alternative way to improve the surface display of recombinant protein on *L. lactis*. The scFv peptide linker is a short flexible peptide that joins the variable region of heavy (V_H) and light (V_L) chains of immunoglobulins (Ahmad *et al.*, 2012). This peptide linker is usually comprised of stretches of Gly and Ser residues $(Gly_4Ser)_n$ for flexibility (Huston *et al.*, 1988; Hoedemaeker *et al.*, 1997; Gu *et al.*, 2010; Chen *et al.*, 2013; Wen *et al.*, 2013) and solubility (Chen *et al.*, 2013), respectively. The peptide linker bears a low charge and is resistant to protease activity (Gu *et al.*, 2010; Wen *et al.*, 2013). Different lengths of peptide linker for the construction of scFv have been reported, however $(Gly_4Ser)_3$ has been the most preferred length used (Chen *et al.*, 2013).

Here, a non-recombinant *L. lactis* surface displaying the influenza HA1 that was fused to the AcmA binding domain via a scFv peptide linker was reported. The binding

parameters, the amount of HA1 recombinant protein added to *L. lactis*, the duration of binding and the buffer used for binding were optimized. The specific immune response elicited upon oral immunization of the constructed non-recombinant *L. lactis* surface displaying HA1, LL-HA1/L/AcmA, in mice was evaluated. Lastly, the protective efficacy of LL-HA1/L/AcmA in immunized mice against a lethal dose challenge with influenza virus was also assessed.

1.1 Study objectives

The present study is divided into two parts. The aim of the first part of this study was to construct a non-recombinant *L. lactis* surface displaying influenza A (H1N1) HA1, LL-HA1/L/AcmA. It was hypothesized that surface display of HA1 can be improved by the inclusion of scFv peptide linker in the recombinant protein. This hypothesis was validated through i) cloning and expression of HA1 in *Escherichia coli*, followed by purification of the produced protein and ii) surface display of HA1 on *L. lactis*. The aim of the second part in this study was to evaluate the protective efficacy of LL-HA1/L/AcmA in immunized mice against a lethal dose challenge with influenza virus. It was hypothesized that this delivery platform would accord protection against lethal challenge with influenza virus in mice. This hypothesis was validated through iii) evaluation of immune response towards oral immunization of LL-HA1/L/AcmA in mice and iv) evaluation of protective potential of LL-HA1/L/AcmA in immunized mice against lethal challenge with influenza virus.

CHAPTER 2: LITERATURE REVIEW

2.1 Influenza virus

2.1.1 Introduction

Influenza viruses belong to the family of Orthomyxoviridae and are classified into four types, namely influenza A, B, C and D (CDC, 2016f). Influenza A virus infects the human respiratory tract, potentially causes pandemic and seasonal epidemics globally. The literature here will be limited predominantly to influenza A virus, unless otherwise stated.

2.1.2 Influenza A virus structure

Influenza A virus is an enveloped virus with a diameter ranging from 80 to 120 nm (Webster *et al.*, 1992). This virus consists of 8 single-stranded negative sense RNA segments which encode 11 genes. The functions of each translated protein are summarized in Table 2.1. The virus envelop is made up of a lipid bilayer which is derived from the host plasma membrane. Three transmembrane proteins are present on the lipid bilayer: hemagglutinin (HA), neuraminidase (NA) and matrix protein 2 (M2). HA is a homotrimer, embedded in the viral membrane at its C-terminal (type 1 membrane protein) (Cox *et al.*, 2004; Lacroix-Desmazes *et al.*, 2008). A HA monomer consists of a globular head connected to a stalk. The globular head is made up of HA1 subunit containing the receptor binding site and 5 antigenic sites that have neutralizing activity, while the stalk is made up of HA2 and part of the HA1 subunit (Cox *et al.*, 2004). To date, 16 functional antigenic subtypes of HA (H1-H16) and two bat HA homologs (H17 and H18) have been identified (Zhang *et al.*, 2015). NA is a tetramer, embedded in the viral membrane at its N-terminal (type 2 membrane protein) (Cox *et al.*, 2004; Lacroix-Desmazes *et al.*, 2008). It has a globular head containing enzymatic

Table 2.1: Influenza A virus gene segments and the functions of the respective encoded protein.

Segment	Encoded protein	Function
1	Basic polymerase protein 2 (PB2)	Initiates viral mRNA translation by recognizes and binds host-mRNAs 5'cap-1 structures as primers for transcription
2	Basic polymerase protein 1 (PB1)	Responsible for elongation of the primed nascent viral mRNA and elongation in template RNA and vRNA synthesis
	PB1-frame 2 (PB1-F2)	Modulates the host response to influenza A virus by hastening the death of immune cells
3	Acidic polymerase protein (PA)	Involves in viral RNA replication
4	Hemagglutinin (HA)	Responsible for virus attachment to host cell receptors and enables the virus entry to the host cell
5	Nucleoprotein (NP)	Encapsidates viral RNA to facilitate the formation of double-helical vRNP. Responsible in switching of viral RNA polymerase activity from mRNA synthesis to cRNA and vRNA synthesis
6	Neuraminidase (NA)	Cleaves terminal sialic acid from glycoproteins and glycolipids, to free progeny virus from infected cells
7	Matrix protein 1 (M1)	Forms a matrix to hold the viral nucleocapsid and responsible in RNP coating during viral assembly
	Matrix protein 2 (M2)	Responsible in the formation of an ion channel tetramer and demonstrating pH-inducible proton transport activity. Regulates the golgi pH during HA synthesis and allows acidification of the virion interior during virus uncoating
8	Non-structural protein 1 (NS1)	Regulates mRNA export and pre-mRNA splicing to involve in viral replication and inhibition of the host's innate immune responses
	Non-structural protein 2 (NS2)/ Nuclear export protein (NEP)	Facilitates the export of newly synthesized vRNP from nucleus to cytoplasm

(Webster *et al.*, 1992; Lambert & Fauci, 2010; Zheng & Tao, 2013; Zhang *et al.*, 2015)

and antigenic sites that are attached to a hydrophobic stalk (Cox *et al.*, 2004). A total of nine functional NA antigenic subtypes (N1- N9) and 2 bat NA homologs (N10 and N11) have been reported (Zhang *et al.*, 2015). M2 is a tetramer, forming an ion channel on the viral membrane (type 3 membrane protein) (Lacroix-Desmazes *et al.*, 2008). Matrix protein 1 (M1) is the most abundant viral protein and it is located underneath the viral lipid membrane. It forms a matrix to hold the viral nucleocapsid consisting of ribonucleoproteins (vRNPs) which are rod-shaped and approximately 10 nm in width (Zheng & Tao, 2013). Each vRNP consists of the negative-stranded viral RNAs which are encapsidated by multiple nucleoprotein (NP) and a small amount of non-structural protein 2 (NS2)/nuclear export protein (NEP) in a helical conformation (Lacroix-Desmazes *et al.*, 2008; Samji, 2009). There are three polymerase proteins: basic polymerase protein 1 (PB1), basic polymerase protein 2 (PB2) and acidic polymerase protein (PA), all of which are located at one end of the vRNPs. Two non-structural proteins, the non-structural protein 1 (NS1) and PB1-frame 2 (PB1-F2), are present in infected host cells but not in the virions.

2.1.3 Influenza virus life cycle

The life cycle of influenza virus can be divided into the following stages: i) receptor binding and host cell entry, ii) membrane fusion and viral core uncoating, iii) RNA replication and translation, and iv) assembly and release of new viral particles (Figure 2.1) (Andre *et al.*, 2008; Polo *et al.*, 2008; Samji, 2009; Zheng & Tao, 2013).

2.1.3.1 Receptor binding and host cell entry

Influenza virus infection is initiated by the binding of HA to glycoproteins or glycolipids sialic acid residues that are present on the host cell surface (Ito *et al.*, 1998; Samji, 2009). Human influenza viruses bind to sialic acid with a α-2,6 linkage, whereas

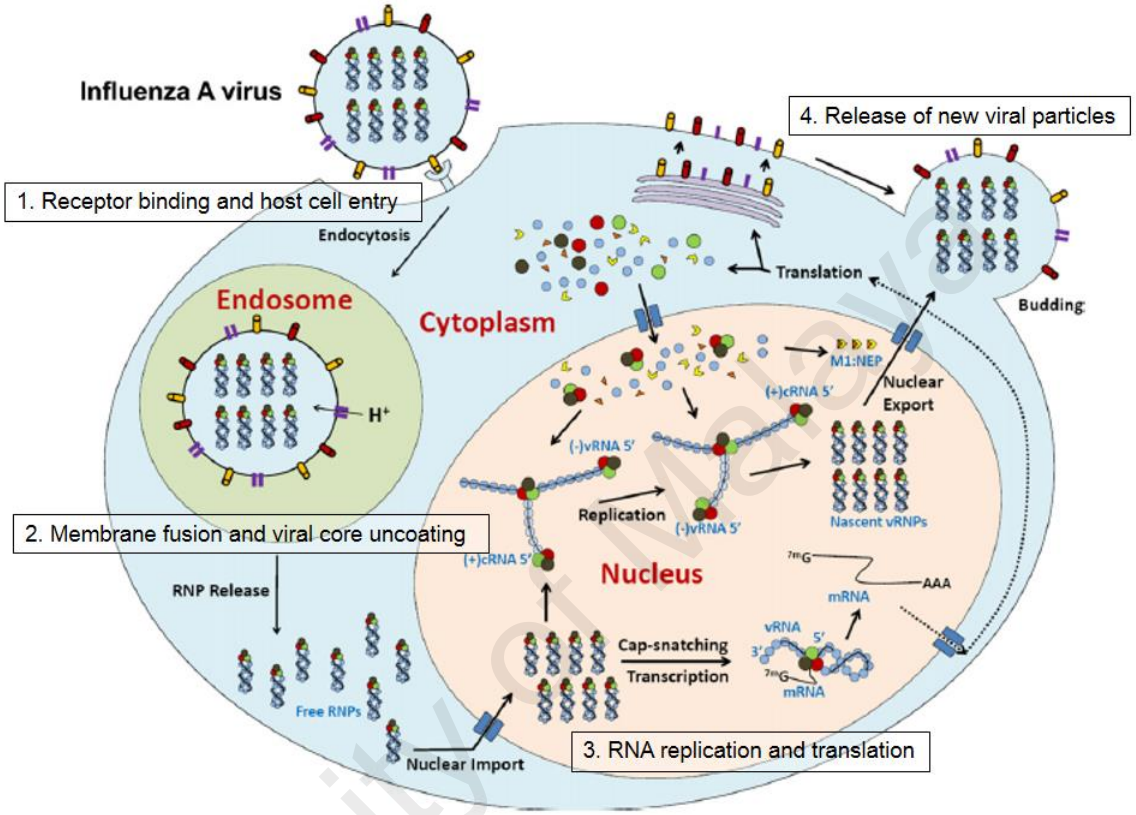

Figure 2.1: Schematic illustration of the influenza A virus life cycle.

The life cycle of influenza A virus can be divided into the following stages: receptor binding and host cell entry, membrane fusion and viral core uncoating, RNA replication and translation, and assembly and release of new viral particles. Figure adapted and modified from Zheng & Tao (2013).

avian and equine influenza viruses bind to sialic acid with a α-2,3 linkage. Swine, on the other hand, recognize both linkages and are susceptible to the infection. Therefore, co-infection of influenza viruses in swine possibly results in the rearrangement of new virus genome which may cause influenza pandemic.

2.1.3.2 Membrane fusion and uncoating of the viral core

Influenza virus enters the host cell through receptor-mediated endocytosis (Andre *et al.*, 2008; Hancock *et al.*, 2008; Lacroix-Desmazes *et al.*, 2008; Polo *et al.*, 2008). The host cell plasma membrane internalizes the virus and results in the formation of an endosome. The virus fuses with the endosomal membrane to escape from degradation by hydrolytic enzymes. The endosome which has low pH (pH 5-6), subsequently induces major acidic pH-promoted conformational change of HA (Lacroix-Desmazes *et al.*, 2008; Rouleau *et al.*, 2008). As a result of the conformational change, HA2 fusion peptide moves upwards to the tip of the homotrimer and allows the insertion to host cell membrane (Rouleau *et al.*, 2008). The homotrimer then folds and induces membrane fusion. Meanwhile, M2 ion channel opens and mediates acidification of viral core to release the vRNPs from M1 to the host cell cytoplasm.

2.1.3.3 RNA replication and translation

Upon release of the vRNPs to host cell cytoplasm, NP which has nuclear-localized signal, facilitates the vRNPs to enter host nucleus for transcription and replication (Polo *et al.*, 2008). The negative-sense RNAs are first transcribed to positive-sense messenger RNAs (mRNAs) by PB1, PB2 and PA transcriptase that are present in the vRNPs (Engelhardt & Fodor, 2006). In this step, the transcriptase snatches cellular mRNA 5'-short cap region as primer to initiate mRNA synthesis (Bouloy *et al.*, 1978; Engelhardt & Fodor, 2006). Subsequently, translation of mRNA takes place in the

cytosol (Engelhardt & Fodor, 2006). The negative-sense RNAs also serve as active templates for positive-sense complementary RNAs (cRNAs) synthesis which in turn direct the synthesis of new negative-sense RNAs. The newly translated HA, NA and M2 are transported to the endoplasmic reticulum for glycosylation and folding into respective structures (Braakman *et al.*, 1991; Polo *et al.*, 2008). Subsequently, the proteins are transported to the cell plasma membrane through the golgi apparatus and trans-golgi network. The NP, PB1, PB2 and PA are then transported back to the nucleus to interact with newly synthesized RNAs to form vRNPs. M1 starts to interact with HA and NA on the plasma membrane, forming patches containing high density of HA and NA. Then, newly formed vRNPs interacts with M1. NEP is also known to facilitate vRNPs export from the nucleus to the cytosol (Lacroix-Desmazes *et al.*, 2008; Zheng & Tao, 2013).

2.1.3.4 Assembly and release of new viral particles

The viral particles budding process starts after attachment of the vRNPs to M1 (Lacroix-Desmazes *et al.*, 2008). The virions bud from the apical side of polarized cells but are still attached to the sialic acid residue on the host plasma membrane by HA. NA then cleaves the sialic acid to release the new virions (Lacroix-Desmazes *et al.*, 2008; Samji, 2009).

2.1.4 Influenza pandemics and epidemics

Influenza viruses are known to continuously undergo antigenic evolution over time specifically of the surface antigens, HA and NA (Treanor, 2004; Subbarao *et al.*, 2006; Carrat & Flahault, 2007). This occurs by two main mechanisms: antigenic drift and antigenic shift. Antigenic drift is point mutation of the viral RNA which occurs all the time, in response to selection pressure from the pre-existing host immunity. Antigenic

drift will result in variation of the influenza viruses, which eventually causes an epidemic, and therefore it is important to identify the circulating virus strain on an annual basis. On the other hand, antigenic shift happens through gene reassortment of two different influenza virus subtypes. It results in the emergence of new influenza virus subtypes, which potentially cause a pandemic. To date, antigenic shift is only reported in influenza A viruses (Cox & Subbarao, 2000; CDC, 2018).

2.1.4.1 Influenza pandemics

Three influenza pandemics in the 20th century (1918 Spanish flu, 1957-1958 Asian influenza and 1968 Hong Kong influenza) and one in the 21st century (2009 pandemic H1N1) had been reported (Zhang *et al.*, 2015). The 1918 Spanish flu caused approximately 50 million deaths globally and has been the most severe pandemic (Johnson & Mueller, 2002; Zhang *et al.*, 2015). The 1957-1958 Asian influenza and the 1968 Hong Kong influenza caused 1 million and 70,000 deaths, respectively (Zhang *et al.*, 2015). The 2009 pandemic H1N1 caused at least 18,449 deaths globally as of 6 August 2010 (WHO, 2010a). Subsequently, on 10th August 2010, WHO declared the end of the 2009 pandemic H1N1 (WHO, 2010b). In Malaysia, the first case of H1N1 was reported on 15th May 2009 (Sam & Abu Bakar, 2009), and as of 24th July 2010, there were 15,421 confirmed cases including 92 deaths (Ong *et al.*, 2010). Of 1,362 children <12-years-old who were hospitalized during 18th June 2009 to 1st March 2010, there were 51 deaths (Muhammad Ismail *et al.*, 2011). The virus contained genes from avian H1N1, swine H1N1 and seasonal human H3N2 (Sam & Abu Bakar, 2009).

2.1.4.2 Influenza epidemics

Influenza epidemics happen during winter months in the Northern hemisphere and May to September in the Southern hemisphere (Cox *et al.*, 2004). Annual epidemics

cause approximately 3-5 million cases of severe illnesses and 250,000-500,000 deaths worldwide (WHO, 2014). In the United States, an estimated 3,000 to 49,000 influenza associated deaths were reported annually from 1976-1977 to 2006-2007 season (CDC, 2010). In Malaysia, it has been reported that, A/Sydney/5/97(H3N2) and B/Beijing/184/93 were the predominant circulating influenza virus in 1997-2000, and it was replaced by A/New Caledonia/20/99(H1N1) and B/Sichuan/379/99 in 2001 (Shahidah *et al.*, 2003). An outbreak involving A/New Caledonia/20/99(H1N1)-like and A/Fujian/411/2002(H3N2)-like isolates was reported in Perak, Malaysia among students in seven residential schools in July and August 2003 (Ayob *et al.*, 2006). There were 1,419 out of 4,989 students affected, including 36 hospitalized students. Subsequently, predominant seasonal influenza virus circulating in Malaysia were A/California/7/2004(H3N2)-like and B/Hong Kong/330/2001-like in 2005, A/New Caledonia/20/99(H1N1)-like and B/Malaysia/2506/2004-like in 2006, A/Brisbane/10/2007(H3N2)-like and B/Fluorida/4/2006-like in 2007 and 2008, and A/Perth/16/2009(H3N2)-like and B/Brisbane/60/2008-like in 2009 (Saat *et al.*, 2010).

2.1.5 Influenza vaccine

Ideally, an influenza vaccine should promote long-term protection towards both homologous and heterologous viruses without compromising vaccine production capacity, manufacturing time and safety. As of 2016, several influenza vaccines, including IIV, LAIV and recombinant vaccine were approved and made available in the United States (CDC, 2016d). The efficacy of the vaccines, however, can be influenced by the recipient's age, health and the antigenic similarity of the strain in the vaccine with the circulating strain in real life. Due to high mutation rates of the virus, influenza vaccine has to be reformulated each year. For the 2016-2017 season, A/California/7/2009(H1N1)pdm09-like virus, A/HongKong/4801/2014(H3N2)-like

virus and B/Brisbane/60/2008-like virus (B/Victoria lineage) in trivalent vaccines and an addition of B/Phuket/3073/2013-like virus (B/Yamagata lineage) in quadrivalent vaccines are recommended (CDC, 2016e). Malaysia has a seasonal influenza vaccine program which began in 1988 (Gupta *et al.*, 2012). The vaccine recommended for the Southern hemisphere is used in Malaysia (Saat *et al.*, 2010). In 2009-2010, monovalent A(H1N1)pdm09 vaccine doses purchased per capita was approximately 1,408 per 100,000 population in Malaysia (Gupta *et al.*, 2012).

2.1.5.1 Inactivated influenza vaccine

IIV is manufactured using embryonated hen's egg in three formulations: whole-virus, split-virus and subunit (Cox *et al.*, 2004; Noh & Kim, 2013; Wong & Webby, 2013). Traditionally, whole virus vaccine is prepared by propagating the virus in eggs and subsequently the allantoic fluid is harvested (Wong & Webby, 2013). The virus is inactivated using formaldehyde or β-propiolactone, and then concentrated and purified to remove contaminants. An additional treatment is applied for split-virus vaccine to dissociate the virus lipid envelop, while an additional purification step is applied for subunit vaccine to further enrich the HA protein. The egg-based trivalent IIVs approved and available in the United States for 2016-2017 season are Affluria, Fluvirin and Fluad-adjuvanted inactivated vaccines (Seqirus, USA), while the quadrivalent IIVs available include Fluarix Quadrivalent (GlaxoSmithKline, USA), Flulaval Quadrivalent (ID Biomedical Corporation of Quebec, USA), Fluzone Quadrivalent (Sanofi Pasteur, USA) and Fluzone Intradermal Quadrivalent (Sanofi Pasteur, USA) (CDC, 2016d). All IIVs are administered intramuscularly except Fluzone Intradermal which is administered intradermally.

In the event of an avian influenza outbreak or other diseases affecting egg production, there will be a limitation in the production of egg-based IIV. In addition, not all of the

influenza viruses replicate well using this system. Numerous attempts to grow A/Fujian/411/02 (H3N2) virus which predominated in 2003-2004 season using embryonated eggs were unsuccessful (Lu *et al.*, 2005; Widjaja *et al.*, 2006). The absence of this strain in vaccine formulated for 2003-2004 season had eventually caused an increase in influenza incidence (Widjaja *et al.*, 2006). A cell-culture based IIV therefore, is developed to overcome the limitations. The first United States licensed cell-culture based IIV was approved by FDA on 20th November 2012 (CDC, 2016b). This vaccine, named Flucelvax, is a trivalent IIV manufactured by Seqirus (USA). On 23rd May 2016, Flucelvax Quadrivalent-cell culture based IIV was approved and is being used for the 2016-2017 season in the United States.

2.1.5.2 Live attenuated influenza vaccine

LAIV contains temperature sensitive and attenuated live influenza viruses. It is manufactured by serially passaging the isolated virus in chicken eggs by cold-adaptation, forcing the virus to replicate at a lower temperature (Cox *et al.*, 2004). LAIV is therefore, unable to replicate in mucosal surface of the lower respiratory tract which has a higher temperature. The first LAIV, Flumist®, manufactured by MedImmune (USA) was approved on 17th June 2003 and is available in the United States (FDA, 2016). This is the first trivalent vaccine which is to be administered intranasally. On 29th February 2012, FluMist Quadrivalent was approved by FDA (CDC, 2016d; FDA, 2016). However, it is not recommended to be used for the 2016-2017 season (CDC, 2016d) due to concerns of its effectiveness (CDC, 2016a).

2.1.5.3 Recombinant influenza vaccine

FluBlock is a recombinant influenza vaccine produced in express+® sf9 insect cell line which is a non-tumorigenic continuous and non-transformed cell line (Cox *et al.*,

2008). It is manufactured by Protein Sciences (USA) and was approved by FDA on 16th January 2013 for use in adults 18 years and older (CDC, 2016c). As of 2016, this recombinant influenza vaccine is still being used only in the United States (CDC, 2016d). Production of this vaccine requires as early as 45 days after reception of the virus and thus, is of advantage especially during a pandemic (Cox & Hashimoto, 2011). In addition, production of this vaccine does not involve eggs and therefore, is suitable for recipients having egg allergy (CDC, 2016c). It also does not require adaptation of the new influenza virus for a better productivity and hence, the vaccine immunogenicity will not be potentially compromised.

2.1.5.4 Next generation influenza vaccine

Although traditional influenza vaccines have been well established, a better influenza vaccine with improved safety and efficacy is still needed. Many approaches in influenza vaccine development have been extensively studied, particularly recombinant proteins, virus-like particles (VLPs), viral vectors and DNA-based vaccines (Lambert & Fauci, 2010; Zhang *et al.*, 2015; Gianchecchi *et al.*, 2016). All these approaches eliminate the need to adapt influenza viruses in eggs or cells by serial passaging, as well as to avoid potential lab-acquired infection by eliminating the need of handling live pathogenic influenza viruses.

In recent years, the production of recombinant influenza antigens has primarily been in mammalian or insect cells, although other expression systems are still being used (Powers *et al.*, 1995; Treanor *et al.*, 2006). Vaxinnate (USA) developed a recombinant vaccine containing influenza HA using bacterial cells (Liu *et al.*, 2011; Tussey *et al.*, 2016). The recombinant HA vaccine was fused with flagellin, which has been reported to play an important role as an adjuvant (Adar *et al.*, 2009; Hong *et al.*, 2012; Song *et*

al., 2015). In addition, plant-based system has also been used for influenza vaccine production (Song, 2016).

VLPs are morphologically similar to native virus, but are replication incompetent due to the lack of genomic component (Wong & Webby, 2013). In order to produce VLPs, recombinant viral vectors expressing HA, NA and M1 are used to infect cells (Lambert & Fauci, 2010). The produced proteins self-assemble at the plasma membrane and bud from the infected cells, forming wild-type VLPs. Novavax (USA) has developed VLPs comprising influenza M1, HA and NA proteins for both seasonal and pandemic vaccines (Song, 2016). In addition, Dow Global Tech. Inc. (USA) has developed chimeric VLPs carrying influenza peptides displayed on the coat protein of cowpea chlorotic mottle virus or cowpea mosaic virus.

Viral vectors have been studied for their application as influenza vaccine carriers. HA gene has been cloned in carrier viruses such as baculoviruses (Prabakaran *et al.*, 2010), adenoviruses (Hoelscher *et al.*, 2006; Tang *et al.*, 2009), Newcastle disease virus (DiNapoli *et al.*, 2010) and vesicular stomatitis virus (Schwartz *et al.*, 2010). The advantage of using a viral vector is that it can be delivered directly to the mucosal surfaces, which mimic the natural infection (Wong & Webby, 2013). The major challenge of a viral vector, however, is likely the presence of anti-vector immunity which could induce tolerance (Soema *et al.*, 2015).

In contrast to virus-based vaccines, DNA-based vaccines involve administration of plasmid DNA encoding viral protein. Immune response is elicited upon viral protein synthesis in host cells. HA and NA genes administered intramuscularly with and without internal gene segments in animals has been extensively studied (Laddy *et al.*, 2008; Kim & Jacob, 2009). DNA-based vaccine was proven to provide equivalent protective efficacy to traditional IIV in mouse model (Rota *et al.*, 1990). In addition, DNA-based vaccine containing consensus antigen was shown to be able to provide

broad protective immunity (Chen *et al.*, 2008). The limitation of DNA-based vaccines, however, is that continued production of antigens in host might induce tolerance (Soema *et al.*, 2015). In addition to that, the introduction of extraneous DNA to the host could lead to unpredictable genetic alteration such as tumor growth.

2.2 Lactic acid bacteria

2.2.1 Introduction

Lactic acid bacteria (LAB) are Gram-positive bacteria which include the genera *Lactococcus*, *Lactobacillus*, *Streptococcus* and *Enterococcus* (Chapot-Chartier & Kulakauskas, 2014). They are usually found in food, plants, as well as the respiratory, intestinal and genital tracts of human and animals (Endo *et al.*, 2014; Endo *et al.*, 2015). The bacteria are extensively used in food fermentation and food processing due to their GRAS status microorganism (Pouwels *et al.*, 1998). LAB metabolize carbohydrates and secrete lactic acid as the major end product which is also used to help in the acidification of raw material (Ammor & Mayo, 2007). Other end products of LAB such as bacteriocins, an antimicrobial compounds, are also of importance to the food industry. In addition, LAB have been widely used as probiotics for human and animals due to their resistance to acid and bile salts. The bacteria have beneficial effects on several diseases, such as inflammatory bowel disease, intestinal infection and allergy reactions (Ljungh & Wadström, 2006). LAB also reduce anxiety-like and depression-like behavior, and help in ameliorating neuropsychiatric disorders (Liu *et al.*, 2016a; Liu *et al.*, 2016b).

2.2.2 *Lactococcus lactis* as a vaccine delivery vector

In recent years, LAB particularly *L. lactis* has been explored extensively as a mucosal vaccine delivery vehicle due to its non-pathogenic and non-colonizing

properties. *L. lactis* has been used to deliver antigens in three forms: intracellular, secreted or membrane-anchored forms.

Antigen delivery via intracellular form has the advantage of allowing the antigen to escape from gastric juices and bile salts, however, cell lysis is required for this delivery method. One of the well characterized expression systems for protein production in intracellular form using the *L. lactis* is the nisin-controlled expression (NICE) system, which is controlled by the addition of nisin (Bermúdez-Humaran, 2009). Proteins such as human papillomavirus type 16 (HPV 16) capsid protein L1 was produced in *L. lactis* intracellularly and it elicited mucosal immunity in mice upon immunization (Cho *et al.*, 2007). Other antigens such as HPV 16 E7 oncoprotein (Bermúdez-Humaran *et al.*, 2004), dengue virus E protein (Sim *et al.*, 2008) and tetanus toxin fragment C (TTFC) (Norton *et al.*, 1996) have also been produced in *L. lactis* intracellularly and used in vaccine delivery.

Antigen delivery via secretion form allows the antigen to have direct interaction with the environment such as the digestive tract. In *L. lactis*, most of the antigens are secreted out by an N-terminal signal peptide (SP). Usp45 is the most effective SP in facilitating secretion. This system has been applied in the production of interleukin 2 (IL-2) and interleukin 6 (IL-6) (Steidler *et al.*, 1998). It has been shown that mice immunized with *L. lactis* co-expressing TTFC intracellularly and secreted IL-2 or IL-6 developed greater serum IgG response when compared to mice immunized with *L. lactis* expressing TTFC intracellularly alone.

Antigen delivery via membrane-anchored form uses anchoring motif such as cell wall anchoring motif (LPXTG) and LysM to target antigens to the cell membrane layer (Michon *et al.*, 2016). This can be achieved by fusing the antigens to the motif prior to anchoring onto the cell layer. Antigens are covalently anchored to the cell membrane layer when LPXTG is used and noncovalently anchored when LysM is used

(Visweswaran *et al.*, 2014). This system has been used to deliver antigens such as merozoite surface antigen MSA2 (Ramasamy *et al.*, 2006), enterovirus type 71 viral capsid protein (VP1) (Varma *et al.*, 2013) and hepatitis A virus VP1 structural protein (Berlec *et al.*, 2013) in membrane-anchored form.

The best method to deliver heterologous antigen using *L. lactis* is still controversial. Previous study had demonstrated that the membrane-anchored form of TTFC on *L. lactis* was more immunogenic than the intracellular and secreted forms (Norton *et al.*, 1996). Bermúdez-Humaran *et al.* (2004) also showed that the membrane-anchored form of E7 protein on *L. lactis* was more immunogenic compared to the intracellular and secreted forms. On the other hand, *L. lactis* secreting rotavirus outer shell protein VP7 was more immunogenic than antigen in intracellular and membrane-anchored forms (Perez *ėt al.*, 2005). In addition, antigens delivered using *L. lactis* via different forms also elicited different types of immune responses. Mice immunized with rotavirus spike-protein subunit VP8 in intracellular form developed significant intestinal IgA, while mice immunized with membrane-anchored VP8 developed both mucosal and systemic immunity (Marelli *et al.*, 2011). Thus, it is important to use a suitable form of delivery that allows the antigen to be taken by the host immune machinery and stimulates the required types of immune responses.

2.2.3 Surface display on *L. lactis* using AcmA binding domain

Surface display of antigens on *L. lactis* using the AcmA binding domain has been well described (Buist *et al.*, 1997; Steen *et al.*, 2003; Raha *et al.*, 2005; Varma *et al.*, 2013; Visweswaran *et al.*, 2014). AcmA is a major autolysin found on *L. lactis* MG1363. It is responsible for bacterial cell separation and is involved in bacterial cell lysis (Buist *et al.*, 1995). AcmA comprises three domains: the N-terminal signal

domain, followed by an N-acetyl-glucosaminidase active domain and the C-terminal LysM binding domain (Buist *et al.*, 1995; Buist *et al.*, 1997).

LysM was first identified in the *Bacillus* phage ϕ29 lysozyme by Garvey in 1986 (Garvey *et al.*, 1986; Visweswaran *et al.*, 2014). The LysM was present as a C-terminal direct repeat composed of 44 amino acids separated by seven amino acids. Subsequently, LysM was identified in the *Enterococcus faecalis* peptidoglycan hydrolase in 1991 at the C-terminal with six repeats (Béliveau *et al.*, 1991; Buist *et al.*, 2008). There are few thousand prokaryotes and eukaryotes proteins that have one or more LysM present at the N-terminal, C-terminal or central domains of their proteins (Buist *et al.*, 2008). This motif ranges from 44 to 65 amino acids, and is well-conserved for the first 16 amino acid residues. The central domain is poorly conserved with exception of the IIe/Leu which is located at positions 23 and 30, and Asn at position 27. LysM containing multiple LysMs is separated by spacing sequences mostly consisting of Ser, Thr and Asp or Pro residues that contribute to the flexibility between the LysMs (Buist *et al.*, 1995). A LysM has a βααβ structure with the two α-helices packing onto the same side of an antiparallel β-sheet (Bateman & Bycroft, 2000; Buist *et al.*, 2008; Visweswaran *et al.*, 2014). A shallow groove is formed by the two loops between the α-helix and β-strand which mediates the binding of LysM onto the peptidoglycan.

LAB cell wall is composed of peptidoglycan which is made up of alternating N-acetylglucosamine (GlcNAc) and N-acetylmuramic acid (MurNAc) linked by β-1,4 bonds (Chapot-Chartier & Kulakauskas, 2014). Peptide chains consisting of one or more amino acids are attached covalently to the MurNac. The peptide chains can be cross-linked to generate a three-dimensional structure of the peptidoglycan layer. The peptide chain sequences vary across species, with stem peptide of L-Ala-γ-D-Glu-X-D-Ala, where X denotes a di-amino acid such as L-Lys in *L. lactis*. LysM binds specifically to GluNAc residues (Mesnage *et al.*, 2014; Visweswaran *et al.*, 2014),

possibly modulated by the short peptide stem that cross-links GluNAc residues with MurNAc (Mesnage *et al.*, 2014). Gly10-Asp11-Tyr12-Leu13 (GDTL) sequence is highly conserved in AcmA LysM (Petrovic *et al.*, 2012). The amino acid Asp11 in the highly conserved GDTL sequence of LysM likely interacts with GlcNAc in the peptidoglycan layer (Bateman & Bycroft, 2000; Petrovic *et al.*, 2012).

The LysM domain binds strongly in a non-covalent manner to peptidoglycan of Gram-positive bacteria, specifically around the pores and septum of the cell where cell lysis takes place (Steen *et al.*, 2003; Buist *et al.*, 2008). Binding of LysM domain occurs at the specific sites because the binding is hindered by the presence of other cell wall components that are associated with the peptidoglycan (Buist *et al.*, 2008), such as techoic acids and polysaccharides (de Ambrosini *et al.*, 1996; Chapot-Chartier, 2014; Chapot-Chartier & Kulakauskas, 2014). Teichoic acids are made up of alditolphosphate repeating units. Two types of teichoic acids, wall teichoic acids (WTA) and LTA, have been reported (Reichmann & Gründling, 2011). WTA is usually composed of ribitol phosphate, glycerolphosphate or other sugar containing polymers that are polymerized within the cytoplasm and covalently bind to the peptidoglycan molecule after being transported across the membrane (de Ambrosini *et al.*, 1996; Chapot-Chartier & Kulakauskas, 2014). LTA consists of polyglycerolphosphate chain that is anchored in the cell cytoplasmic membrane by a glycolipid anchor. On the other hand, there are three types of polysaccharides associated with the bacteria cell wall, exopolysaccharide (EPS), capsular polysaccharide (CPS) and cell wall polysaccharide (WPS) (Chapot-Chartier & Kulakauskas, 2014). EPS loosely attaches to the cell surface and is released to the surrounding environment. CPS permanently attaches to the cell and forms a shield around the cell, while WPS attaches to the cell wall without forming a capsule. Several studies have demonstrated the hindrance effect of cell wall components on the binding of LysM to peptidoglycan using an atomic force microscopy, which measured

the interaction forces by scanning of a sharp tip coated with LysM over the bacterial cells surface (Andre *et al.*, 2008; Tripathi *et al.*, 2012).

2.3 Mucosal immunity

2.3.1 Introduction

Mucosal surfaces cover the largest area within the body and separate the internal environment from the external environment. It therefore presents as the first line of defense against pathogens. In order to provide protection and combat infection, mucosal surfaces are equipped with specialized defense mechanism, particularly the mucosal immune system. The mucosal immune system is different from the systemic immune system as it mounts an immune response to pathogenic antigens and maintains active suppression to non-pathogenic antigens at the same time. The mucosal immune system is composed of mucosal surfaces lymphoid tissues (MALT) which is comprised of a few components: gut-associated lymphoid tissue (GALT), bronchus-associated lymphoid tissue (BALT), nasopharynx-associated lymphoid tissue (NALT), mammary glands, salivary glands and the genitourinary organs. The GALT is discussed in greater details here.

2.3.2 GALT

GALT comprises organized lymphoid tissues in two forms: the Peyer's patches (PPs) and the solitary lymph nodes.

The PPs are located at the small intestine anti-mesenteric side (Shakya *et al.*, 2016). PPs comprise lymphoid follicles made up of three regions: the top epithelial, the sub epithelium dome and the germinal center at the basal part (Figure 2.2). The top epithelial, follicle associated epithelium (FAE), is single-cell thick and comprises columnar epithelial cells, microfold (M) cells and intraepithelial lymphocytes (IELs).

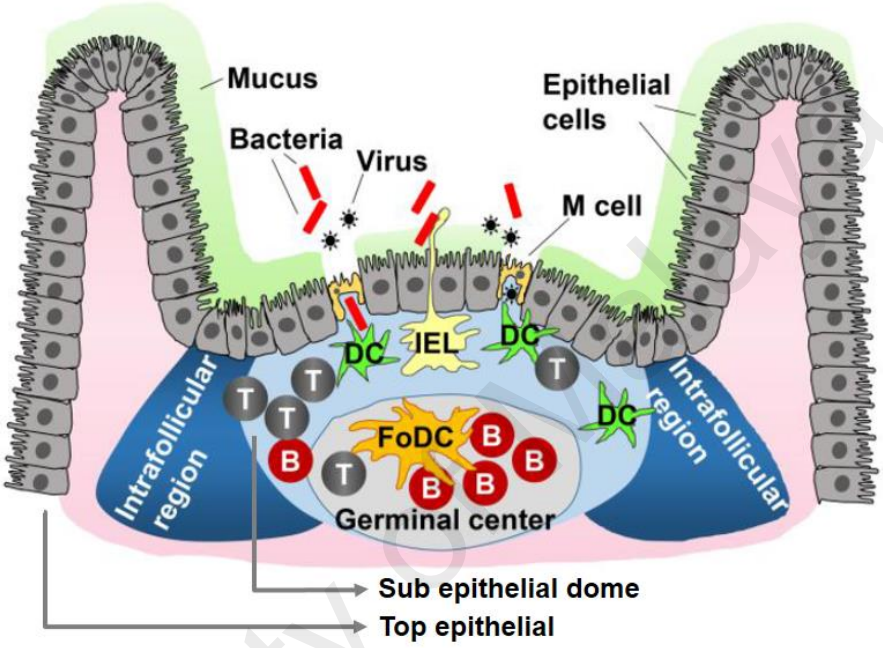

Figure 2.2: Schematic illustration of a Payer's patch (PP) located at the small intestine.

The PP comprises three parts: the top epithelial, the sub epithelial dome and the germinal center. T: T cell; B: B cell; DC: dendritic cell; IEL: intraepithelial lymphocyte; FoDC: follicular dendritic cell. Figure adapted and modified from Shakya *et al.* (2016).

M cells transport foreign antigens from the lumen to the underlying lymphoid tissue by transcytosis (De Magistris, 2006; Kim *et al.*, 2012; Kunisawa *et al.*, 2012; Shakya *et al.*, 2016). There is no mucus layer on the M cells apical side, therefore, allowing antigen sampling from the luminal space (Shakya *et al.*, 2016). IELs are located in between the epithelial cells and/or M cells, and they sample antigens from the intestinal lumen by extending their appendages out. The sub epithelium dome consists of dendritic cells (DCs) which rapidly take up the transcytosed antigens and present them to the B and T cells. The germinal center is rich in follicular dendritic cells (FoDCs), B and T cells to help in induction of immune response. The germinal center is also important for the switching of B cells to IgA-producing plasma cells (Kim *et al.*, 2012; Shakya *et al.*, 2016).

Solitary lymph nodes, on the other hand, uptake the antigen through M cells and the DCs residing at the M cells basal process the antigen to induce antigen-specific immune responses (Shakya *et al.*, 2016). In contrast to PP, solitary lymph nodes have high amounts of DCs and B cells but very few T cells.

2.3.3 Production of IgA in the gastrointestinal tract

IgA is present in two forms, typically a monomeric form in serum and a dimeric form in the mucosal secretions (Shakya *et al.*, 2016). Dimeric form IgA is produced in the gastrointestinal tract in T cell-dependent and T cell-independent pathways (Kim *et al.*, 2012).

In the T cell-dependent pathway, B cell differentiation takes place in the PP. DCs residing underneath the M cells take up antigens and present them to the T cells located in the T cell zone. The activated T cells then express CXCR5 and migrate towards CXCL13 in the follicular DC network, and activate B cells to form IgA-producing plasma cells. Expression of integrins (homing receptors) on the mucosal lymphocytes

direct their migration to the addressins (ligand to the homing receptors) secreted at the respective mucosal sites (Figure 2.3) (Kunkel & Butcher, 2003; Shakya *et al.*, 2016). Expression of CCR9, which is a homing receptor of CCL25, and integrin α4β7, which is homing receptor of mucosal addressin cell-adhesion molecule 1 (MADCAM1), are induced during IgA plasma cell development. This specifically directs the migration of IgA plasma cells from PP to lamina propia of small intestine for further differentiation into IgA-secreting plasma cells. The expression of CCR10, which is a homing receptor of CCL28, is also induced by intestinally derived IgA plasma cells (Kunkel & Butcher, 2003). CCL28 is produced by various mucosal epithelial tissues at sites such as the large intestine, stomach, trachea, bronchi, mammary glands and salivary glands. This allows the intestinal IgA plasma cells to populate the mucosal sites. Therefore, oral immunization leads to presence of antigen specific IgA at both intestinal and non-intestinal mucosal tissues (Czerkinsky *et al.*, 1991; VanCott *et al.*, 1994). In other words, mucosal immunity activated at intestine can stimulate immunity at other mucosal surfaces (De Magistris, 2006).

The dimeric IgA secreted by the IgA-secreting plasma cells in effector sites migrates and attaches to the polymeric immunoglobulin receptor (pIgR) located on the mucosal epithelial cell basolateral surface (Kim *et al.*, 2012; Kunisawa *et al.*, 2012; Shakya *et al.*, 2016). A portion of pIgR is cleaved and the remaining portion called secretory component (SC) stays attached to IgA during transcytosis of IgA to the apical surface (Renegar *et al.*, 1998). The dimeric IgA attached with SC is named secretory IgA (sIgA). sIgA is more stable than polymeric IgA (pIgA) without SC (Asahi *et al.*, 2002).

In the T cell-independent pathway, IgA is produced in isolated lymphoid follicles and lamina propia (Kim *et al.*, 2012). Stimulated DCs ($iNOS^+$) express TNFα, which induces matrix metalloproteinase (MMPs) expression (Brandtzaeg, 2003; Kim *et al.*, 2012). The MMPs such as MMP9 and A Proliferation-Inducing Ligand (APRIL)

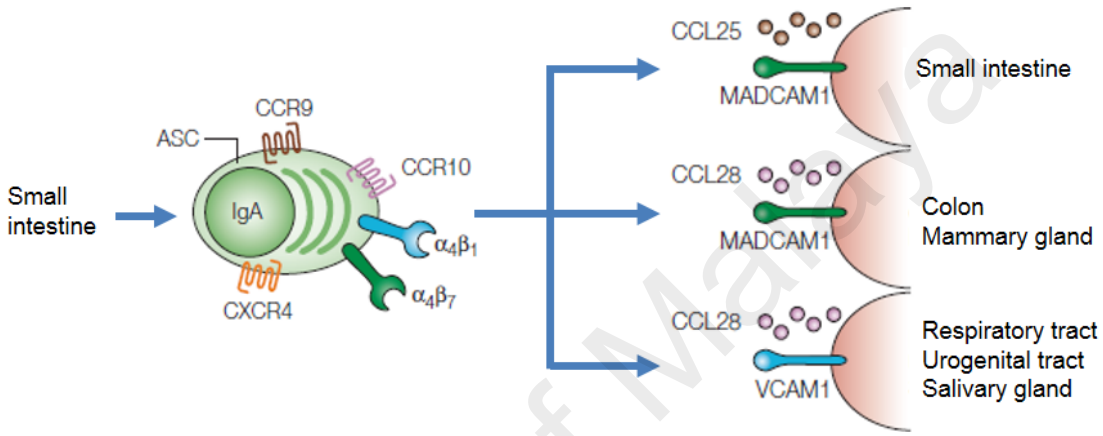

Figure 2.3: Model of trafficking IgA-producing plasma cells induced in the small intestine.

Recruitment of lymphoid cells to a target site requires specific addressin and homing receptor recognition. This specific recognition allows the IgA-producing plasma cell induced in the small intestine to populate other mucosal sites in addition to the small intestine. Figure adapted and modified from Kunkel & Butcher (2003).

subsequently activate TGF-β1, which facilitates class switching of B cells from IgM to IgA. BAFF, APRIL, IL-6 and IL-10 in lamina propia also facilitates the proliferation and differentiation of B cells to IgA-producing plasmacytes.

2.3.4 The role of IgA in protection from influenza infection

Mechanisms including steric hindrance, agglutination, neutralization and mucus trapping are believed to be the protective role of sIgA (Brandtzaeg, 2003; Shakya *et al.*, 2016). The sIgA-antigen complex can be "reverse transcytosed" by the M cells for presenting and processing by the antigen presenting cells (APCs) that reside underneath the M cells.

In influenza virus infection, sIgA is believed to be the first line of defense. Infection in knockout mice suggested that sIgA played a pivotal role in protection against influenza virus infection (van Riet *et al.*, 2012). sIgA eliminates pathogen before it passes the mucosal barrier and enters the human body (Taylor & Dimmock, 1985; Asahi-Ozaki *et al.*, 2004; Renegar *et al.*, 2004; van Riet *et al.*, 2012). It has been shown that monoclonal pIgA and sIgA are far more effective than monoclonal monomeric IgA in neutralizing viruses (Renegar *et al.*, 1998). Moreover, sIgA has been reported to be more important than IgG in the protection of the upper respiratory tract (Renegar *et al.*, 2004) and it has been shown to provide cross-protection against influenza virus infection (Liew *et al.*, 1984; Tamura *et al.*, 1990; Tamura *et al.*, 1991; Asahi-Ozaki *et al.*, 2004). Monoclonal pIgA administered intravenously was transported to the nasal surface more efficiently as compared to the monomeric IgA or IgG1 (Renegar & Small, 1991). However, a study reported that IgG1, IgG2a, IgM and pIgA were all effective in preventing influenza virus infection to varying degrees (Mbawuike *et al.*, 1999).

2.3.5 Mucosal vaccines

Mucosal vaccines have received increasing attention due to their advantages over conventional vaccines. Mucosal vaccines eliminate the use of needles during vaccine administration which would eliminate potential blood transmissible infections such as human immunodeficiency virus and hepatitis B virus infections (Levine, 2003). Mucosal vaccines can be easily administered in the absence of trained personnel and thus, are more suitable for mass vaccination of large population during pandemics. Moreover, mucosal vaccination can induce both systemic and mucosal immunity in contrast to parenteral vaccination which is poor in inducing mucosal immunity. Among the mucosal vaccines, oral vaccines are considered a more favorable approach due to the ease of administration. It is, however, generally poorly immunogenic due to induced tolerance in the gastrointestinal tract. In addition, the acid and enzyme rich stomach also form a major barrier to oral vaccination (Shakya *et al.*, 2016). Such harsh conditions may result in antigen degradation or instability. Oral immunization has proven to be difficult in stimulating strong sIgA, particularly in the administration of soluble antigens (Brandtzaeg, 2003). Examples of mucosal vaccines that have been approved for human use are the cholera vaccine (Dukoral®, Shanchol™ and mORAC-vax™), influenza virus vaccine (FluMist™), polio vaccine (Biopolio™ B1/3), rotavirus vaccine (Rotarix® and RotaTeq®) and typhoid vaccine (Vivotif®) (Holmgren & Czerkinsky, 2005; Shakya *et al.*, 2016).

2.4 Linkers

2.4.1 Introduction

Linkers have been widely used in the construction of recombinant fusion proteins. In general, linkers are categorized into three main types: flexible linkers, rigid linkers and cleavable linkers (Chen *et al.*, 2013; Klein *et al.*, 2014). Flexible linkers are used

when the domains in the fusion protein require flexibility for mobility or interaction. They ordinarily comprise small and non-polar amino acid such as Gly, or polar amino acids such as Ser or Thr (Chen *et al.*, 2013). Linkers consisting Gly and Ser amino acids, particularly $(GGGGS)_n$, have been the most widely used flexible linkers (Chen *et al.*, 2013). Gly and Ser also contribute to fusion protein stability in solution by forming hydrogen bonds with water molecules instead of interacting with the protein domains (Chen *et al.*, 2013). Other flexible linkers are KESGSVSSEQLAQFRSLD, EGKSSGSGSESKST, GSAGSAAGSGEF and $(Gly)_8$ (Chen *et al.*, 2013). Rigid linkers are applied when fixed distance between the domains in a fusion protein is of interest. Examples of rigid linkers are $(EAAAK)_n$ (Huang *et al.*, 2013) and $(Ala/LyS/Glu\text{-}Pro)_n$ (Chen *et al.*, 2013). Cleavable linkers are used when the functional domains in fusion protein are to be released free *in vivo*. Examples of cleavable linkers are LEAGCKNFFPRSFTSCGSLE, a disulfide linker, and CRRRRRREAEAC, a dithiocyclopeptide linker (Chen *et al.*, 2013).

A linker to join two domains is necessary in the recombinant fusion protein development. Direct fusion of protein domains without the addition of linker between domains may cause fusion protein misfolding (Zhao *et al.*, 2008), lower yield in protein production (Amet *et al.*, 2009) or reduction in biological activity (Bai & Shen, 2006; Zhao *et al.*, 2008; Amet *et al.*, 2009). Linkers have been proven to be able to improve protein folding and stability. Insertion of $(Gly)_8$ linker in fusion protein consisting of the Myc epitope tag and Est2p contributed to correct folding of the fusion protein (Sabourin *et al.*, 2007). Linkers help to improve fusion protein production and this was shown when the insertion of $(H4)_2$, two copies of helical linker $[A(EAAAK)_4]_2$ successfully enhanced the production of G-CSF-$(H4)_2$-Tf and Tf-$(H4)_2$-G-CSF fusion proteins (Amet *et al.*, 2009). The mechanism of the linker in the improvement of the production is however, not clear. Another study also demonstrated that insertion of

$(GGGGS)_3$ or $(EAAAK)_3$ linkers in fusion protein improved the fusion protein production (Werner *et al.*, 2006). In addition, linkers have been shown to improve the biological activity of fusion protein, possibly because the protein domains are brought far from each other. A study demonstrated that direct fusion of human serum albumin (HSA) and interferon-α2b (IFN-α2b) caused a reduction in IFN-α2b antiviral activity due to the inability of the disulphide bond formation between Cys in IFN-α2b (Zhao *et al.*, 2008). The insertion of a flexible linker, (GGGS), Pro-rich linker, (PAPAP) or helical linker, (AEAAAKEAAAKA), however, increased the antiviral activity of the fusion protein.

Suitable linkers used in fusion protein development can be complicated and is often neglected. A study demonstrated that the fusion protein consisting of acid phosphatase and green fluorescent protein linked by a rigid linker, $(EAAAK)_5$, exhibited higher biological activity when compared to the fusion protein linked by a flexible linker, $(GGGGS)_5$ (Huang *et al.*, 2013). In addition, surface display activity of fusion protein was not observed when GGGGS linker was used to link anchor protein and *Helicobacter acinonychis* urease subunit A protein (Hinc *et al.*, 2013). Fusion protein linked by a linker consisting of EAAAK motif, on the other hand, resulted in binding activity. Indeed, the choice of a suitable linker used in the construction of a fusion protein is crucial. In addition, linker length is also an important parameter in fusion protein construction as it could affect the overall performance of the constructed fusion protein (Iliades *et al.*, 1997; Kortt *et al.*, 1997; Atwell *et al.*, 1999; Shan *et al.*, 1999; Arai *et al.*, 2001; Cunliffe *et al.*, 2002; Lu & Feng, 2008; Zhao *et al.*, 2008; Klein *et al.*, 2014; Klement *et al.*, 2015).

2.4.2 scFv peptide linker, $(GGGS)_3$

The scFv peptide linker, $(GGGS)_3$, is a short peptide that joins the V_H and V_L chains of immunoglobulin (Ahmad *et al.*, 2012). This peptide linker comprises Gly and Ser residues for flexibility (Huston *et al.*, 1988; Hoedemaeker *et al.*, 1997; Gu *et al.*, 2010; Chen *et al.*, 2013; Wen *et al.*, 2013). NMR data has demonstrated that the $(GGGS)_3$ peptide linker enhanced flexibility of the scFv (Freund *et al.*, 1993). It was applied for the first time in the construction of the scFv by Huston *et al.* (1988), in which an anti-digoxin scFv comprising 26-10 V_H and V_L chains was produced. The scFv expressed in *E. coli* displayed specificity for digoxin and other related cardiac glycosides, which is comparable to the natural 26-10 fragment antigen-binding fragment. Thereafter, the peptide linker has been used widely in the development of antibodies, particularly in scFv development (Huston *et al.*, 1988; Freund *et al.*, 1993; Hoedemaeker *et al.*, 1997; Chee & AbuBakar, 1998; Dimasi *et al.*, 2009; Ahmad *et al.*, 2012). Examples of scFv constructed using the $(GGGS)_3$ peptide linker are scFv for anti-P-glycoprotein monoclonal antibody C219 (Hoedemaeker *et al.*, 1997), anti-dengue 2 virus envelop protein (Chee & AbuBakar, 1998), anti-plumbagin (Sakamoto *et al.*, 2009), anti-parasporal crystal protein (Zhang *et al.*, 2014) and anti-carbaryl insecticide (Zhang *et al.*, 2015). The peptide linker has also been used in the construction of hybrid endonucleases comprising the zinc-finger protein and *Fok* I endonuclease cleavage domain (Kim *et al.*, 1996). In addition, this peptide linker has been used in the construction of a proinflammatory cytokine fusion protein comprising a high-mobility group box 1 A box and C box (Gong *et al.*, 2010). Moreover, the peptide linker has been applied in the construction of fusion proteins which have other medical value, such as the bone morphogenetic proteins (BMP) 7-BMP2 fusion protein for osteogenic activity (Dang *et al.*, 2015) and polyethylene glycol-aldehyde-Cyanovirin-N for human

immunodeficiency virus type 1 inhibition (Chen *et al.*, 2014). In the present study, the scFv peptide linker is used in the construction of the recombinant HA1 fusion protein.

CHAPTER 3: METHODOLOGY

3.1 Cells and virus

3.1.1 Cell culture

Madin-Darby canine kidney (MDCK) cells (CCL-34) was purchased from the American Type Culture Collection (ATCC, Manassas, VA, USA). MDCK cells were cultured in complete Dulbecco's modified Eagle's medium (DMEM) containing DMEM supplemented with 10% heat-inactivated fetal bovine serum (FBS), 0.2% bovine serum albumin (BSA), 25 mM HEPES buffer, 100 U/ml penicillin and 100 µg/ml streptomycin. The cells were maintained at 37°C in a humidified atmosphere containing 5% CO_2.

3.1.2 Virus strain and propagation

Influenza A virus [A/Malaysia/2097724/2009(H1N1)] was obtained from the Diagnostic Virology Laboratory Repository, University Malaya Medical Center, Kuala Lumpur, Malaysia. Mouse adapted influenza A virus [A/TN/1-560/2009-MA2(H1N1)] propagated in embryonated eggs was kindly provided by Dr. Richard J. Webby (St. Jude Children's Research Hospital, Memphis, TN, USA).

Influenza virus was propagated in MDCK cells following WHO's guidelines (WHO, 2011). All experiments which involved handling of infectious virus were conducted in the biosafety level 2 (BSL2) containment laboratories of the Tropical Infectious Diseases Research and Education Centre (TIDREC), University of Malaya. Briefly, MDCK cells were cultured in 25 cm^2 tissue culture flasks (Corning Inc., Corning, NY, USA) to approximately 90% confluence. The cells were washed thrice with phosphate buffered saline (PBS) and inoculated with 200 µl of influenza virus inoculum. The inoculum was allowed to adsorb at 37°C for 30 min. The inoculum was then removed

and replaced with 6 ml of complete DMEM for virus growth containing DMEM supplemented with 0.2% BSA, 25 mM HEPES buffer, 100 U/ml penicillin, 100 µg/ml streptomycin and 2 µg/ml TPCK-trypsin. The cells were incubated at 35°C with 5% CO_2 until the cells showed 75-100% cytopathic effect (CPE). Following manifestation of CPE, the culture medium was added with 0.5% stabilizer such as 7.5% bovine albumin fraction V. The suspension was centrifuged at 1,811 ×g for 10 min using aerosol-resistant centrifuge to remove all residual cells. The supernatant was used as virus inoculum. The inoculum was aliquoted into screw-cap tubes (Axygen, Corning, NY, USA) and stored at -80°C until needed. The mock-infected inoculum was similarly prepared using uninfected MDCK cells.

3.1.3 Virus titration

Virus titer for all the viruses was determined using plaque assay. Briefly, MDCK cells were seeded in 24-well tissue culture plate (BD Bioscience, Bedford, MA, USA) at cell density of 2×10^5 cells per well. After overnight incubation at 37°C with 5% CO_2, the cell monolayer was washed with PBS. A ten-fold serially diluted virus inoculum (200 µl) prepared using complete DMEM for virus growth was added to the wells in duplicate. The plates were incubated at 37°C for 1 h. Subsequently, the cells were washed thrice with PBS and overlaid with 1.5% (w/v) carboxymethyl-cellulose sodium salt (CMC) in complete DMEM for virus growth (1 ml). After incubation at 35°C for 84 h post-infection (p.i.), the cells were fixed with 4% (w/v) paraformaldehyde for 1 h and subsequently stained with 1% (w/v) crystal violet in 20% ethanol for 30 min. After removal of crystal violet solution, the plates were washed gently with water and left to dry. The plaques in each well were counted using a stereo-microscope (Nikon, Tokyo, Japan) and the titer of the virus in plaque-forming unit per mililiter (PFU/ml) was determined.

3.2 Influenza virus hemagglutinin (HA) gene sequencing

3.2.1 RNA extraction

Viral RNA was extracted from the A/Malaysia/2097724/2009(H1N1) influenza virus-infected MDCK cell culture supernatant using QIAamp Viral RNA Mini Kit (Qiagen, Hilden, Germany) following the manufacturer's instructions. The extracted RNA sample was eluted in 60 µl of nuclease-free water and stored at -80°C until needed.

3.2.2 Reverse transcription-polymerase chain reaction (RT-PCR) amplification

Forward and reverse specific primers designed by the WHO Collaborating Centre for influenza at CDC Atlanta, USA (WHO, 2009) were used to obtain the complete HA sequence (Table 3.1). A total of six primer sets was used to amplify six fragments of the influenza HA gene (Figure 3.1). The fragments were amplified from the extracted RNA by one step reverse transcription-polymerase chain reaction (RT-PCR) using the Access Quick RT-PCR System (Promega, Madison, WI, USA). The reaction mixture (25 µl) consisted of 2× AccessQuick Master Mix (12.5 µl), 30 pmol forward and reverse primers (1 µl), RNA template (2 µl), AMV reverse transcriptase (0.5 µl) and nuclease-free water (8 µl). Conditions applied for the RT-PCR amplification were; reverse-transcription at 48°C for 45 min; initial denaturation at 94°C for 2 min; 30 cycles of denaturation at 94°C for 20 sec, annealing at 50°C for 30 sec, extension at 72°C for 1 min; followed by final extension at 72°C for 7 min. The RT-PCR reactions were performed using a Veriti 96-well Thermal Cycler (Applied Biosystems, Foster City, CA, USA). The amplified DNA fragments were separated in 1.5% (w/v) agarose gel. Following that, the bands of interest were excised and purified using QIAquick™ Gel Extraction Kit (Qiagen, Hilden, Germany) following the manufacturer's instructions.

Table 3.1: Primers used in the RT-PCR amplification of influenza virus HA gene.

Primer set	Primer	Position (5'-3')	Sequence (5'-3') [a, b]	Expected size (bp) [c]
1	HAF1-F	1	**TGTAAAACGACGGCCAGT**ATACG ACTAGCAAAAGCAGGGG	507
	HAF1-R	471	**CAGGAAACAGCTATGACC**TCATG ATTGGGCCAYGA	
2	HAF2-F	356	**TGTAAAACGACGGCCAGT**ACRTG TTACCCWGGRGATTTCA	649
	HAF2-R	968	**CAGGAAACAGCTATGACC**GAAAK GGGAGRCTGGTGTTTA	
3	HAF3-F	356	**TGTAAAACGACGGCCAGT**ACRTG TTACCCAGGRGATTTC	959
	HAF3-R	1278	**CAGGAAACAGCTATGACC**TCTTT ACCYACTRCTGTGAA	
4	HAF4-F	767	**TGTAAAACGACGGCCAGT**AGRAT GRACTATTACTGGAC	633
	HAF4-R	1363	**CAGGAAACAGCTATGACC**TTCTK CATTRTAWGTCCAAA	
5	HAF5-F	1129	**TGTAAAACGACGGCCAGT**TGGAT GGTAYGGTTAYCAYCA	453
	HAF5-R	1545	**CAGGAAACAGCTATGACC**TCATA AGTYCCATTTYTGA	
6	HAF6-F	1244	**TGTAAAACGACGGCCAGT**AAGAT GAAYACRCARTTCACAG	584
	HAF6-R	1791	**CAGGAAACAGCTATGACC**GTGTC AGTAGAAACAAGGGTGTTT	

[a] The bold letters indicate M13 forward universal sequencing primer (TGT AAA ACG ACG GCC AGT) in all forward primers and M13 reverse universal sequencing primer (CAG GAA ACA GCT ATG ACC) in all reverse primers.

[b] Y=T/C, R=G/A, W=A/T, K=G/T

[c] A/California/07/2009(H1N1) HA gene (accession number: CY121680.1) was used as the reference strain to calculate the expected size.

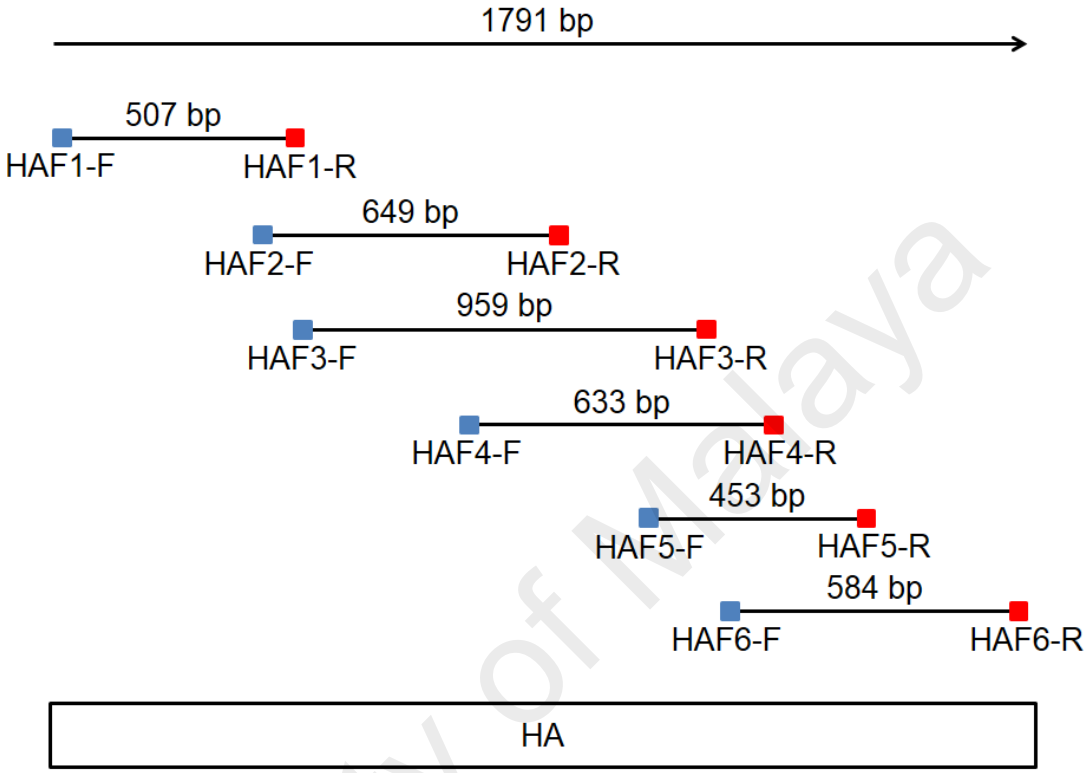

Figure 3.1: Schematic illustration of the influenza HA gene and the locations of the primers used to derive the complete HA sequence.

A total of six primer sets were used in the RT-PCR amplification with overlapping regions spanning the entire HA gene. The forward primers were marked in blue and the reverse primers were marked in red. The size in base pairs (bp) for each amplified fragments were also indicated.

3.2.3 Nucleotide sequencing

The purified DNA fragments obtained from Section 3.2.2 were sequenced with M13 forward and M13 reverse primers using BigDye Terminator v3.1 Cycle Sequencing Kit (Applied Biosystems, Foster City, CA, USA). The reaction mixture (5 µl) consisted of 5× BigDye Terminator sequencing buffer (0.5 µl), BigDye Terminator Ready Reaction Premix (0.5 µl), 10 pmol primer (0.5 µl), DNA template (2 µl) and nuclease-free water (1.5 µl). Conditions applied for the amplification were; initial denaturation at 96°C for 2 min; 30 cycles of denaturation at 96°C for 10 sec, annealing at 52°C for 5 sec, extension at 60°C for 4 min. The sequencing reaction was purified using ethanol/sodium acetate precipitation method. The precipitation solution containing 3 M sodium acetate (2.55 µl), 95% ethanol (54.74 µl) and nuclease-free water (22.71 µl) was added to the sequencing reaction. The mixture was incubated at room temperature for 30 min followed by centrifugation at 3,000 ×g at 4°C for 10 min. The precipitated pellet was washed twice with 70% ethanol (150 µl) and air dried. The pellet was resuspended in 10 µl of Hi-Di Formamide (Applied Biosystems, Foster City, CA, USA) and the sample was denatured at 95°C for 2 min. Subsequently, the sequencing reaction was performed using a DNA sequencer 3730xl DNA analyser (Applied Biosystems, Foster City, CA, USA). The nucleotide sequences were then analyzed using Sequencher version 4.9 (Gene Codes, Ann Arbor, MI, USA).

3.3 Bacterial strains, plasmids and culture conditions

The bacteria strains and plasmids used in this work are listed in Table 3.2. *E. coli* was grown in Luria-Bertani (LB) broth at 37°C with aeration. *L. lactis* MG1363 was grown in M17 broth supplemented with 0.5% (w/v) glucose (GM17) at 30°C without aeration. When necessary, antibiotics were added as follow: 12.5 µg/ml tetracycline, 34 µg/ml chloramphenicol and 50 µg/ml ampicillin.

Table 3.2: Bacteria strains and plasmids used in the study.

Bacteria strain or plasmid	Characteristics	Sources or references
Bacteria strains		
E. coli NovaBlue	Host for gene cloning; Plasmid free; tet^r	Novagen Inc (Madison, WI, USA)
E. coli RosettaBlue (DE3) pLacI	Host for gene expression; Plasmid free; tet^r cam^r	Novagen Inc (Madison, WI, USA)
L. lactis MG1363	Wild type; Plasmid free	(Raha *et al.*, 2005)
Plasmids		
pSVac	Recombinant plasmid containing AcmA binding domain; amp^r	(Raha *et al.*, 2005)
pTriEx-3 Hygro	*E. coli* cloning vector; amp^r	Novagen Inc (Madison, WI, USA), Appendix A
pTriEx_HA1/L/AcmA	amp^r	This work
pTriEx_Tag/HA1/L/AcmA	amp^r	This work
pTriEx_Tag/HA1/AcmA	amp^r	This work
pTriEx_Tag/HA1	amp^r	This work

3.4 Construction of pTriEx_HA1/L/AcmA recombinant plasmid

3.4.1 Polymerase chain reaction (PCR) amplification

Extracted RNA from the A/Malaysia/2097724/2009(H1N1) influenza virus was used as template for complementary DNA (cDNA) synthesis using SuperScript™ III reverse transcriptase (Invitrogen Life Technologies, Carlsbad, CA, USA). The reaction mixture (13 µl) consisted of 10 mM dNTP mix (1 µl), 2 pmol primer (1 µl), RNA template (5 µl) and nuclease free water (6 µl). The reaction mixture was incubated at 65°C for 5 min and 4°C for 1 min. Subsequently, 5× First-Strand Buffer (4 µl), 0.1 M DTT (1 µl), SuperScript™ III reverse transcriptase (1µl) and nuclease-free water (1 µl) were added to the reaction mixture. Conditions applied for the cDNA synthesis were; 50°C for 2 h and 70°C for 15 min. The cDNA was subsequently used in polymerase chain reaction (PCR) amplification of HA1_L fragment using Platinum® Taq DNA Polymerase High Fidelity (Invitrogen Life Technologies, Carlsbad, CA, USA) with HA1F1 and HA1R1 primers (Table 3.3, Figure 3.2). The reaction mixture (50 µl) consisted of 10× High Fidelity PCR buffer (5 µl), 10 mM dNTP (1 µl), 50 mM $MgSO_4$ (2 µl), 30 pmol of each primers (1 µl), cDNA template (4 µl), Platinum® *Taq* DNA polymerase High Fidelity (0.2 µl) and nuclease-free water (35.8 µl). Conditions applied for the amplification were; initial denaturation at 94°C for 2 min; 40 cycles of denaturation at 94°C for 30 sec, annealing at 50°C for 1 min, extension at 68°C for 1 min 30 sec; and final extension at 68°C for 7 min. The recombinant plasmid pSVac containing the AcmA binding domain was used for amplification of AcmA_L fragment using AcmAF1 and AcmAR1 primers (Table 3.3, Figure 3.2). The reaction mixture (50 µl) consisted of 10× High Fidelity PCR buffer (5 µl), 10 mM dNTP (1 µl), 50 mM $MgSO_4$ (2 µl), 30 pmol of each primers (1 µl), DNA template (1 µl), Platinum® *Taq* DNA polymerase High Fidelity (0.2 µl) and nuclease-free water (38.8 µl). Conditions applied for the amplification were; initial denaturation at 94°C for 30 sec; 25 cycles of denaturation at

Table 3.3: Primers used for amplification of gene fragments in the construction of recombinant plasmids.

Oligonucleotide	Sequence (5'-3') [a, b, c, d, e, f, g]
HA1F1	CTACATG*CTGCAG*GACACATTATGTATAGGTTATCATGC
HA1R1	GGATCCACCTCCGCCTGAACCGCCTCCACCTCTAGATTGAATAGAAGGGACATTCCTCAATCC
AcmAF1	GGTGGAGGCGGTTCAGGCGGAGGTGGATCCGGCGGTGGCGGTTCGGACGGAGCTTCTTCAGC
AcmAR1	GCCGCGCG*CTCGAG*TGAACCACCTGAATTTGTAGAAGAAGCTGAAC
HA1F2	CCGGG*CTGCAG*CACCACCATCACCATCACGACTACAAGGACGACGATGACAAGGACACATTATGTATAGGTTATCATG
HA1R2	GCTCCGTC**TCTAGATTGAATAGAAGGGAC**
HA1R3	GCGCG*CTCGAG*TTATTATCTAGATTGAATAGAAGGGACATTCC
AcmAF2	GGAAT**GTCCCTTCTATTCAATCTAGA**GACGGAGCTTCTTCAGC
AcmAR2	GCCGGCGCG*CTCGAG*TTATTATGAACCACCTGAATTTGTAGAAG
TriEx2403	GACCTTGCTTCCTTTGG

[a] The italicized letters indicate the restriction site overhangs used in the cloning procedure.

[b] The underlined letters indicate the overlapping parts of the scFv peptide linker.

[c] The double underlined letters indicate the six-histidine (His)-tag.

[d] The dotted underlined letters indicate the FLAG-tag including an enterokinase cleavage site.

[e] The dashed underlined letters indicate the overlapping parts of the AcmA fragment.

[f] The bold letters indicate the overlapping parts of the HA1 fragment.

[g] The boxed letters indicate the stop codon.

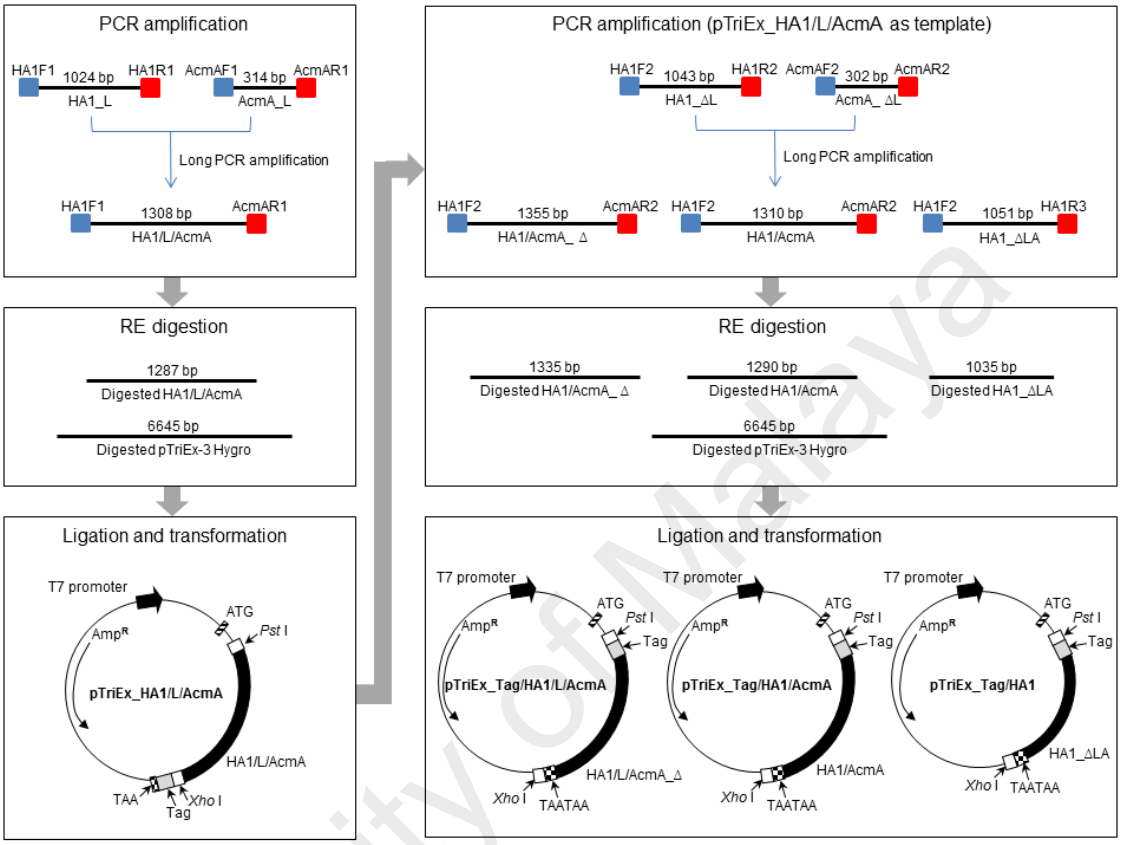

Figure 3.2: Flow chart for the construction of pTriEx_HA1/L/AcmA, pTriEx_Tag/HA1/L/AcmA, pTriEx_Tag/HA1/AcmA and pTriEx_Tag/HA1 recombinant plasmids.

Primer sets used in the PCR amplification of each fragment were indicated. The forward primers were marked in blue and the reverse primers were marked in red. The sizes in bp for each amplified and RE digested fragment were indicated. The map of each recombinant plasmid was also shown.

94°C for 15 sec, annealing at 58°C for 1 min, extension at 72°C for 2 min; and final extension at 72°C for 7 min. The amplified HA1_L and AcmA_L DNA fragments were analyzed by 1.5% (w/v) agarose gel electrophoresis and purified using QIAquick™ Gel Extraction Kit (Qiagen, Hilden, Germany) following the manufacturer's instructions. These fragments were used as template for long PCR amplification to generate HA1/L/AcmA fusion fragment using HA1F1 and AcmAR1 primers (Figure 3.2). The reaction mixture (50 µl) consisted of 10× High Fidelity PCR buffer (5 µl), 10 mM dNTP (1 µl), 50 mM $MgSO_4$ (2 µl), 30 pmol of each primers (1 µl), HA1_L DNA template (1 µl), AcmA_L DNA template (1 µl), Platinum® *Taq* DNA polymerase High Fidelity (0.2 µl) and nuclease-free water (37.8 µl). Conditions applied for the amplification were; initial denaturation at 94°C for 2 min; 30 cycles of denaturation at 94°C for 30 sec, annealing at 50°C for 1 min, extension at 68°C for 2 min; and final extension at 68°C for 7 min. The PCR reactions were performed using a PTC-100® Peltier Thermal Cycler (Bio-Rad Laboratories, Hercules, CA, USA). The amplified HA1/L/AcmA fusion fragment were separated by 1.5% (w/v) agarose gel electrophoresis and purified using QIAquick™ Gel Extraction Kit (Qiagen, Hilden, Germany) following the manufacturer's instructions.

3.4.2 Restriction endonuclease (RE) digestion

The purified HA1/L/AcmA fusion fragment and the pTriEx-3 Hygro vector extracted using QIAprep® Spin Miniprep kit (Qiagen, Hilden, Germany) following the manufacturer's instructions weredigested using *Pst*I and *Xho*I restriction enzymes (New England Biolabs, Ipswich, MA, USA). The restriction endonuclease (RE) digestion mixture (20 µl) consisted of 10× NEBuffer 3 (2 µl), 10× BSA (2 µl), *Pst*I (0.5 µl), *Xho*I (0.5 µl), DNA template (10 µl) and nuclease-free water (5 µl). The conditions for digestion were; incubation at 37°C for 2 h and heat inactivation at 80°C for 20 min.

The digested DNA fragments were analyzed by 1.5% (w/v) agarose gel electrophoresis and purified using QIAquick™ Gel Extraction Kit (Qiagen, Hilden, Germany) following the manufacturer's instructions for subsequent used.

3.4.3 Ligation

The HA1/L/AcmA fusion fragment was ligated into pTriEx-3 Hygro vector as a *Pst*I-*Xho*I fragment using T4 DNA ligase (Promega, Madison, WI, USA). The ligation mixture (12 µl) consisted of 10× T4 DNA Ligase buffer (1.2 µl), digested HA1/L/AcmA fusion fragment (9.3 µl), digested pTriEx-3 Hygro vector (0.5 µl) and T4 DNA ligase (1 µl). The conditions for ligation were; incubation at 16°C for overnight and inactivation at 65°C for 10 min. The ligated recombinant construct was named pTriEx_HA1/L/AcmA (Figures 3.2 and 3.3a).

3.4.4 Transformation into *Escherichia coli* NovaBlue

The recombinant plasmid pTriEx_HA1/L/AcmA was transformed into *E. coli* NovaBlue competent cells prepared using calcium chloride ($CaCl_2$) procedure. Briefly, *E. coli* was inoculated in LB broth containing antibiotics and incubated overnight at 37°C. Following that, the *E. coli* was subcultured and incubated at 37°C until the OD_{600} reading reached 0.5. The culture was transferred into 1.5 ml microcentrifuge tubes (1 ml per tube) and sedimented by centrifugation at 5,000 ×g for 3 min. The cell pellet was resuspended with 500 µl of cold 100 mM $CaCl_2$ gently after the removal of supernatant. Subsequently, 100 µl of cold 100 mM $CaCl_2$ was added and the mixture was mixed by inversion, followed by incubation on ice for 2 h. Following centrifugation at 1,000 ×g for 3 min, the pellet was resuspended with 80 µl of cold 100 mM $CaCl_2$. Ligation mix (12 µl) was then added to the suspension. After incubation on ice for 45 min, the sample was mixed prior to heat shock at 42°C for 1 min and placed

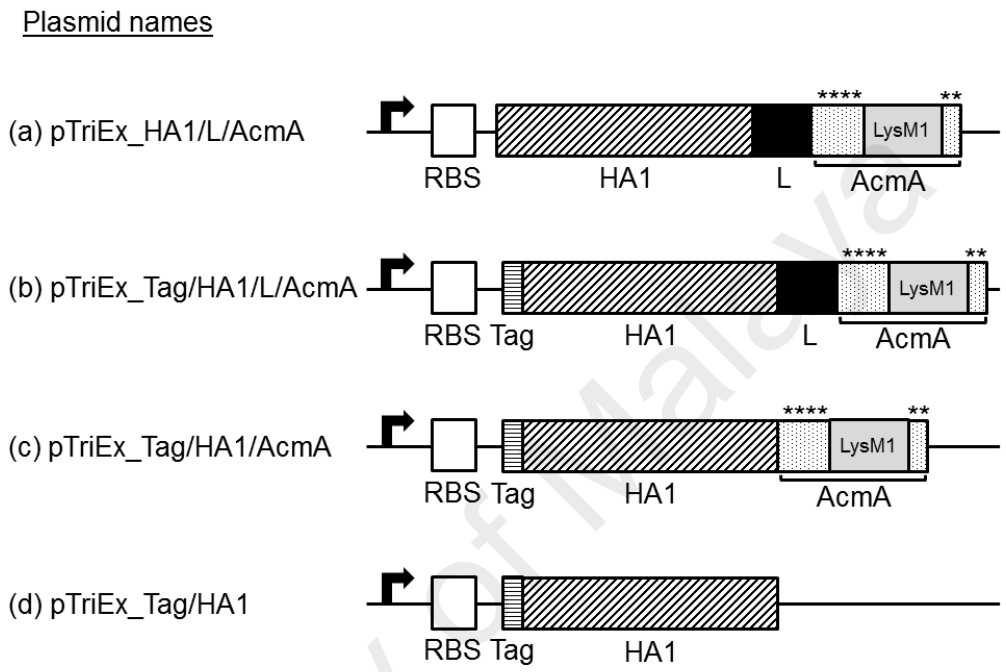

Figure 3.3: Schematic illustration of the recombinant plasmid constructs, pTriEx_HA1/L/AcmA, pTriEx_Tag/HA1/L/AcmA, pTriEx_Tag/HA1/AcmA and pTriEx_Tag/HA1.

RBS: ribosome binding site; Tag: six-histidine (His)-tag; HA1: influenza A (H1N1) 2009 hemagglutinin 1; L: scFv peptide linker $(Gly_4Ser)_3$; AcmA: N-acetylmuramidase binding domain (including Ser, Thr and Asp rich region, marked with asterisks, followed by LysM1, shaded in grey). Details for the plasmids construction are as stated in the experimental procedures.

back on ice for 5 min. A total of 1 ml of LB broth was added and the mixture was mixed by inversion, followed by incubation at 37°C for 1 h. The mixture was centrifuged at 5,000 ×g for 3 min and the supernatant was discarded. The pellet was then resuspended with the leftover LB broth, plated onto LB agar containing antibiotics for selection (12.5 µg/ml tetracycline and 50.0 µg/ml ampicillin) and incubated overnight at 37°C.

3.4.5 Screening and verification of positive transformants

Colony PCR was performed to screen for positive transformants containing pTriEx_HA1/L/AcmA. Briefly, putative bacterial colonies were picked and streaked on a grid plate. After overnight incubation at 37°C, bacteria from each grid was picked, resuspended in 20 µl of nuclease-free water and immediately placed on ice. The samples were heated in boiling water for 6 min. The samples were centrifuged at 15,000 ×g for 3 min and the supernatant was used in PCR amplification. PCR amplification was performed using GoTaq® Flexi DNA polymerase (Promega, Madison, WI, USA). The reaction mixture (25 µl) consisted of 10× Green GoTaq® Flexi buffer (2.5 µl), 10 mM dNTP (0.5 µl), 25 mM $MgCl_2$ (1 µl), 30 pmol gene-specific primers (0.5 µl), DNA template (5 µl), GoTaq® Flexi DNA polymerase (0.5 µl) and nuclease-free water (14.5 µl). Conditions applied for the amplification were; initial denaturation at 94°C for 2 min; 30 cycles of denaturation at 94°C for 30 sec, annealing at 50°C for 1 min, extension at 68°C for 2 min; and final extension at 68°C for 7 min. The amplified DNA fragments were separated by 1.5% (w/v) agarose gel electrophoresis. The positive transformants carrying pTriEx_HA1/L/AcmA were cultured in LB broth containing antibiotics overnight at 37°C. A 20% (v/v) glycerol stock of the culture was prepared from the overnight culture and kept at -80°C until needed.

3.4.6 Nucleotide sequencing

Recombinant plasmid pTriEx_HA1/L/AcmA was extracted from the positive transformants using QIAprep® Spin Miniprep kit (Qiagen, Hilden, Germany) following the manufacturer's instructions. The extracted recombinant plasmids were sequenced using T7 promoter, Triex2403, HA1F1 and AcmAR1 primers (Table 3.3) as previously described in Section 3.2.3.

3.5 Construction of pTriEx_Tag/HA1/L/AcmA, pTriEx_Tag/HA1/AcmA and pTriEx_Tag/HA1 recombinant plasmids

Subsequent PCR amplifications to introduce a N-terminal hexahistidine tag (HHHHHH) and a C-terminal stop codon were performed using pTriEx_HA1/L/AcmA recombinant plasmid as the template. Briefly, for the construction of pTriEx_Tag/HA1/L/AcmA (Figure 3.3b), HA1/L/AcmA_Δ fusion fragment was amplified from pTriEx_HA1/L/AcmA using HA1F2 and AcmAR2 primers (Table 3.3, Figure 3.2). For the construction of pTriEx_Tag/HA1/AcmA (Figure 3.3c), the HA1_ΔL fragment was amplified using HA1F2 and HA1R2 primers (Table 3.3, Figure 3.2), while AcmA_ΔL fragment was amplified using AcmAF2 and AcmAR2 primers (Table 3.3, Figure 3.2). These two amplified fragments (HA1_ΔL and AcmA_ΔL) overlapped each other at 29 nucleotides at the HA1_ΔL C-terminal and the AcmA_ΔL N-terminal, were subsequently used as templates in long PCR amplification with HA1F2 and AcmAR2 primers to generate HA1/AcmA fusion fragment (Figure 3.2). Primers HA1F2 and HA1R3 (Table 3.3, Figure 3.2) were used to amplify HA1_ΔLA fragment for construction of pTriEx_Tag/HA1 (Figure 3.3d). The reaction mixture and conditions applied for the PCR and long PCR amplification were as previously described in Section 3.4.1. Similarly, the amplified fragments were digested using *Pst*I and *Xho*I restriction enzymes, ligated into *Pst*I and *Xho*I digested pTriEx-3 Hygro and

transformed into *E. coli* NovaBlue as previously described in Sections 3.4.2, 3.4.3 and 3.4.4, respectively. The putative bacterial colonies were screened and verified by colony PCR as previously described in Section 3.4.5. Nucleotide sequencing for each positive recombinant plasmid was performed using T7 promoter, TriEx2403 and the respective gene-specific primers as previously described in Section 3.2.3.

3.6 Production, purification and refolding of HA1/L/AcmA, HA1/AcmA and HA1 recombinant proteins

3.6.1 Transformation into *E. coli* RosettaBlue (DE3) pLacI

The positive pTriEx_Tag/HA1/L/AcmA, pTriEx_Tag/HA1/AcmA and pTriEx_Tag/HA1 recombinant plasmids verified by nucleotide sequencing, were extracted from among the positive transformants using QIAprep® Spin Miniprep kit (Qiagen, Hilden, Germany) following the manufacturer's instructions. Subsequently, the positive recombinant plasmids were transformed into expression host, *E. coli* RosettaBlue (DE3) pLacI, respectively, as previously described in Section 3.4.4 with the exception that the ligation mix (12 µl) was replaced with recombinant plasmid (1 µl). Transformants were screened by colony PCR and sequenced by nucleotide sequencing as previously described in Sections 3.4.5 and 3.4.6, respectively.

3.6.2 Computational analysis of recombinant protein biochemical properties

The molecular masses of HA1/L/AcmA, HA1/AcmA and HA1 recombinant proteins to be produced in *E. coli* RosettaBlue (DE3) pLacI carrying pTriEx_Tag/HA1/L/AcmA, pTriEx_Tag/HA1/AcmA and pTriEx_Tag/HA1 recombinant plasmids, respectively, were predicted using ExPASy ProtParam tool (http://web.expasy.org/protparam/). The recombinant proteins theoretical isoelectric point (pI) value and instability index were also predicted using the same tool to determine the optimal buffers pH to be used for the

separation of recombinant proteins and the stability of the recombinant proteins, respectively.

3.6.3 Protein production

The positive clones were cultured overnight in LB broth supplemented with antibiotics and 1% (w/v) glucose. The overnight culture was inoculated in fresh LB broth (1:100 ratio) containing the same concentration of antibiotics and glucose, and cultured until an OD_{600} reading of 0.7 was achieved. Production of HA1/L/AcmA, HA1/AcmA and HA1 recombinant proteins was induced by the addition of a final concentration of 1 mM isopropyl β-D thiogalactosidase (IPTG). After 4 h, the bacterial cells were harvested by centrifugation at 10,000 ×g for 10 min. The resulting bacteria pellet was stored at -80°C until needed. Simultaneously, 1 ml of induced and uninduced bacteria cells were also sedimented and resuspended with 100 µl of PBS for analysis by sodium dodecyl sulphate-polyacrylamide gel electrophoresis (SDS-PAGE) and immunoblotting.

3.6.4 Sodium dodecyl sulphate-polyacrylamide gel electrophoresis (SDS-PAGE) and immunoblotting analysis

The induced and uninduced bacterial cells obtained from Section 3.6.3 were analyzed by SDS-PAGE and immunoblotting. Samples were prepared by adding one volume of bacteriasample with half volume of 3× reducing SDS sample buffer [187.5 mM Tris-HCl (pH 6.8), 6% (w/v) SDS, 30% (w/v) glycerol, 0.03% (w/v) bromophenol blue and 0.125 M dithioethreitol]. The protein samples were heated at 95°C for 5 min prior to loading into 12.5% SDS-PAGE. The samples were separated under denaturing condition in tank buffer [0.02 M Tris, 0.2 M glycine, 0.1% (w/v) SDS] at 120 V for 80 min. After electrophoresis, the gel was fixed in fixative solution [40% (v/v) ethanol, 10%

(v/v) acetic acid] for 1 h. Following that, the gel was washed with water thrice, each time for 10 min, and then stained with Colloidal Coomassie solution [0.08% (w/v) Commassie Brilliant Blue G250, 8% (w/v) ammonium suphate, 0.82% (v/v) phosphoric acid, 20% (v/v) methanol] for overnight. The gel was then destained with water thrice, each time for 30 min.

For immunoblotting, the proteins separated on SDS-PAGE were transferred onto nitrocellulose membrane (Millipore, Billerica, MA, USA) using a Trans-Blot SD Semi-Dry Electrophoretic Transfer Cell (Bio-Rad Laboratories, Hercules, CA, USA) at 15 V for 45 min. The membrane was blocked with 3% (w/v) BSA in TBS-T [TBS (50 mM Tris-base, 150 mM NaCl), 0.05% (v/v) Tween-20] for 1 h. The membrane was washed with TBS-T for 10 min before incubation with AP-conjugated HisDetector Nickel (KPL, Gaithersburg, MD, USA) at 1:5,000 dilution in 1% (w/v) BSA in TBS-T for 1 h. The membrane was then washed vigorously using TBS-T thrice, each time for 20 min, and TBS twice, each time for 10 min. After washing, the membrane was developed using BCIP/NBT (KPL, Gaithersburg, MD, USA). The reaction was stopped by the addition of water onto the membrane. All incubations were performed with constant agitation at room temperature.

3.6.5 Protein extraction

Bacterial pellet sedimented from 100 ml of induced bacteria cells culture from Section 3.6.3 was resuspended in 10 ml of lysis buffer (20 mM NaH_2PO_4, 500 mM NaCl, 20 mM imidazole, pH 7.4), containing 2 mg/ml of lysozyme and incubated on ice for 30 min. Subsequently, the cells were sonicated using a Branson Sonifier 250 (Branson Ultrasonics, Danbury, CT, USA) at 30% output intensity for 40×10 sec at constant duty cycle. The suspension was centrifuged at 10,000 ×g for 10 min at 4°C. The supernatant (soluble protein) and pellet (insoluble protein) fractions were subjected

to 12.5% SDS-PAGE and immunoblotting analysis as previously described in Section 3.6.4 to detect the presence of the recombinant protein.

3.6.6 Protein purification

The insoluble fraction, containing the inclusion bodies was washed with PBS for five times and recovered by centrifugation at 10,000 ×g for 10 min. The inclusion bodies were solubilized in 20 ml denaturing buffer (6 M urea, 20 mM NaH_2PO_4, 1 M NaCl, 20 mM imidazole) for 2 h with mild agitation at room temperature. The solubilized recombinant proteins were purified using a HisTrap HP 1 ml column (GE Healthcare, Uppsala, Sweden) attached to the Akta™ Purifier system (GE Healthcare, Uppsala, Sweden). Briefly, sample (16 ml) was applied to the pre-equilibrated column and the column was washed with 10 column volume (CV) of Buffer A (6 M urea, 20 mM NaH_2PO_4, 1 M NaCl, 20 mM imidazole). The target recombinant protein was then eluted with step gradients using 5 CV of 10% and 50% Buffer B (6 M urea, 20 mM NaH_2PO_4, 1 M NaCl, 500 mM imidazole). Buffers with pH 7.4 were used for HA1/L/AcmA and HA1/AcmA recombinant proteins, while buffers with pH 7.2 were used for HA1 recombinant protein. The chromatography was performed at a flow rate of 1 ml/min and the recombinant proteins were detected at UV wavelength of 280 nm. The eluted fractions were subjected to 12.5% SDS-PAGE as previously described in Section 3.6.4. Eluted fractions containing the target recombinant protein were pooled. The concentration of the purified recombinant proteins was determined using Micro BCA protein assay kit (Pierce, Rockford, IL, USA) following the manufacturer's instructions.

3.6.7 Protein refolding

The purified recombinant proteins were diluted to a final concentration of <100 μg/ml and refolded through 4 M, 2 M and 0 M urea solutions (dissolved in 20 mM NaH_2PO_4, 0.5 M NaCl) using the Slide-A-Lyzer dialysis cassette (Pierce, Rockford, IL, USA). Residual urea was removed by dialysis twice against the same dialysis buffer containing no urea. Dialysis buffer with pH 7.4 was used for the HA1/L/AcmA and HA1/AcmA recombinant proteins, while buffer with pH 7.2 was used for the HA1 recombinant protein. Centrifugation at 15,000 ×g for 20 min was performed to remove any protein aggregate generated during the dialysis process. The refolded recombinant proteins were concentrated using a Vivaspin 6 centrifugal filter device (Sartorius AG, Goettingen, Germany) with a MWCO of 10 kDa. All steps were performed at 4ºC to avoid protein degradation. The concentrated recombinant proteins were analyzed by 12.5% SDS-PAGE and immunoblotting as previously described in Section 3.6.4. The purity of the recombinant proteins was determined using the Gel Pro Analyzer 4.0 (Media Cybernetics, Rockville, MD, USA). The concentration of the recombinant proteins was quantified using Micro BCA protein assay kit (Pierce, Rockford, IL, USA) following the manufacturer's instructions.

3.6.8 Protein identification

The identity of the recombinant proteins was confirmed by mass spectrometry. Briefly, protein spots from Colloidal Coomassie blue R250-stained gel were excised using Ettan™ Spot Picker (GE Healthcare, Uppsala, Sweden) and transferred to a 96-well plate. The gel plugs were destained thrice using 150 μl of 50% (v/v) methanol containing 50 mM ammonium bicarbonate, each time for 30 min. The destaining solution was removed and the gel plugs were dried at 42°C for 17 min. Subsequently, 10 μl of 0.02 μg/μl sequencing grade modified trypsin (Promega, Madison, WI, USA)

was added into each well and incubated at 37°C for 2 h. Peptide from the gel plugs were then extracted using 60 µl of solvent solution containing 0.1% (v/v) trifluoroacetic acid (TFA) and 50% (v/v) acetonitrile (ACN). After 30 min incubation, the extracted peptides were transferred to new wells, respectively. The extraction step was repeated using 40 µl of the solvent solution and transferred to the same new wells, respectively. The plate was subsequently placed in a 37°C incubator for overnight to allow the evaporation of the solvent solution. The dried peptides were reconstituted with 2 µl of saturated matrix containing 5 mg/ml α-cyano-4-hydroxy cinnamic acid (LaserBio Labs, Sophia-Antipolis, France) prepared in 0.5% (v/v) TFA and 50% (v/v) ACN. Following that, the peptide-matrix mixture (0.7 µl) was spotted twice onto the sample slide immediately and then air-dried. The sample slide was analyzed using the 4800 plus MALDI-TOF/TOF analyzer™ (Applied Biosystems, Foster City, CA, USA).

Mass spectrometry/mass spectrometry (MS/MS) analysis was performed using 20 most abundant ions in the peptide mass fingerprinting (PMF) mass spectrum. MS/MS ion search was performed using the MASCOT server (http://www.matrixscience.com) against all entries of the Swiss-Prot protein database. The parameters used were fixed modification of carboxymethylation of cysteine, variable modification of oxidation of methionine, maximum of one missed cleavage per peptide, peptide mass tolerance at 100 ppm, monoisotopic masses and MS/MS fragment tolerance of 0.2 Da. Mowse scores greater than 41 were considered significant ($p<0.05$).

3.7 Hemagglutination activity of HA1/L/AcmA, HA1/AcmA and HA1 recombinant proteins

3.7.1 Guinea pig red blood cells (RBCs) preparation

Functional HA1 activity of the HA1/L/AcmA, HA1/AcmA and HA1 recombinant proteins was assessed in a hemagglutination assay using guinea pig red blood cells

(RBCs). Guinea pig RBCs were prepared following WHO's guideline (WHO, 2011) with minor modifications. Briefly, guinea pig blood was collected into an equal volume of Alserver's solution [2.05% (w/v) dextrose, 0.8% (w/v) sodium citrate dihydrate, 0.42% (w/v) NaCl, 0.055% (w/v) citric acid, pH 6.1±0.1]. The mixture was centrifuged at 259 ×g for 10 min and the supernatant containing buffy layer of white blood cells was removed. The pellet was washed with 50 ml of 0.01 M PBS (pH 7.2) gently by inversion followed by centrifugation at 259 ×g for 5 min. The washing step was repeated twice. The RBCs was resuspended in 12 ml of 0.01 M PBS (pH 7.2) in a 15 ml centrifuge tube and centrifuged at 259 ×g for 10 min. The volume of packed cells was estimated and diluted with 0.01 M PBS (pH 7.2) to appropriate concentration. All procedures involving use of guinea pig blood were reviewed and approved by the FOM-Institutional Animal Care and Use Committee (FOM-IACUC), University of Malaya with ethics reference no. 2014-11-07/MMB/R/JPF.

3.7.2 Hemagglutination assay

Two-fold dilutions of 30 µg purified recombinant protein in 0.01 M PBS (pH 7.2) in volumes of 50 µl were distributed in V-bottomed 96-well microplates (Cooke Engineering Co., Alexandria, VA, USA). Subsequently, each well was added with 50 µl of 0.75% guinea pig RBCs suspension freshly prepared as previously described in Section 3.7.1. Agglutination was read after incubation at room temperature for 60 min.

3.8 Binding analysis of HA1/L/AcmA, HA1/AcmA and HA1 recombinant proteins to *L. lactis*

3.8.1 Binding of recombinant proteins to *L. lactis*

An overnight culture of *L. lactis* MG1363 was subcultured in GM17 broth and incubated at 30ºC until the OD_{600} reading reached 0.5. The *L. lactis* culture (2 ml) was

harvested by centrifugation at 2,000 ×g for 10 min. The cell pellet was resuspended in fresh GM17 broth (0.6 ml). Subsequently, 200 µg/ml refolded recombinant proteins (100 µl) in protein buffer (20 mM NaH_2PO_4, 0.5 M NaCl) were added to the cell suspension, respectively. Protein buffer containing no recombinant protein was used as a control. After incubation at 30ºC for 2 h, the cells were harvested and washed with PBS thrice. The mixtures were centrifuged at 2,000 ×g for 10 min and the cell pellet was eventually resuspended in 200 µl of PBS for subsequent binding analysis using flow cytometry.

3.8.2 Determination of *L. lactis* surface displaying recombinant proteins by flow cytometry analysis

Briefly, 100 µl of *L. lactis* cells pre-mixed with the refolded recombinant proteins and control *L. lactis* cells prepared as previously described in Section 3.8.1 were fixed with 200 µl of 4% (w/v) paraformaldehyde for 20 min. The fixed cells were then washed with PBS thrice and blocked with 200 µl of 3% (w/v) BSA for 30 min. After washing with PBS thrice, the cells were incubated with 200 µl of mouse monoclonal anti-polyhistidine (Sigma-Aldrich, St. Louis, MO, USA) at 1:1,000 dilution for 1 h. Following that, the cells were washed with PBS thrice and incubated with 200 µl of Alexa Fluor® 488 goat anti-mouse IgG (Invitrogen Life Technologies, Carlsbad, CA, USA) at 1:500 dilution in the dark for 1 h. The cells were washed again with PBS thrice and finally suspended in 1 ml of PBS. All washing steps were performed using 1 ml of PBS and the samples were subsequently recovered by centrifugation at 2,000 ×g for 10 min.

The stained cells were examined using a fluorescence-activated cell sorting (FACS) CANTO ™ II Flow cytometer (BD Biosciences, Bedford, MA, USA). The bacterial cells population on scatter was gated based on the forward angle light scatter (FS) and

side angle light scatter (SS) profile. Cell debris was eliminated by setting the FS threshold. A total of 5×10^4 cells falling into the bacterial gate defined on the FS-SS plot were acquired for each sample. The positive cell count and mean fluorescence intensity (MFI) were determined. All samples were acquired using identical instrument settings.

3.8.3 Determination of recombinant proteins bound to *L. lactis* by protein band density analysis

The amount of recombinant proteins surface displayed on *L. lactis* was determined by immunoblotting analysis. Briefly, ~1.5×10^{10} CFU/ml *L. lactis* cells pre-mixed with the refolded recombinant proteins, control *L. lactis* cells and HA1/L/AcmA recombinant protein with previously determined concentrations of 5, 10, 20, 40 and 60 µg/ml were separated in a 12.5% SDS-PAGE gel. The separated proteins on SDS-PAGE were transferred onto nitrocellulose membrane (Millipore, Billerica, MA, USA) and analyzed by immunoblotting as previously described in Section 3.6.4. Subsequently, the Integrated Optical Density (IOD) of each band was quantified using Gel Pro Analyzer 4.0 (Media Cybernetics, Rockville, MD, USA). A standard curve for band IOD was established using the HA1/L/AcmA recombinant protein. The amount of the recombinant proteins surface displayed on *L. lactis* was then determined from the established standard curve.

3.8.4 Structural modeling analysis of recombinant proteins

The structural models of HA1/L/AcmA and HA1/AcmA recombinant proteins were generated using the HHpred server (http://toolkit.tuebingen.mpg.de/hhpred). The crystal structure of influenza A virus HA [A/Brevig Mission/1/1918(H1N1), Protein Data Bank (PDB) ID: 4GXX], the solution structure of the *Enterococcus faecalis* autolysin AtlA LysM peptidoglycan binding domain (AtlA-LysM2, PDB ID: 2MKX)

and the solution structure of *E. coli* MltD LysM (MltD-LysM2, PDB ID: 1E0G) were used as the templates for modeling. The image of the structural models were created using PyMOL 1.3 (Schrödinger, New York, NY, USA).

3.9 Binding optimization and binding stability of HA1/L/AcmA recombinant protein on *L. lactis*

3.9.1 Binding optimization

The binding of HA1/L/AcmA recombinant protein onto *L. lactis* was optimized. Briefly, *L. lactis* displaying HA1/L/AcmA recombinant protein was prepared as previously described in Section 3.8.1. Binding optimizations were performed by varying the binding parameters, specifically the amount of recombinant protein (25, 20, 15, 10 and 5 µg) added to equal number of *L. lactis* cells, the duration of binding (1, 2, 3 and 4 h) and the type of binding buffer (GM17 and PBS). After binding, the *L. lactis* cells pre-mixed with the recombinant protein were analyzed by flow cytometry as previously described in Section 3.8.2.

3.9.2 Binding stability

The binding stability of HA1/L/AcmA recombinant protein on *L. lactis* at 4ºC was examined. Briefly, *L. lactis* surface displaying HA1/L/AcmA recombinant protein was prepared as previously described in Section 3.8.1 using the optimal conditions determined in Section 3.9.1. The samples were stored in PBS at 4ºC. Samples were collected every day for 8 days and analyzed by flow cytometry as previously described in Section 3.8.2. *L. lactis* pre-mixed with protein buffer containing no recombinant protein was similarly prepared to use as a control.

3.10 Immunogenicity studies of *L. lactis* displaying HA1/L/AcmA recombinant protein

3.10.1 Immunogen preparation

L. lactis displaying HA1/L/AcmA was prepared using the optimal conditions determined in Section 3.9.1 and scaled-up by proportionally increasing the amount of recombinant protein and *L. lactis* cells to be used in the binding. The *L. lactis* displaying HA1/L/AcmA recombinant protein was eventually resuspended in endotoxin-free PBS to a concentration of 1×10^{11} CFU/ml and 5×10^{11} CFU/ml for study group A and B, respectively. The constructed non-recombinant *L. lactis* displaying HA1/L/AcmA recombinant protein was named LL-HA1/L/AcmA.

3.10.2 Animals and immunization

Six to eight-weeks-old specific-pathogen-free female BALB/c mice were purchased from InVivos Pte Ltd. (Singapore). Animals were housed in specific-pathogen-free conditions with free access to food and water at the Association for Assessment and Accredidation of Laboratory Animal Care International certified Animal Experimental Unit, Faculty of Medicine, University of Malaya. A total of two study groups were performed to evaluate the immunogenicity of the LL-HA1/L/AcmA. In study group A, mice (n=8) were immunized orally with 0.1 ml of 1×10^{10} CFU of LL-HA1/L/AcmA (25 µg/dosage) or endotoxin-free PBS using intra-gastric lavage for three consecutive days. The immunization regimen was repeated thrice at two weeks intervals. In study group B, mice (n=8) were immunized orally with 0.1 ml of 5×10^{10} CFU of LL-HA1/L/AcmA (125 µg/dosage), HA1/L/AcmA (125 µg/dosage) or endotoxin-free PBS for three consecutive days. The immunization regimen was repeated thrice at two weeks intervals. Simultaneously, mice (n=8) were immunized subcutaneously with HA1/L/AcmA (50 µg/dosage) emulsified with complete Freund's adjuvant (CFA;

Sigma-Aldrich, St. Louis, MO, USA), HA1/L/AcmA-FA, to serve as a positive control. The immunization regimen was repeated thrice at two weeks intervals using incomplete Freund's adjuvant (IFA; Sigma-Aldrich, St. Louis, MO, USA) instead of CFA. The details of the immunogen and immunization regimen are shown in Table 3.4. All procedures involving animals were reviewed and approved by the FOM-IACUC with ethics reference no. 2014-01-07/MMB/R/JPF.

3.10.3 Sample collection

In study group A, blood and faeces were collected two weeks after the last immunization. Thereafter, the mice were sacrificed by intraperitoneal injection of an overdose of ketamine-xylazine (ketamine: 240-360 mg/kg; xylazine: 30-48 mg/kg) and samples such as small intestine, bronchoalveolar lavage (BAL) and nasal fluid were collected. In study group B, only blood and faecal samples were collected.

Briefly, blood sample was collected and sera was obtained by centrifugation at 1,000 ×g for 5 min. Faecal pellet (100 mg) was collected and resuspended in 0.5 ml sterile PBS containing 1 mM phenylmethanesulfonyl fluoride (PMSF). The suspension was vortexed vigorously and the faecal extract was obtained by centrifugation at 10,000 ×g for 5 min. Small intestine was harvested and flushed thrice with 1 ml PBS containing 1 mM PMSF. The sample from small intestine was then obtained following centrifugation at 10,000 ×g for 5 min. BAL (Arulanandam *et al.*, 1999; Saluja *et al.*, 2010) and nasal fluids (Saluja *et al.*, 2010) were collected as previously described with minor modifications. Briefly, mouse trachea was cannulated with an intravenous catheter (BD Bioscience, Bedford, MA, USA) and connected to a 3 ml syringe. BAL fluid was obtained by flushing the lung with 1 ml cold PBS for 5 times. The washing step was repeated once and the lavage fluid recovered from two washings was pooled. Nasal fluid was obtained by flushing the nasopharynx with 1 ml cold PBS for 5 times

Table 3.4: Details of the immunogen and immunization regimen.

Study group	Immunization route	Immunogen	Dose	Immunization regimen (Day)
A	Oral	LL-HA1/L/AcmA	0.1 ml of 1×10^{10} CFU *L. lactis* displaying HA1/L/AcmA (25 µg/dosage)	0, 1, 2, 14, 15, 16, 28, 29, 30, 42, 43 and 44
	Oral	PBS	0.1 ml of endotoxin-free PBS	0, 1, 2, 14, 15, 16, 28, 29, 30, 42, 43 and 44
B	Oral	LL-HA1/L/AcmA	0.1 ml of 5×10^{10} CFU *L. lactis* displaying HA1/L/AcmA (125 µg/dosage)	0, 1, 2, 14, 15, 16, 28, 29, 30, 42, 43 and 44
	Oral	HA1/L/AcmA	0.1 ml of HA1/L/AcmA (125 µg/dosage)	0, 1, 2, 14, 15, 16, 28, 29, 30, 42, 43 and 44
	Oral	PBS	0.1 ml of endotoxin-free PBS	0, 1, 2, 14, 15, 16, 28, 29, 30, 42, 43 and 44
	Subcutaneous	HA1/L/AcmA-FA	0.1 ml of HA1/L/AcmA with CFA/IFA[a,b] (50 µg/dosage)	0, 14, 28 and 42

[a, b] Complete Freund adjuvant (CFA) at priming and incomplete Freund adjuvant (IFA) at the following immunizations.

and the nasal wash fluid was recovered from the mouse nostril. The BAL and nasal fluids were centrifuged at 200 ×g for 5 min and the supernatant samples were collected. All samples were stored at -20°C for subsequent analysis.

3.10.4 Enzyme-linked immunosorbent assay (ELISA)

HA1-specific IgG and IgA antibodies were detected by enzyme-linked immunosorbent assay (ELISA) following the protocol described by Joan *et al.* (2016) with some modifications. Briefly, 96-well microtiter plate (Costar Corporation, Cambridge, MA, USA) was coated with 100 µl of HA1/L/AcmA recombinant protein (1 µg/well) diluted in 50 mM sodium carbonate (15 mM Na_2CO_3, 35 mM $NaHCO_3$, pH 9.6) at 4°C for overnight. The plate was washed with PBS thrice prior to blocking with 200 µl of 3% (w/v) BSA for 1 h. Subsequently, the plate was washed with PBS thrice before incubation with 100 µl of sera or mucosal samples for 1 h. Following washing with PBS thrice, 100 µl of HRP-conjugated goat anti-mouse IgG (Abcam, Cambridge, MA, USA) at 1:10,000 dilution or HRP-conjugated rat anti-mouse IgA (Abcam, Cambridge, MA, USA) at 1:1,000 dilution was added and incubated for 1 h. The plate was washed with PBS thrice prior to the addition of 50 µl of TMB microwell peroxidase substrate system (KPL, Gaithersburg, MD, USA). After incubation for 20 min, 50 µl of TMB stop solution (KPL, Gaithersburg, MD, USA) was added and the absorbance value at 450 nm was measured using a microplate reader (Tecan, Männedorf, Switzerland). The assay was performed with three technical replicates.

3.10.5 Fifty percent mouse lethal dose (MLD_{50}) determination

Six to eight-weeks-old specific-pathogen-free female BALB/c mice (n=5) were fully anesthetized by intraperitoneal injection of ketamine-xylazine (ketamine: 80-120 mg/kg; xylazine: 10-16 mg/kg) and then inoculated intranasally with 50 µl of 10-fold serial

diluted A/TN/1-560/2009-MA2(H1N1) influenza virus in order to determine the fifty percent mouse lethal dose (MLD_{50}). Mice inoculated with only 50 µl of endotoxin-free PBS served as control. Body weight and survival of the mice were monitored daily up to 14 days. Animals that showed weight loss of >20% were humanely sacrificed by intraperitoneal injection of an overdose of ketamine-xylazine (ketamine: 240-360 mg/kg; xylazine: 30-48 mg/kg). The MLD_{50} value was calculated by the Reed-Muench method. All animal studies involving influenza virus were conducted in the animal biosafety level 2 (ABSL2) laboratory at the Animal Experimental Unit, Faculty of Medicine, University of Malaya.

3.10.6 Challenge of vaccinated mice

At 18 days following the last immunization, all mice in study group B were fully anesthetized with ketamine-xylazine as previously described in Section 3.10.5 and intranasally inoculated with 50 µl of 10 MLD_{50} of A/TN/1-560/2009-MA2(H1N1) influenza virus. After inoculation, the body weight and survival rate of the mice were monitored daily up to 14 days. Mice that showed body weight loss of >20% were considered to have reached the experimental end-point and were humanely sacrificed with an overdose of ketamine-xylazine as previously described in Section 3.10.5.

3.11 Statistics

Statistical analysis and graphical representations were performed using GraphPad Prism 5 software (GraphPad Software, La Jolla, CA, USA). Data analysis was performed using Student's t test for the comparison of two groups. The log-rank (Mantel-Cox) test was used for statistical comparison of the survival between groups.

3.12 Summary of work flow for each objective

The work flows for the four objectives are depicted in flow charts presented in Figure 3.4, 3.5, 3.6 and 3.7, respectively.

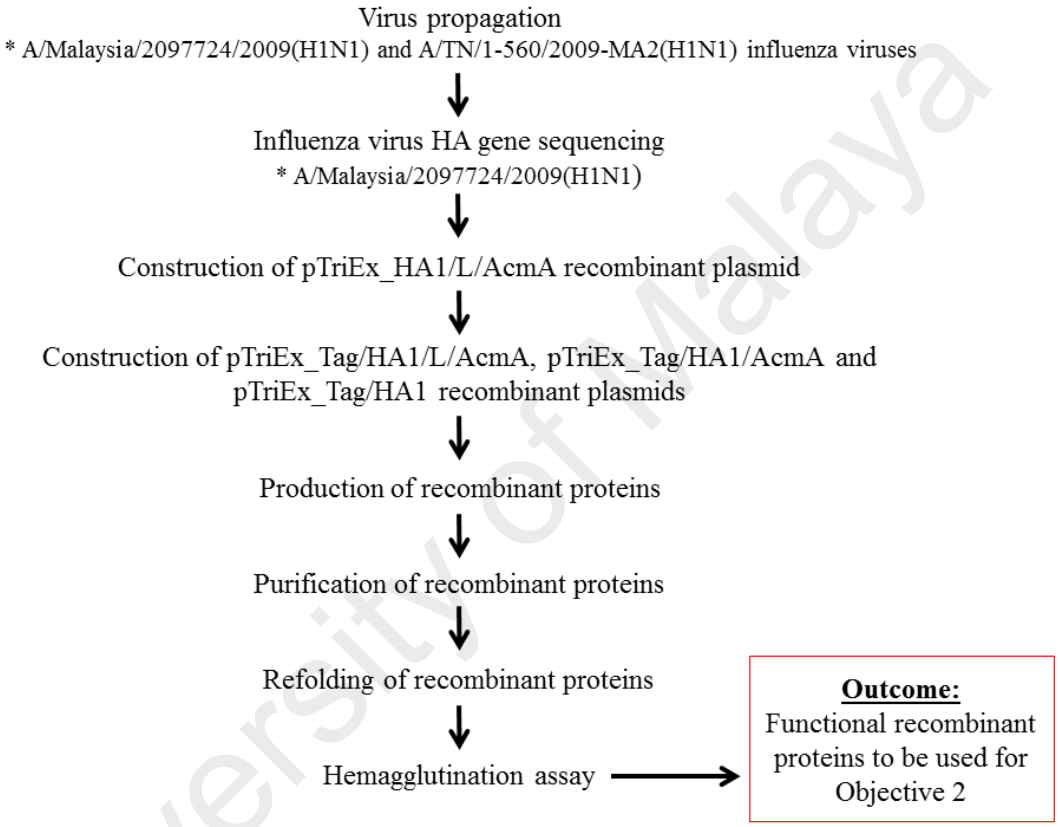

Figure 3.4: Flow chart for Objective 1: Cloning and expression of HA1 in *E. coli*, followed by purification of the produced protein.

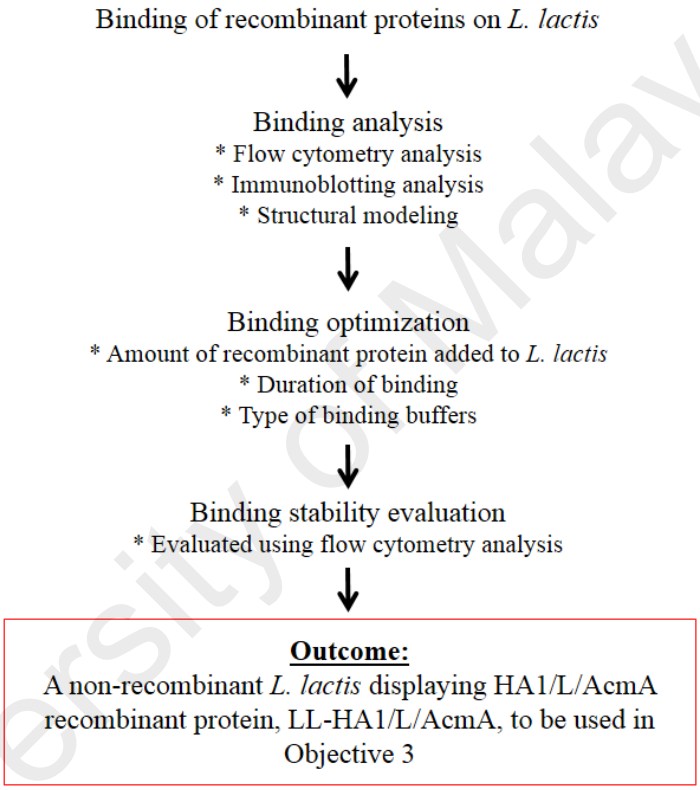

Figure 3.5: Flow chart for Objective 2: Surface display of HA1 on *L. lactis*.

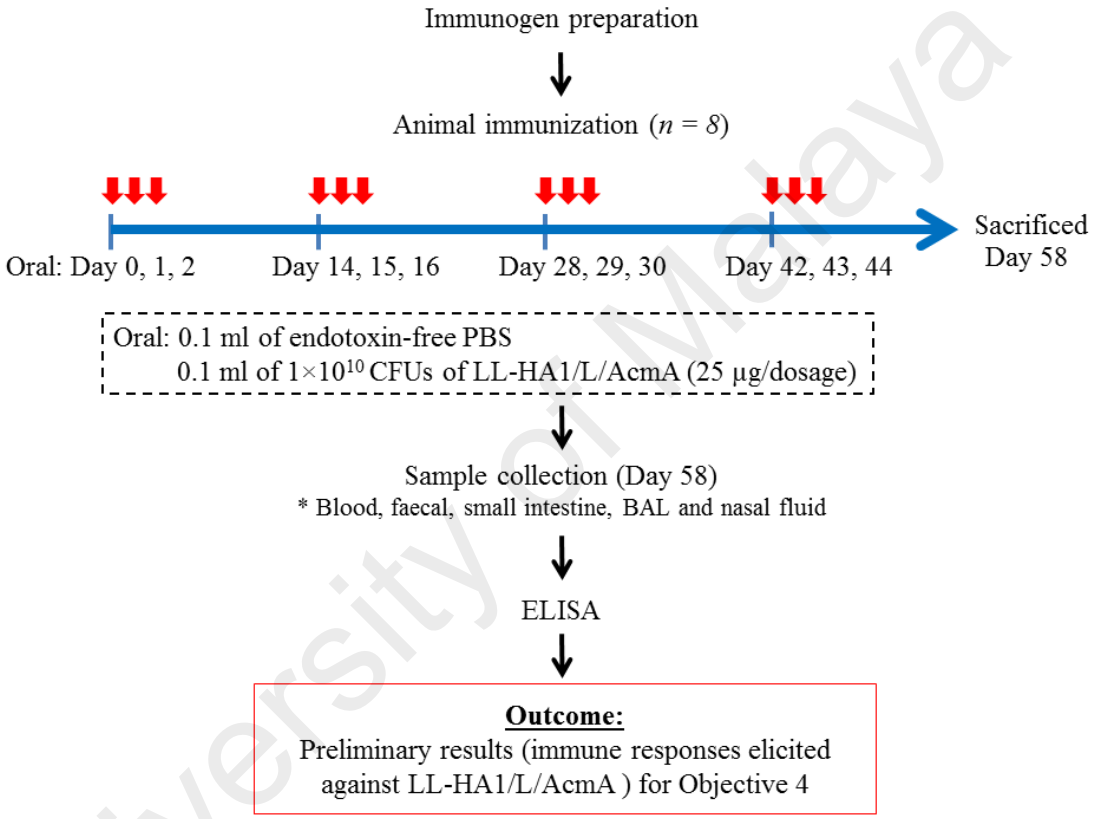

Figure 3.6: Flow chart for Objective 3: Evaluation of immune response towards oral immunization of LL-HA1/L/AcmA in mice.

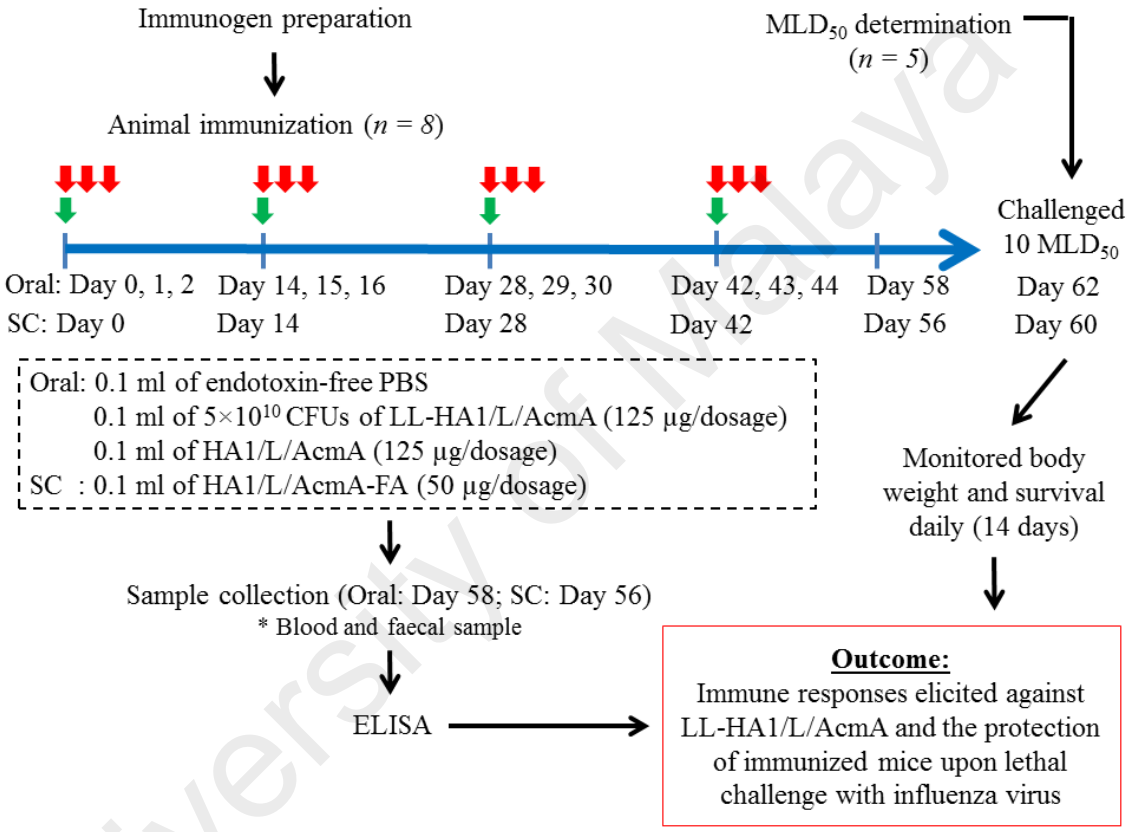

Figure 3.7: Flow chart for objective 4: Evaluation of protective potential of LL-HA1/L/AcmA in immunized mice against lethal challenge with influenza virus.

CHAPTER 4: RESULTS

4.1 Virus propagation

CPE was observed when MDCK cells were inoculated with A/Malaysia/2097724/2009(H1N1) and A/TN/1-560/2009-MA2(H1N1) influenza virus, respectively (Figure 4.1). The infected cells were noted to be rounded and detached from the flask after 48 h of infection. Complete CPE was observed at 72 h p.i. No detectable CPE was observed in the mock-infected cells. The virus titer was determined to be 5.75×10^5 PFU/ml for A/Malaysia/2097724/2009(H1N1) and 1.03×10^6 PFU/ml for A/TN/1-560/2009-MA2(H1N1) influenza virus (Appendix B).

4.2 Influenza virus HA gene sequencing

Six overlapping HA fragments were successfully amplified from the extracted viral RNA of influenza A virus [A/Malaysia/2097724/2009(H1N1)]. The fragments, HAF1, HAF2, HAF3, HAF4, HAF5 and HAF6, were observed as single bands in agarose gel electrophoresis with the expected size of approximately 507 bp, 649 bp, 959 bp, 633 bp, 453 bp and 584 bp, respectively (Figure 4.2). A faint band was observed for the HAF6 fragment in comparison to other fragments possibly due to the non-optimal annealing temperature or specificity of primers used. All amplified fragments were sequenced and the results obtained were successfully assembled into contigs. The assembled HA gene was 1696 nucleotides in length and the sequence was presented in Appendix C. The gene sequence was deposited in the EMBL database under the accession number LN612606.

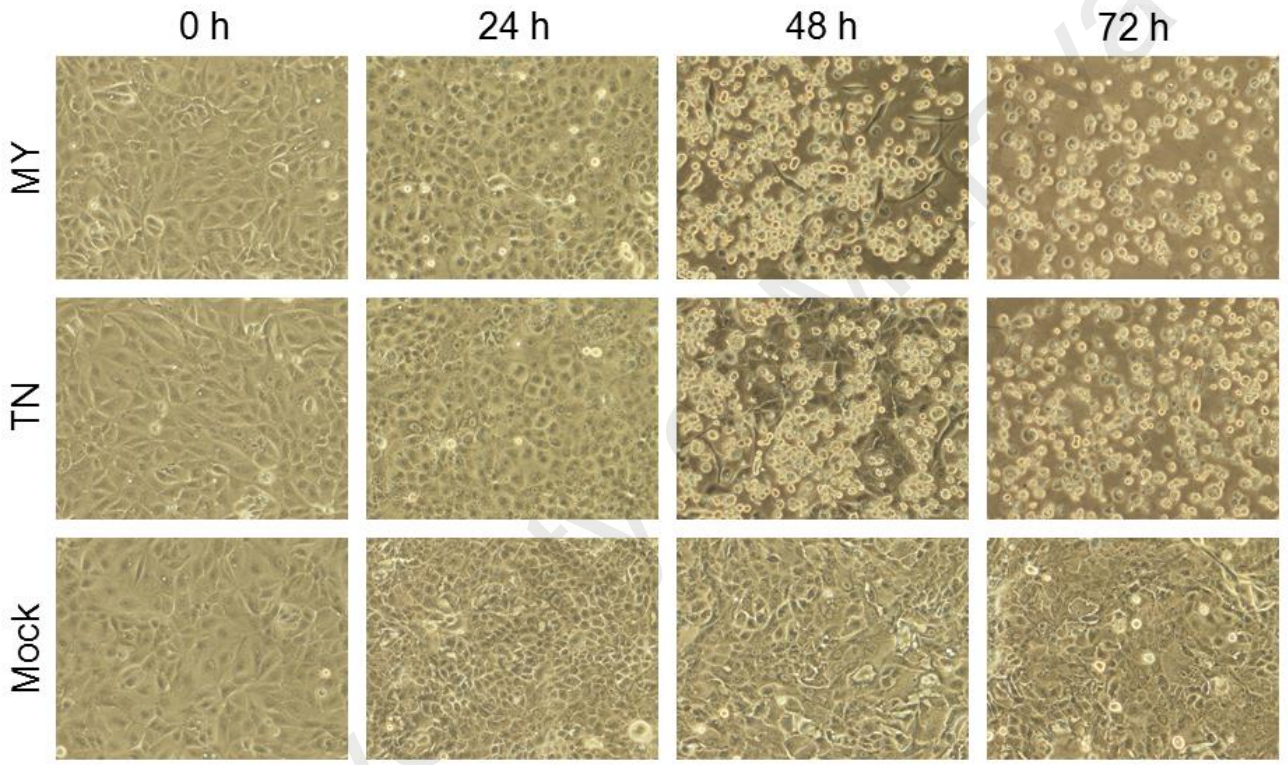

Figure 4.1: Phase contrast images of influenza A virus-infected or mock-infected MDCK cells at 0 h, 24 h, 48 h and 72 h, respectively, observed under an inverted light microscope (200×).

MY and TN represent A/Malaysia/2097724/2009(H1N1) and A/TN/1-560/2009-MA2(H1N1) influenza virus, respectively.

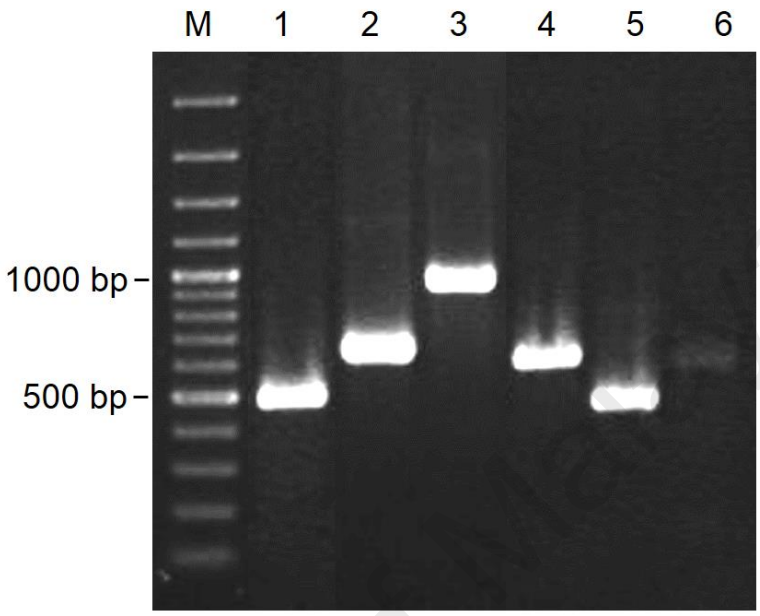

Figure 4.2: Amplification of A/Malaysia/2097724/2009(H1N1) influenza virus HA gene.

Six overlapping HA fragments were amplified using primer sets designed by the WHO Collaborating Centre for influenza at CDC Atlanta (Atlanta, GA, USA). The amplified fragments were gel purified and analyzed on a 1.5% (w/v) agarose gel. The size of the amplified fragments were as expected at 507 bp for HAF1 (lane 1), 649 bp for HAF2 (lane 2), 959 bp for HAF3 (lane 3), 633 bp for HAF4 (lane 4), 453 bp for HAF5 (lane 5) and 584 bp for HAF6 (lane 6). Lane M represents GeneRuler 100 bp DNA Ladder Plus (Thermo Scientific, Waltham, MA, USA).

4.3 Construction of pTriEx_HA1/L/AcmA recombinant plasmid

4.3.1 Cloning of HA1/L/AcmA fusion fragment into pTriEx-3 Hygro vector

The HA1_L fragment (1024 bp), encoding the influenza HA globular head domain (HA1-without transmembrane; 981 bp) was amplified from the extracted A/Malaysia/2097724/2009(H1N1) influenza virus genomic RNA. The AcmA_L fragment (314 bp) was amplified from the plasmid pSVac carrying the most N-terminal AcmA LysM sequence, LysM1, and 43 amino acid spacer (255 bp). The amplified HA1_L and AcmA_L fragments were checked on agarose gel and confirmed to be of the expected sizes (Figures 4.3a and 4.3b). The HA1/L/AcmA fusion fragment was successfully assembled by long PCR amplification using HA1_L and AcmA_L fragments as templates. A single band of DNA fragment was observed on agarose gel and the size of HA1/L/AcmA fusion fragment was corresponded to the expected size of approximately 1308 bp (Figure 4.3c).

The HA1/L/AcmA fusion fragment and the vector, pTriEx-3 Hygro, were then digested using *Pst*I and *Xho*I restriction enzymes. Two single bands on agarose gel which correlated with the expected size of approximately 1287 bp and 6645 bp for the digested HA1/L/AcmA fusion fragment and pTriEx-3 Hygro, respectively, were observed (Figure 4.4). The HA1/L/AcmA fusion fragment was cloned into the pTriEx-3 Hygro vector as a *Pst*I-*Xho*I fragment and transformed into *E. coli* NovaBlue. This recombinant plasmid obtained was named pTriEx_HA1/L/AcmA.

4.3.2 Screening and verification of positive transformants carrying pTriEx_HA1/L/AcmA recombinant plasmid

After transformation, ten putative transformants were picked and subjected to colony PCR to determine the presence of the insert in the recombinant plasmid. Single band corresponded to the predicted fragment size of 1308 bp was observed for all

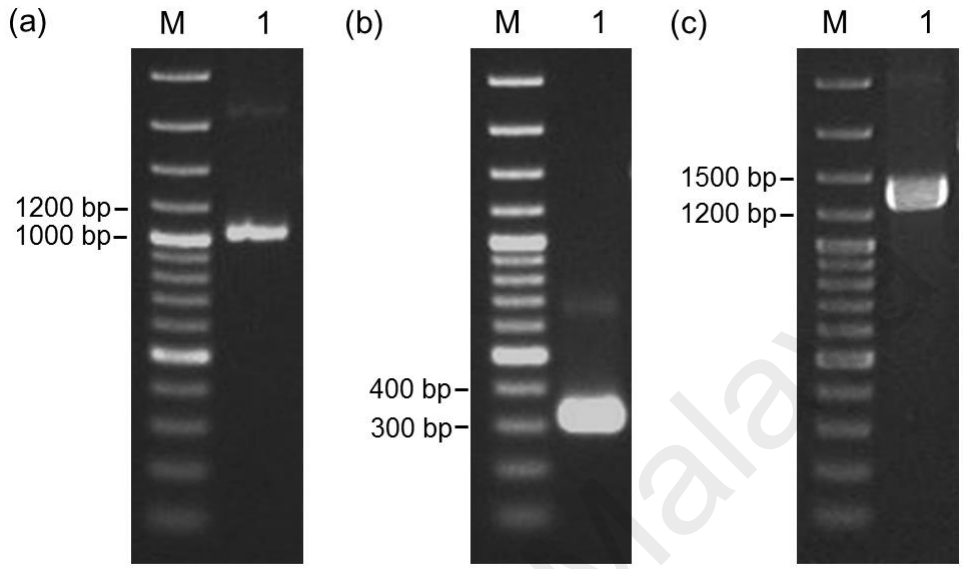

Figure 4.3: Amplification of HA1_L, AcmA_L and HA1/L/AcmA fragments.

(a) HA1_L and (b) AcmA_L were amplified from extracted A/Malaysia/2097724/2009(H1N1) influenza genomic RNA and plasmid pSVac carrying the AcmA sequence, respectively. (c) HA1/L/AcmA fragment was obtained by long PCR amplification using HA1_L and AcmA_L fragments as the template. The amplification products were gel purified and analyzed on a 1.5% (w/v) agarose gel. The sizes of the amplification fragments were as expected at 1024 bp for HA1_L, 314 bp for AcmA_L and 1308 bp for HA1/L/AcmA. Lane M represents GeneRuler 100 bp DNA Ladder Plus (Thermo Scientific, Waltham, MA, USA).

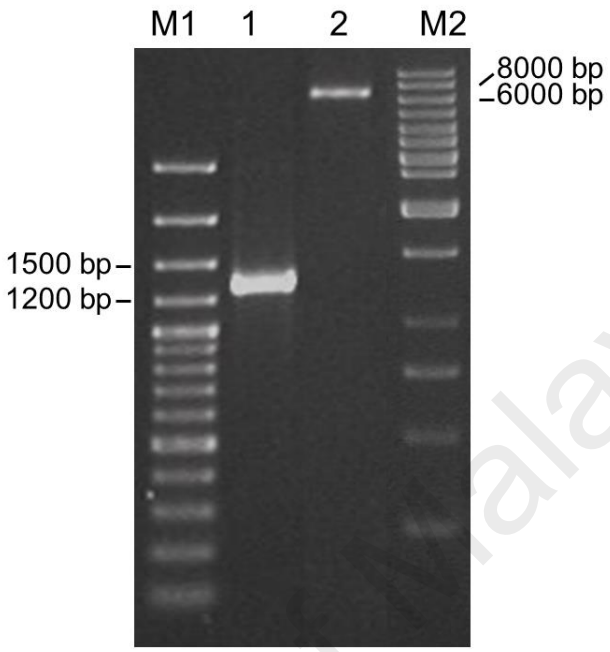

Figure 4.4: RE digestion of HA1/L/AcmA fragment and pTriEx-3 Hygro using *Pst*I and *Xho*I restriction enzymes.

The RE-digested HA1/L/AcmA fragment and pTriEx-3 Hygro were gel purified and analyzed on a 1.5% (w/v) agarose gel. The RE-digested fragments were as expected at 1287 bp for HA1/L/AcmA fragment (lane 1) and 6645 bp for pTriEx-3 Hygro (lane 2) in size. Lanes M1 and M2 represent GeneRuler 100 bp DNA Ladder Plus (Thermo Scientific, Waltham, MA, USA) and GeneRuler 1 kb DNA ladder (Thermo Scientific, Waltham, MA, USA), respectively.

recombinant clones (Figure 4.5), thus, confirming successful transformation.

4.3.3 Nucleotide sequencing of pTriEx_HA1/L/AcmA recombinant plasmid

The recombinant plasmids with the inserted HA1/L/AcmA fusion fragment were extracted from the positive transformants and sequenced to determine the nucleotide sequence and the open reading frame. Nucleotide sequencing results showed that there were two nucleotide changes in the HA1 gene when compared to the previously sequenced A/Malaysia/2097724/2009(H1N1) influenza virus HA gene (Figure 4.6a). These nucleotide changes were noted at position 348 and 858. Nonetheless, these changes occurred within wobble position of a codon and did not result in any amino acid substitution (Figure 4.6b). Therefore, the recombinant construct pTriEx_HA1/L/AcmA was used in the subsequent amplifications. The nucleotide and amino acid sequence of the HA1/L/AcmA fusion fragment in pTriEx_HA1/L/AcmA recombinant plasmid was presented in Appendix D.

4.4 Construction of pTriEx_Tag/HA1/L/AcmA, pTriEx_Tag/HA1/AcmA and pTriEx_Tag/HA1 recombinant plasmids

4.4.1 Cloning of HA1/L/AcmA_Δ, HA1/AcmA and HA1 fragments into pTriEx-3 Hygro vector

For the construction of pTriEx_Tag/HA1/L/AcmA, HA1/L/AcmA_Δ fusion fragment was amplified from pTriEx_HA1/L/AcmA. The gel purified HA1/L/AcmA_Δ fusion fragment validated in agarose gel was of the expected size of 1355 bp (Figure 4.7). For the construction of pTriEx_Tag/HA1/AcmA, HA1_ΔL and AcmA_ΔL fragments were amplified from pTriEx_HA1/L/AcmA. The gel purified HA1_ΔL and AcmA_ΔL fragments were of the expected size of 1043 bp and 302 bp, respectively (Figure 4.8a). The HA1_ΔL and AcmA_ΔL fragments were assembled together using

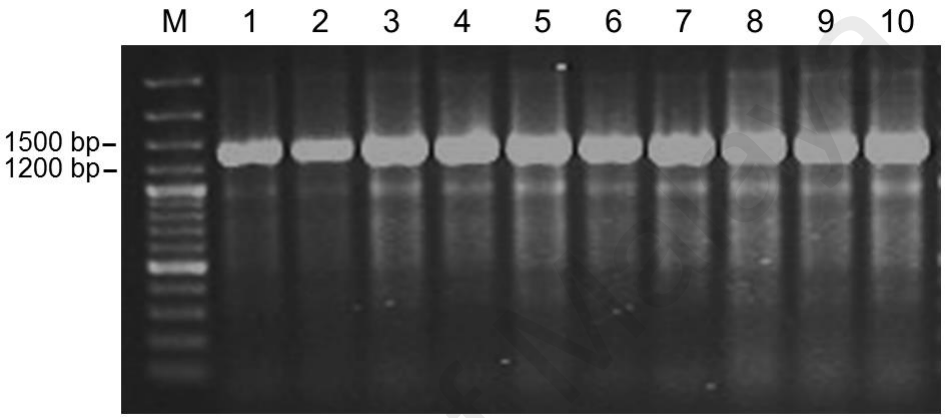

Figure 4.5: Screening of positive transformants by colony PCR to select for recombinant pTriEx-3 Hygro plasmids with the inserted HA1/L/AcmA gene fragment.

Amplification of cloned HA1/L/AcmA gene was performed using gene-specific primer pair. The amplification products (lanes 1-10) analyzed on a 1.5% (w/v) agarose gel were as expected at 1308 bp in size. Lane M represents GeneRuler 100 bp DNA Ladder Plus (Thermo Scientific, Waltham, MA, USA).

(a)

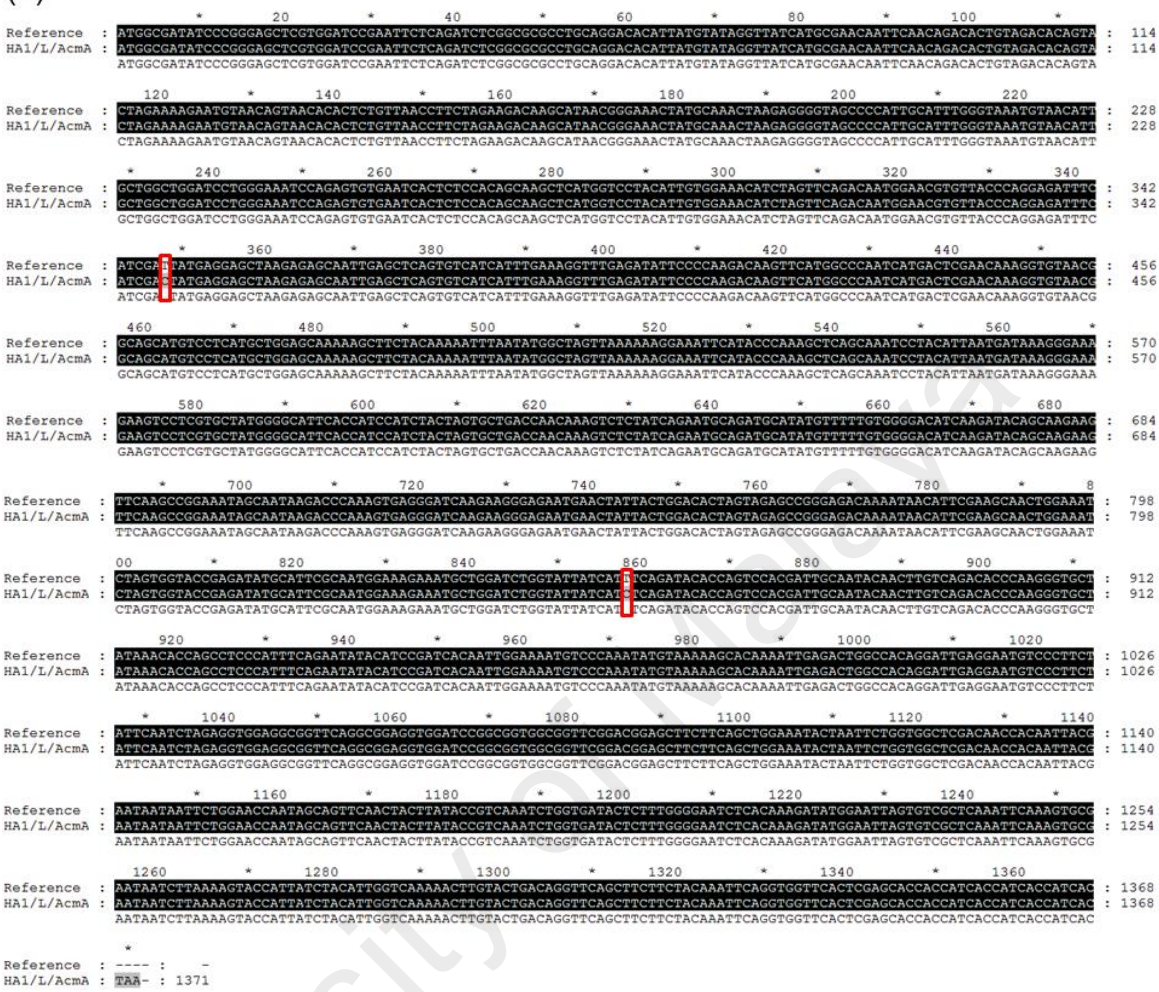

Figure 4.6: Analysis of the assembled nucleotide sequence and deduced amino acid sequence of the HA1/L/AcmA fusion fragment.

The HA1/L/AcmA represented the sequence obtained from the sequencing of pTriEx_HA1/L/AcmA recombinant plasmid. The reference sequence consisted of the HA1 (accession number: LN612606.1), the scFv peptide linker and the AcmA (accession number: U17696.1) gene sequences. In the (a) nucleotide sequence and (b) deduced amino acid alignment, the nucleotides and amino acids are shaded for similarity, while the nucleotide changes are unshaded.

(b)

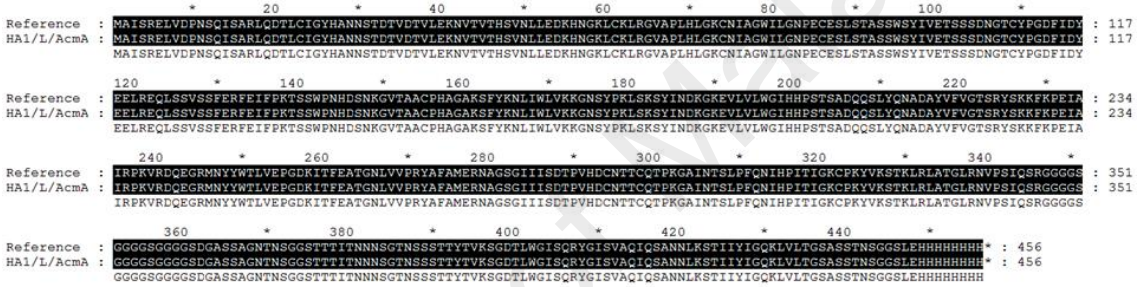

Figure 4.6: Continued.

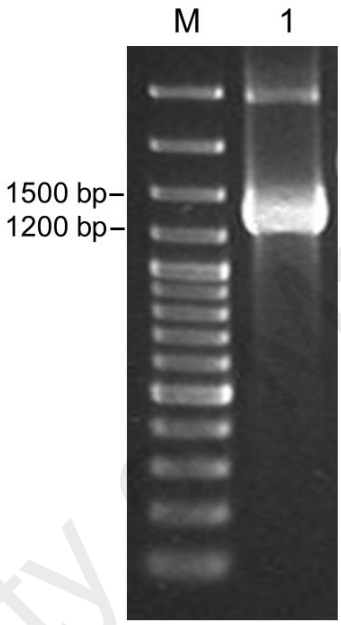

Figure 4.7: Amplification of HA1/L/AcmA_Δ fusion fragment.

HA1/L/AcmA_Δ fusion fragment was amplified from pTriEx_HA1/L/AcmA. The amplification product was gel purified and analyzed on a 1.5% (w/v) agarose gel. The size of the amplified fragment was as expected at 1355 bp. Lane M represents GeneRuler 100 bp DNA Ladder Plus (Thermo Scientific, Waltham, MA, USA).

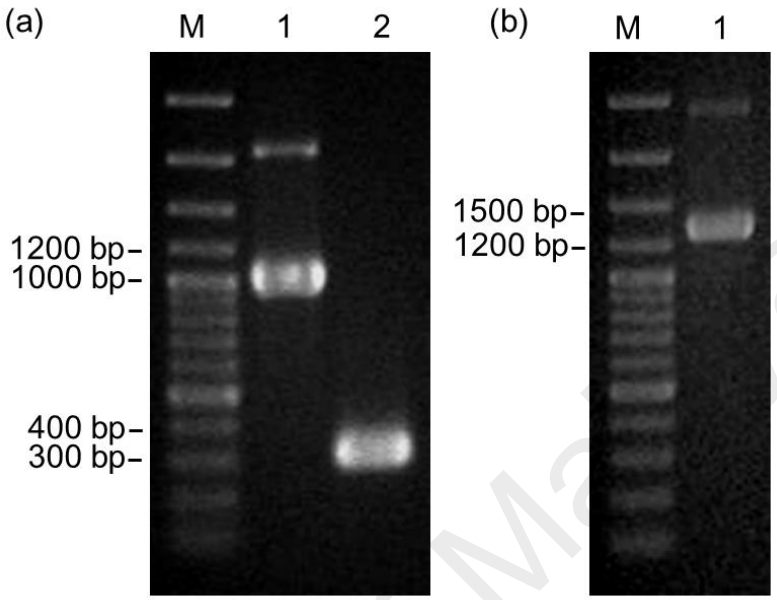

Figure 4.8: Amplification of HA1_ΔL and AcmA_ΔL and HA1/AcmA fragments.

HA1_ΔL (panel a, lane 1) and AcmA_ΔL (panel a, lane 2) fragments were amplified from pTriEx_HA1/L/AcmA. HA1/AcmA (panel b, lane 1) fusion fragment was amplified by long PCR amplification using HA1_ΔL and AcmA_ΔL as template. The amplification products were gel purified and analyzed on a 1.5% (w/v) agarose gel. The gel purified HA1_ΔL (1043 bp), AcmA_ΔL (302 bp) and HA1/AcmA (1310 bp) fragments were of the expected size. Lane M represents GeneRuler 100 bp DNA Ladder Plus (Thermo Scientific, Waltham, MA, USA).

long PCR amplification to generate HA1/AcmA fusion fragment with 1310 bp in size (Figure 4.8b). For pTriEx_Tag/HA1, HA1_ΔLA fragment was amplified from pTriEx_HA1/L/AcmA and a fragment which was as expected at 1051 bp was generated (Figure 4.9). A 6× His-tag (HHHHHH) and a FLAG tag (DYKDDDDK) sequence were introduced upstream of the HA1/L/AcmA_Δ, HA1/AcmA and HA1_ΔLA fragments during PCR amplification as an alternative to downstream of the fragments. The rationale for this design was to avoid any sequence located at the downstream end of the AcmA LysM sequence, which could possibly interfere the binding of the translated recombinant protein on *L. lactis*. The introduction of these sequences was to facilitate the purification of the recombinant proteins. In addition, sequence encoding two stop codons, TAATAA, were successfully inserted immediately downstream of the fragments to assure translation termination. After RE digestion, four single bands were observed in agarose gel for *Pst*I-*Xho*I digested HA1/L/AcmA_Δ (1335 bp), HA1/AcmA (1290 bp), HA1_ΔLA (1035 bp) and pTriEx-3 Hygro (6645 bp), respectively (Figure 4.10). The respective band size corresponded to the expected size, suggesting that all samples were RE digested. The digested HA1/L/AcmA_Δ, HA1/AcmA and HA1_ΔLA fragments were ligated into pTriEx-3 Hygro and transformed into *E. coli* NovaBlue. The recombinant plasmids were named pTriEx_Tag/HA1/L/AcmA, pTriEx_Tag/HA1/AcmA and pTriEx_Tag/HA1, respectively.

4.4.2 Screening and verification of positive transformants carrying pTriEx_Tag/HA1/L/AcmA, pTriEx_Tag/HA1/AcmA and pTriEx_Tag/HA1 recombinant plasmids

Ten putative transformants were picked and subjected to colony PCR to determine the presence of the insert in the recombinant plasmid. Single bands which corresponded to the predicted fragment size of 1355 bp for HA1/L/AcmA_Δ (Figure 4.11a), 1310 bp

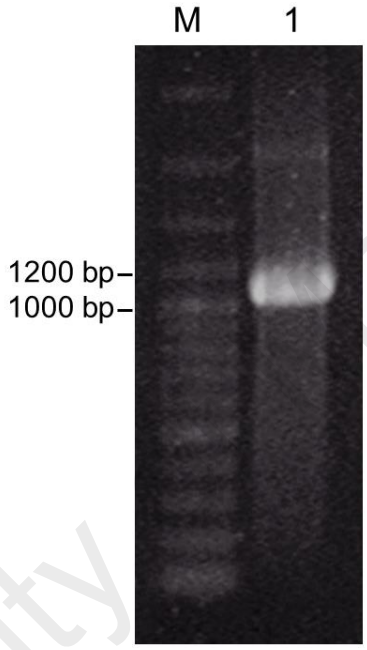

Figure 4.9: Amplification of HA1_ΔLA fragment.

The HA1_ΔLA fragment was amplified from pTriEx_HA1/L/AcmA. The amplification product was gel purified and analyzed on a 1.5% (w/v) agarose gel. The size of the amplified fragment was as expected at 1051 bp. Lane M represents GeneRuler 100 bp DNA Ladder Plus (Thermo Scientific, Waltham, MA, USA).

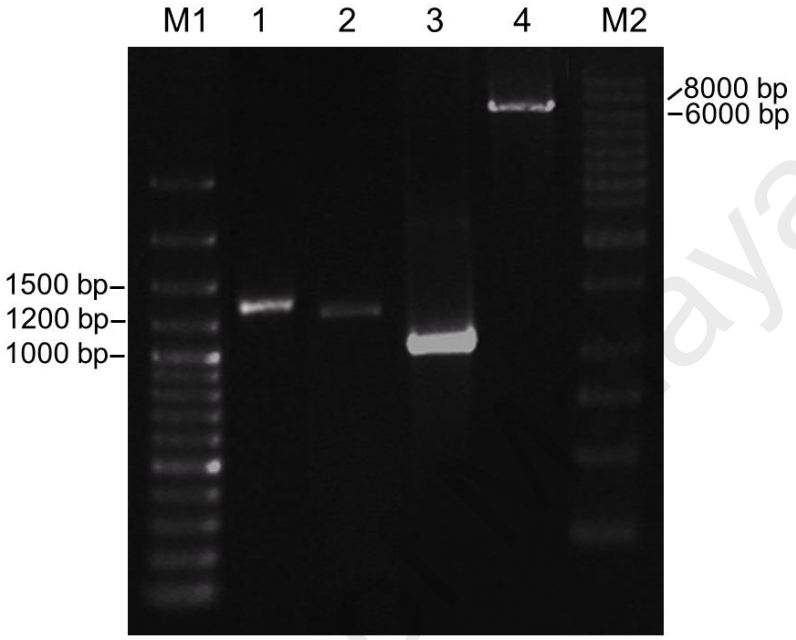

Figure 4.10: RE digestion of HA1/L/AcmA_Δ, HA1/AcmA, HA1_ΔLA and pTriEx-3 Hygro using *Pst*I and *Xho*I restriction enzymes.

The *Pst*I-*Xho*I digested products were gel purified and analyzed on a 1.5% (w/v) agarose gel. The RE-digested fragments were as expected at 1335 bp for HA1/L/AcmA_Δ (lane 1), 1290 bp for HA1/AcmA (lane 2), 1035 bp for HA1_ΔLA (lane 3) and 6645 bp for pTriEx-3 Hygro (lane 4) in size. Lane M1 and M2 represent GeneRuler 100 bp DNA Ladder Plus (Thermo Scientific, Waltham, MA, USA) and GeneRuler 1 kb DNA ladder (Thermo Scientific, Waltham, MA, USA), respectively.

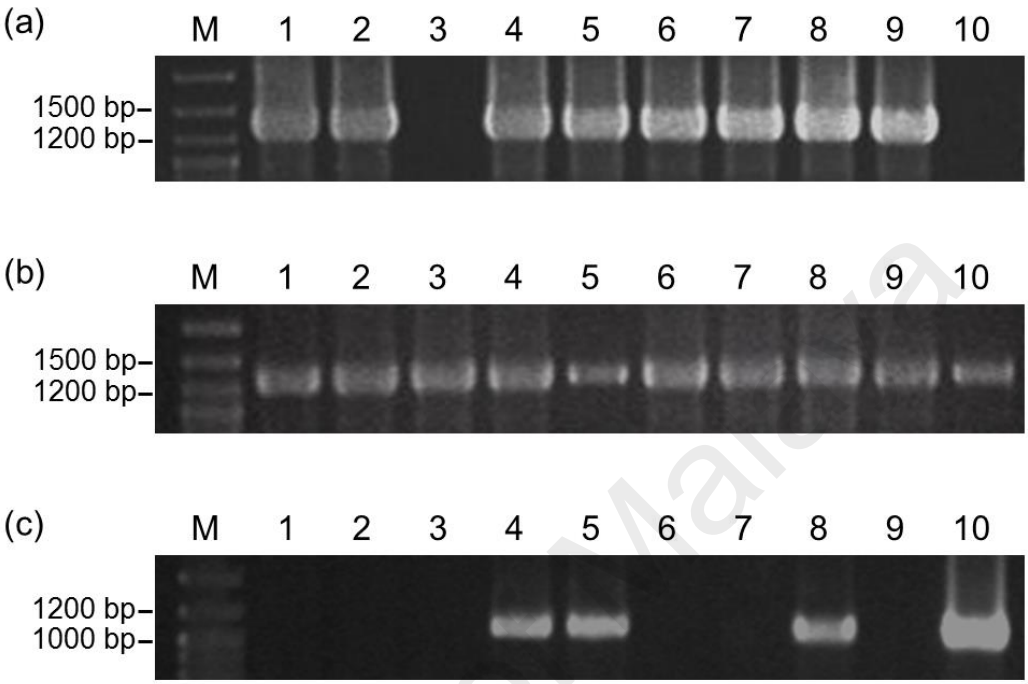

Figure 4.11: Screening of *E. coli* NovaBlue positive transformants by colony PCR to select for recombinant pTriEx-3 Hygro plasmids with the inserted HA1/L/AcmA_Δ, HA1/AcmA and HA1_ΔLA, respectively.

Amplification of cloned (a) HA1/L/AcmA_Δ, (b) HA1/AcmA and (c) HA1_ΔLA genes was performed using gene-specific primer pair and analyzed on a 1.5% (w/v) agarose gel. The expected size of each fragment was 1355 bp for HA1/L/AcmA_Δ, 1310 bp for HA1/AcmA and 1051 bp for HA1_ΔLA. Lane M represents GeneRuler 100 bp DNA Ladder Plus (Thermo Scientific, Waltham, MA, USA).

for HA1/AcmA (Figure 4.11b) and 1051 bp for HA1_ΔLA (Figure 4.11c) were observed in some putative clones and were therefore identified as positive transformants. Results showed that 8, 10 and 4 out of 10 putative transformants carried recombinant pTriEx-3 Hygro plasmids with the inserted HA1/L/AcmA_Δ, HA1/AcmA and HA1, respectively.

4.4.3 Nucleotide sequencing of pTriEx_Tag/HA1/L/AcmA, pTriEx_Tag/HA1/AcmA and pTriEx_Tag/HA1 recombinant plasmids

The pTriEx_Tag/HA1/L/AcmA, pTriEx_Tag/HA1/AcmA and pTriEx_Tag/HA1 recombinant plasmids from the positive transformants were extracted and subjected to nucleotide sequencing to confirm the inserts were in correct sequence and reading frame. Results from nucleotide sequencing showed that there were no nucleotide changes occurred in the gene compared to the initial HA1 and AcmA gene in pTriEx_HA1/L/AcmA, confirming the successful modification of the recombinant fragments. The translated encoded amino acid sequences were also in correct reading frame. The nucleotide and amino acid sequences of HA1/L/AcmA_Δ, HA1/AcmA and HA1 in the pTriEx_Tag/HA1/L/AcmA, pTriEx_Tag/HA1/AcmA and pTriEx_Tag/HA1 recombinant plasmids, respectively, were presented in Appendix D.

4.5 Production, purification and refolding of HA1/L/AcmA, HA1/AcmA and HA1 recombinant proteins

4.5.1 Transformation into *E. coli* RosettaBlue (DE3) pLacI

The pTriEx_Tag/HA1/L/AcmA, pTriEx_Tag/HA1/AcmA, and pTriEx_Tag/HA1 recombinant plasmids were extracted from positive *E. coli* NovaBlue transformants and transformed into *E. coli* RosettaBlue (DE3) pLacI for protein production. Single bands which corresponded to the predicted fragment size of HA1/L/AcmA_Δ (1355 bp),

HA1/AcmA (1310 bp) and HA1 (1051 bp) were observed after colony PCR amplification, suggesting successful transformation (Figure 4.12). There were 9, 10 and 10 out of 10 putative transformants carried recombinant pTriEx-3 Hygro plasmids with the inserted HA1/L/AcmA_Δ, HA1/AcmA and HA1, respectively. In addition, results from nucleotide sequencing showed that there were no nucleotide changes in the gene compared to the initial HA1 and AcmA gene in pTriEx_HA1/L/AcmA and the translated encoded amino acid sequences were in correct order and in-frame.

4.5.2 Properties of the recombinant proteins

The properties of HA1/L/AcmA, HA1/AcmA and HA1 recombinant proteins predicted using ExPASy ProtParam tool are summarized in Table 4.1. HA1/L/AcmA, HA1/AcmA and HA1 recombinant proteins have predicted molecular masses of approximately 50, 49 and 40 kDa, respectively. HA1/L/AcmA and HA1/AcmA recombinant proteins have the same theoretical pI value of 8.56, while HA1 recombinant protein has a lower theoretical pI value of 8.26. The instability index for HA1/L/AcmA, HA1/AcmA and HA1 recombinant proteins were determined to be 28.60, 26.92 and 30.93, respectively, indicating all the recombinant proteins were stable in a test tube.

4.5.3 Protein production and purification

The HA1/L/AcmA, HA1/AcmA and HA1 recombinant proteins were produced upon induction with IPTG. HA1/L/AcmA (Figure 4.13a), HA1/AcmA (Figure 4.13b) and HA1 (Figure 4.13c) recombinant proteins were observed as distinctive protein bands with molecular masses of approximately 50, 49 and 40 kDa, respectively, on SDS-PAGE. The observed protein bands corresponded to the predicted mass values of the recombinant proteins, respectively. All the recombinant proteins reacted to the AP-

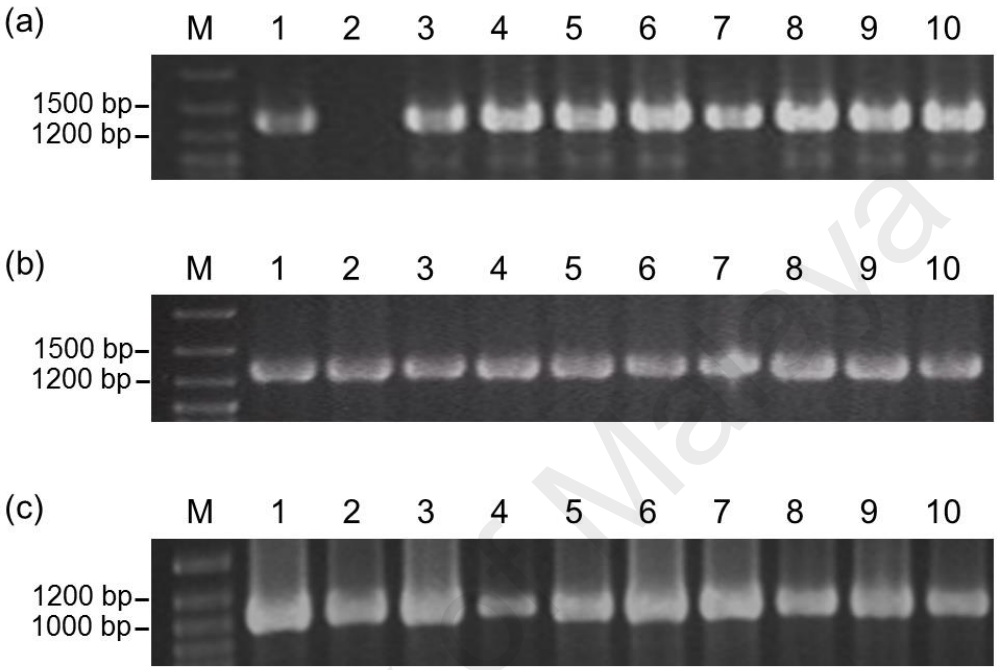

Figure 4.12: Screening of *E. coli* RosettaBlue (DE3) pLacI positive transformants by colony PCR to select for recombinant pTriEx-3 Hygro plasmids with the inserted HA1/L/AcmA_Δ, HA1/AcmA and HA1_ΔLA, respectively.

Amplification of cloned (a) HA1/L/AcmA_Δ, (b) HA1/AcmA and (c) HA1_ΔLA genes was performed using gene-specific primer pair and analyzed on a 1.5% (w/v) agarose gel. The expected size of each fragment was 1355 bp for HA1/L/AcmA_Δ, 1310 bp for HA1/AcmA and 1051 bp for HA1_ΔLA. Lane M represents GeneRuler 100 bp DNA Ladder Plus (Thermo Scientific, Waltham, MA, USA).

Table 4.1: Properties of the HA1/L/AcmA, HA1/AcmA and HA1 recombinant proteins.

Recombinant protein	Number of amino acid	Molecular mass (kDa)	Theoretical pI value	Instability index[a]
HA1/L/AcmA	460	50	8.56	28.60
HA1/AcmA	445	49	8.56	26.92
HA1	360	40	8.26	30.93

[a] Instability index <40 was predicted as stable and >40 was predicted as unstable.

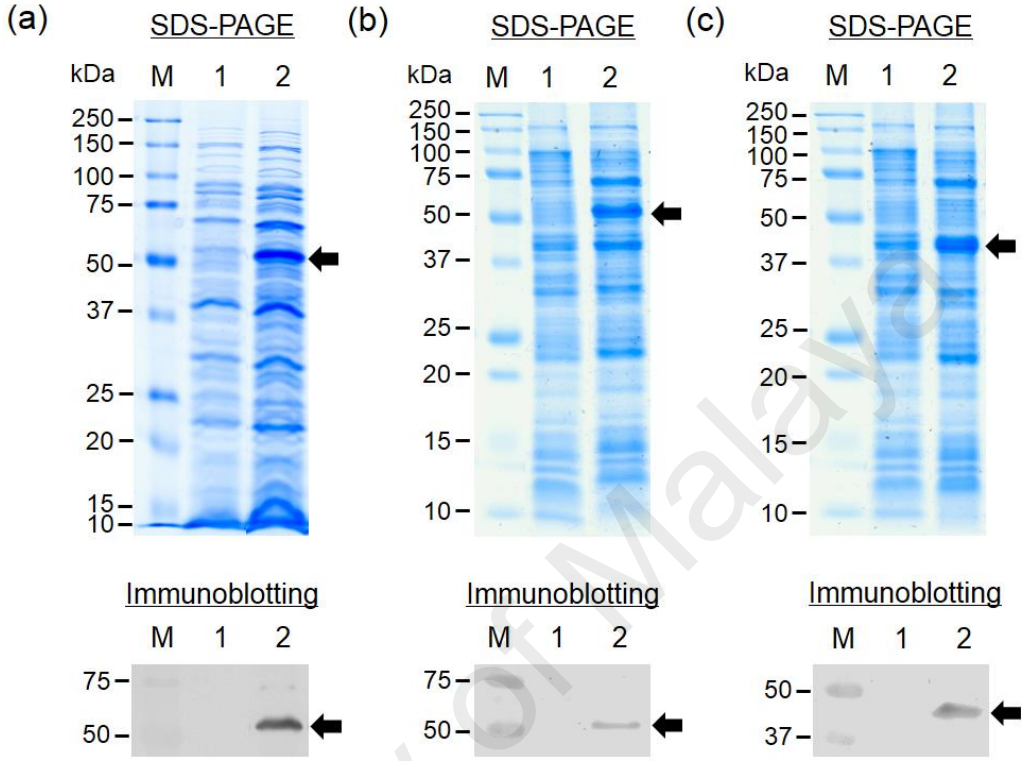

Figure 4.13: Production of HA1/L/AcmA, HA1/AcmA and HA1 recombinant proteins.

(a) HA1/L/AcmA, (b) HA1/AcmA and (c) HA1 recombinant proteins were produced for 4 h upon induction with IPTG. The uninduced (lane 1) and induced (lane 2) bacterial cells were analyzed using 12.5% SDS-PAGE and immunoblotting. The SDS-PAGE gels were stained with Colloidal Coomassie solution, while AP-conjugated HisDetector Nickel was used for detection in immunoblotting. Lane M represents Precision Plus Protein™ All Blue Standards (Bio-Rad Laboratories, Hercules, CA, USA). Arrows indicate the position of the produced recombinant proteins.

conjugated HisDetector Nickel when analyzed by immunoblotting, suggesting the successful cloning and production, as the recombinant proteins have a His-tag at the N-terminus. There were no production of HA1/L/AcmA, HA1/AcmA and HA1 recombinant proteins noted in the uninduced cells.

HA1/L/AcmA, HA1/AcmA and HA1 recombinant proteins were extracted from the induced bacterial cell cultures to determine the solubility of the recombinant proteins. The supernatant and pellet fractions which corresponded to the soluble and insoluble proteins, respectively, were analyzed by 12.5% SDS-PAGE and immunoblotting. The recombinant proteins were found to be present in both the supernatant and pellet fractions (Figure 4.14). Nonetheless, the recombinant proteins were present mainly in the pellet fractions, suggesting that most of the recombinant proteins were insoluble and were produced as inclusion bodies. Considering majority of the recombinant proteins were present in inclusion bodies, therefore the pellet fractions containing inclusion bodies instead of the supernatant fractions were selected for subsequent used.

HA1/L/AcmA, HA1/AcmA and HA1 recombinant proteins were purified from urea-solubilized inclusion bodies using the Akta™ Purifier system. All three recombinant proteins were engineered with a His-tag and therefore, were purified using the HisTrap HP column 1 ml. The affinity chromatography profiles were as shown in Figure 4.15. A single elution peak was observed for all three recombinant proteins. The elution fractions which contained HA1/L/AcmA (Figure 4.16a), HA1/AcmA (Figure 4.16b) and HA1 (Figure 4.16c) recombinant proteins were determined to be in B2-C13 fractions from SDS-PAGE analysis. These fractions were pooled accordingly for subsequent refolding of the respective proteins.

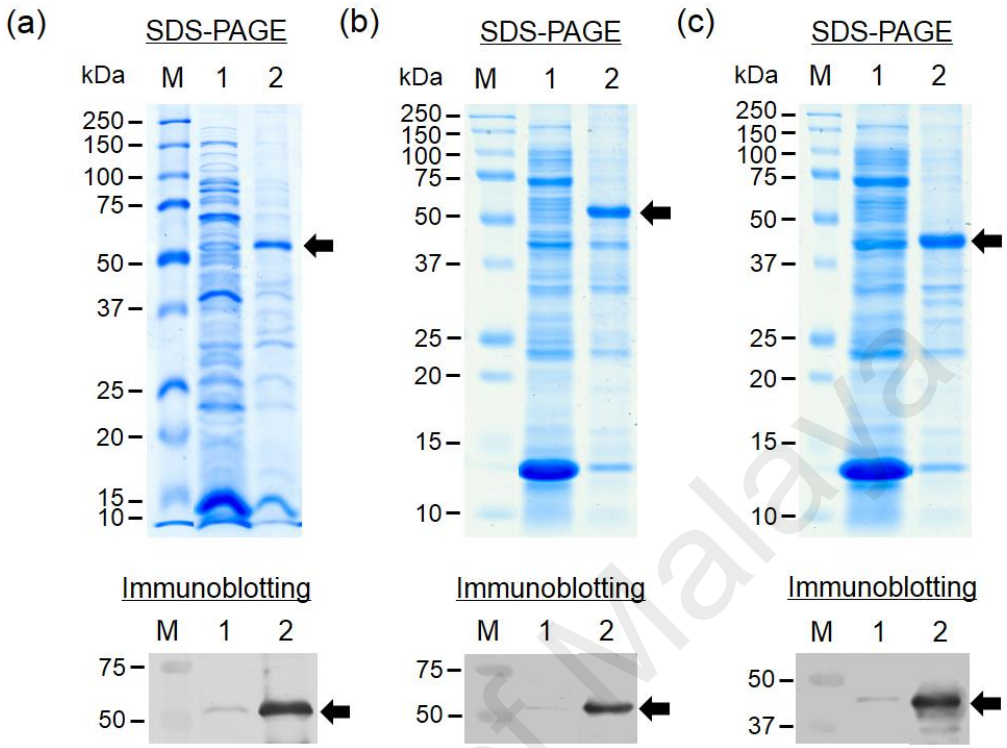

Figure 4.14: Extraction of HA1/L/AcmA, HA1/AcmA and HA1 recombinant proteins.

(a) HA1/L/AcmA, (b) HA1/AcmA and (c) HA1 recombinant proteins were extracted from the induced bacteria cells culture. The supernatant (lane 1) and pellet (lane 2) fractions which corresponded to the soluble and insoluble proteins, respectively, were analyzed in 12.5% SDS-PAGE and immunoblotting analysis. In SDS-PAGE, gels were stained with Colloidal Coomassie solution. In immunoblotting, the membranes were incubated with AP-conjugated HisDetector Nickel for detection. Lane M represents Precision Plus Protein™ All Blue Standards (Bio-Rad Laboratories, Hercules, CA, USA). Arrows indicate the position of the produced recombinant proteins.

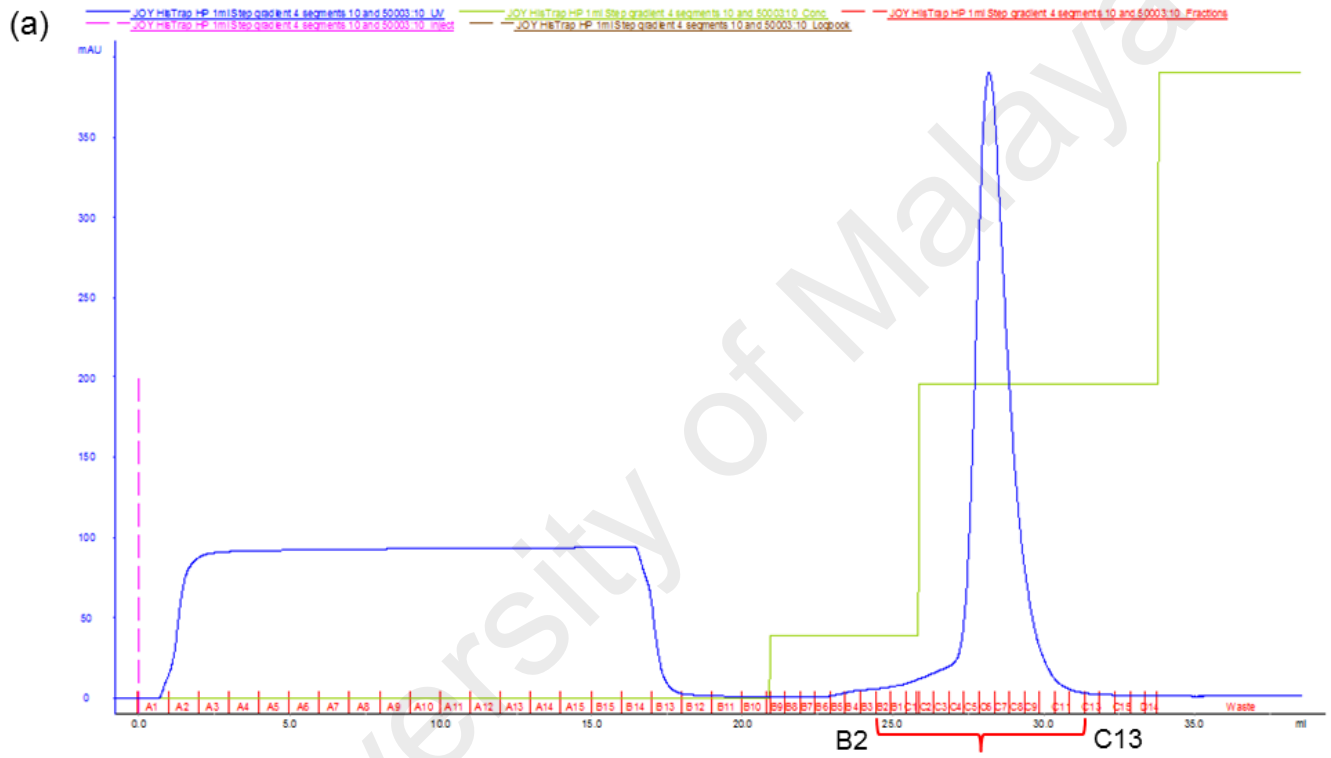

Figure 4.15: The affinity chromatography profile of the HA1/L/AcmA, HA1/AcmA and HA1 recombinant proteins.

The (a) HA1/L/AcmA, (b) HA1/AcmA and (c) HA1 recombinant proteins were purified using Akta™ Purifier system. The recombinant proteins were eluted with step gradients using 10% and 50% Buffer B (green line). A single elution peak detected at UV wavelength of 280 nm (blue line) was observed for all three recombinant proteins.

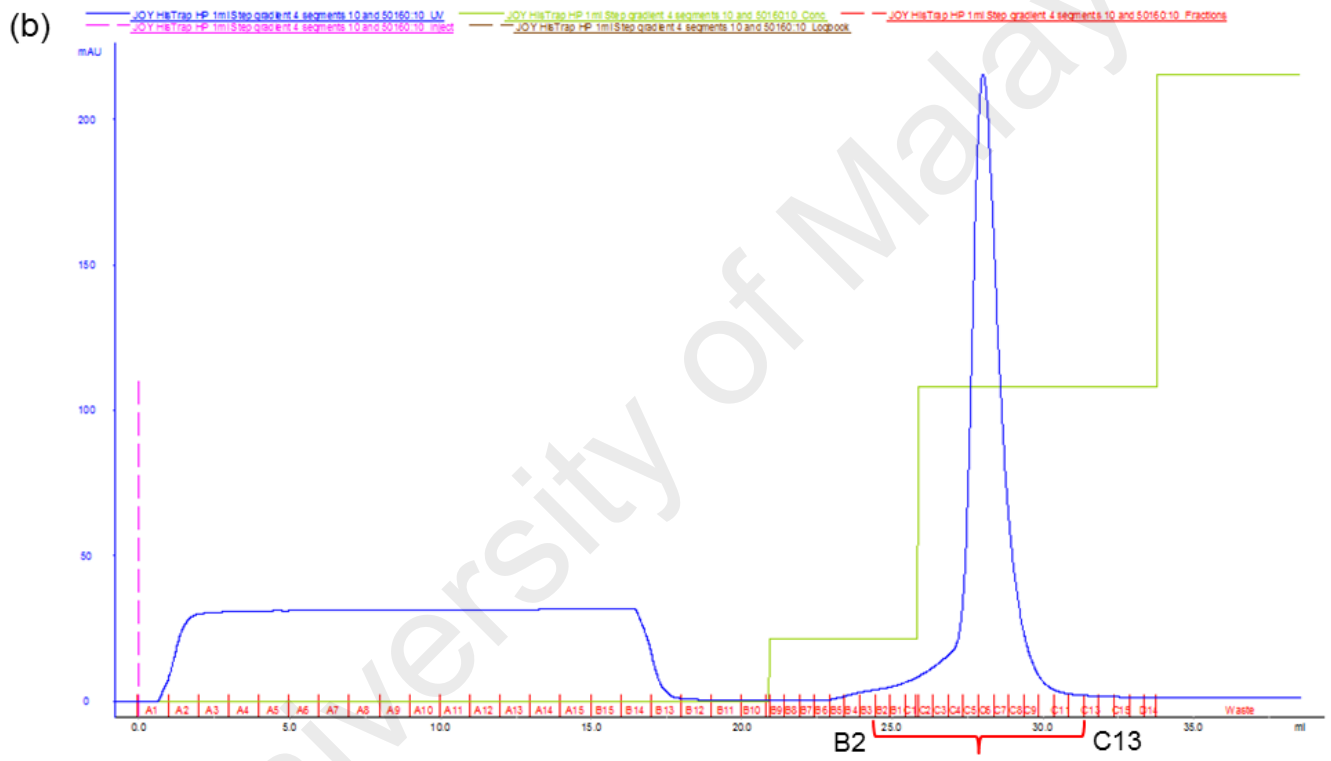

Figure 4.15: Continued.

(c)

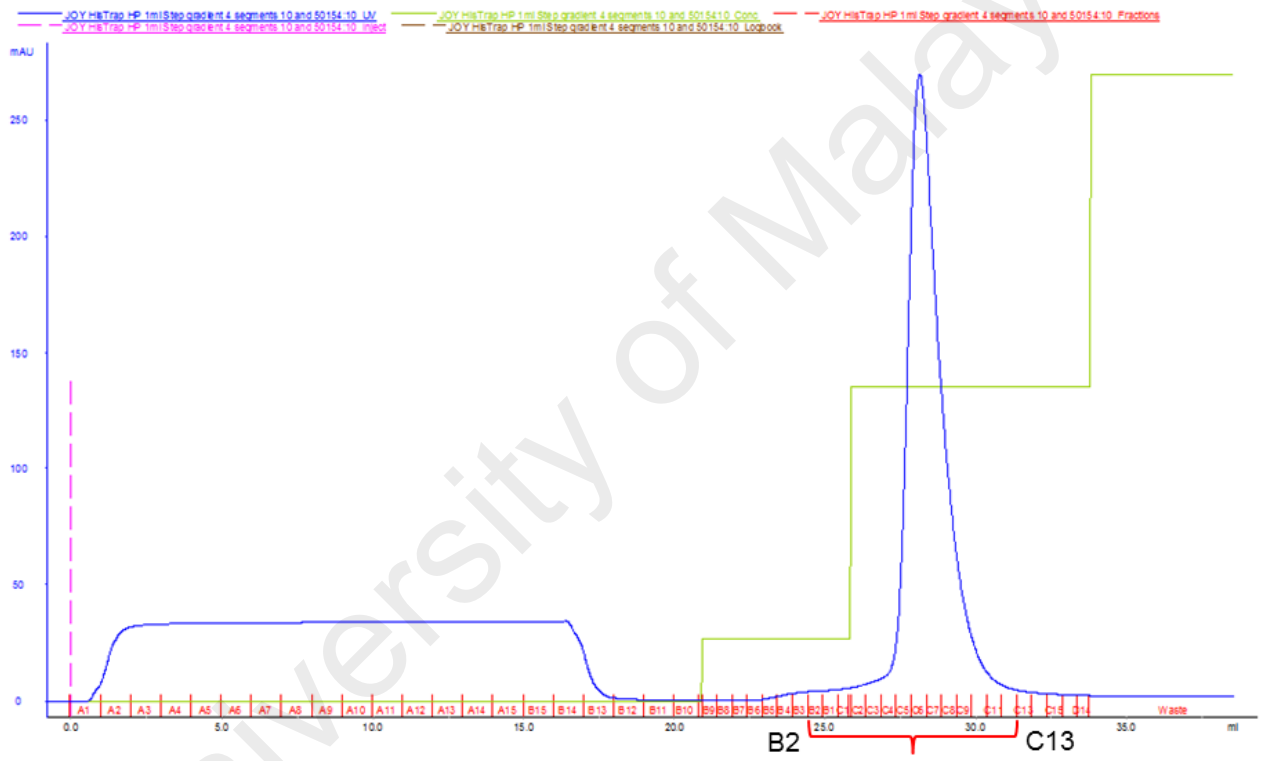

Figure 4.15: Continued.

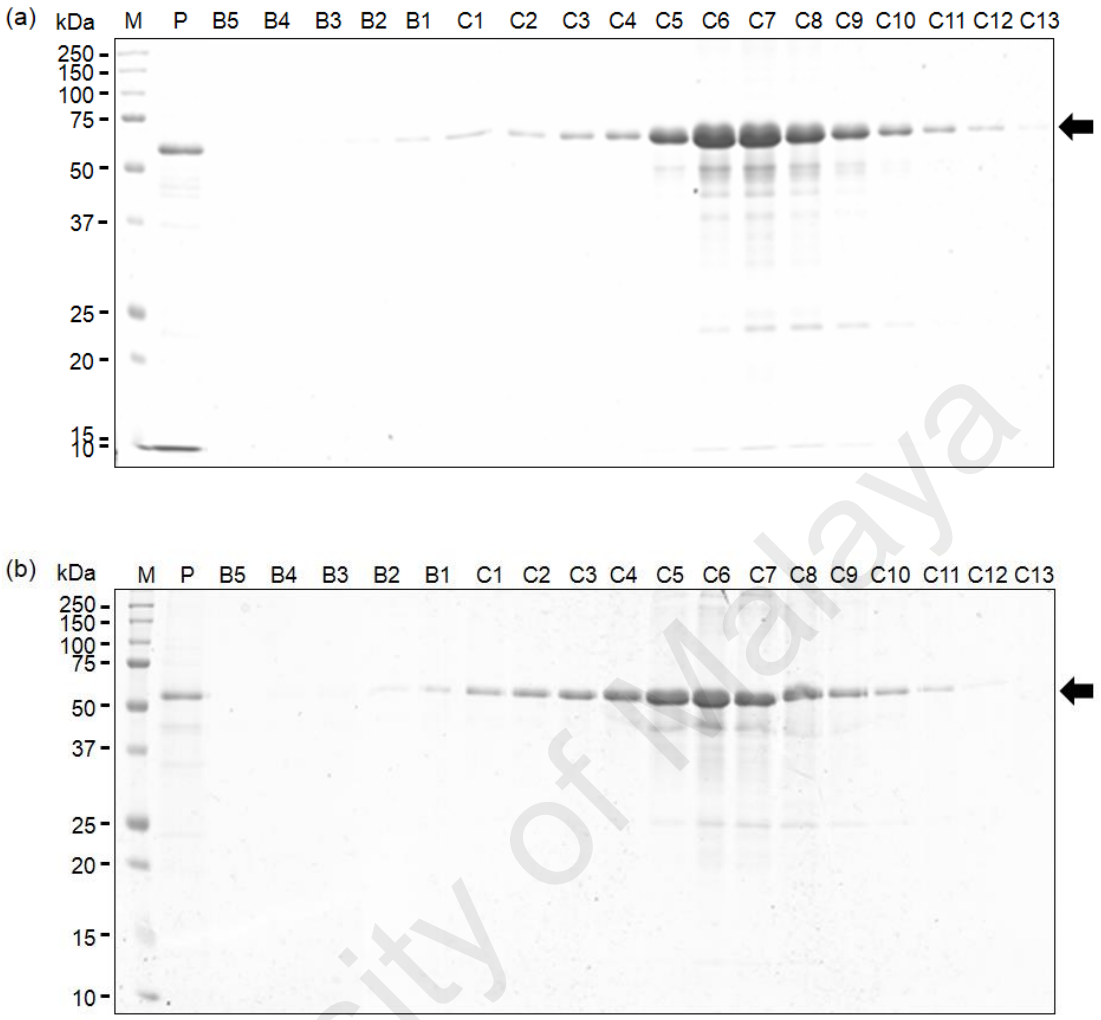

Figure 4.16: Purification of HA1/L/AcmA, HA1/AcmA and HA1 recombinant proteins.

The urea-solubilized (a) HA1/L/AcmA, (b) HA1/AcmA and (c) HA1 recombinant proteins (P) and the respective elution fractions (B5-C13) were analyzed on 12.5% SDS-PAGE. The gels were stained with Colloidal Coomassie solution. Elution fractions containing HA1/L/AcmA, HA1/AcmA and HA1 recombinant proteins were observed in B2-C13 fractions. Lane M represents Precision Plus Protein™ All Blue Standards (Bio-Rad Laboratories, Hercules, CA, USA). Arrows indicate the position of the produced recombinant proteins.

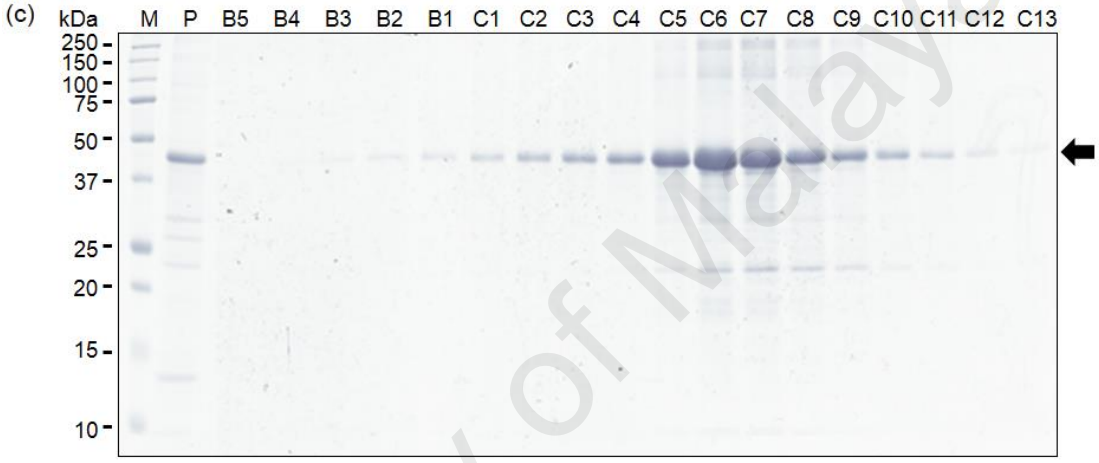

Figure 4.16: Continued.

4.5.4 Protein refolding

Biologically functional recombinant proteins were initially obtained by refolding the purified recombinant proteins using one-step dialysis by exchanging buffer consisting of 6 M to 0 M urea (dissolved in 20 mM NaH_2PO_4, 0.5 M NaCl). Complete protein aggregation however, was observed. Subsequently, the recombinant proteins were refolded using a step-wise dialysis method to gradually remove the denaturing reagent in order to reduce the occurrence of protein aggregation. The recombinant proteins were also diluted to a lower concentration (<100 μg/ml) before the start of refolding to reduce the tendency of intermolecular interactions, which could be one of the possible factors responsible for protein aggregation. Additionally, the pH of the dialysis buffer could be another factor attributing to protein aggregation. The recombinant proteins were found to be stable in buffers with pH lower than their respective pI value. HA1/L/AcmA (pI=8.56) and HA1/AcmA (pI=8.56) recombinant proteins were noted to be stable in a buffer of pH 7.4, while the HA1 (pI=8.26) recombinant protein was noted to be stable in a buffer of pH 7.2. Using the optimized refolding condition, the denatured HA1/L/AcmA, HA1/AcmA and HA1 recombinant proteins were recovered in soluble forms. The soluble recombinant proteins obtained were concentrated and analyzed on SDS-PAGE (Figure 4.17a) and immunoblotting (Figure 4.17b). The recombinant proteins were observed as distinctive protein bands with molecular masses of approximately 50, 49 and 40 kDa, respectively, which corresponded to the respective predicted mass values. These distinctive protein bands were also detected by immunoblotting using AP-conjugated HisDetector Nickel, suggesting successful recombinant protein purification and refolding. However, an additional protein band of a lower molecular mass was observed in the purified HA1/L/AcmA recombinant protein. This could be a minor degradation of the recombinant protein because the band reacted to the AP-conjugated HisDetector Nickel in immunoblotting. The purity of the

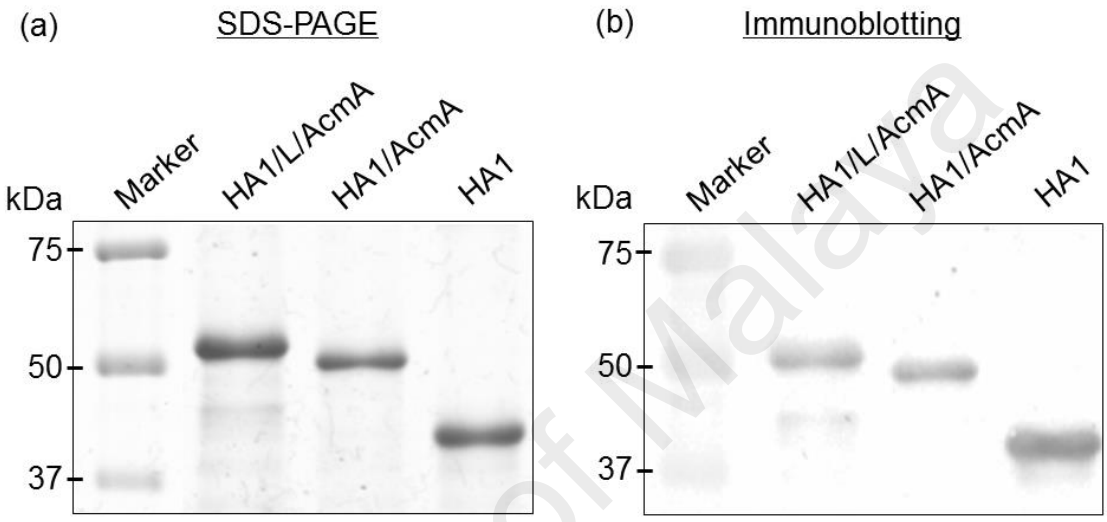

Figure 4.17: Refolded HA1/L/AcmA, HA1/AcmA and HA1 recombinant proteins.

Refolded recombinant proteins were concentrated and analyzed on (a) SDS-PAGE and (b) immunoblotting. The recombinant proteins were detected using Colloidal Coomassie solution on SDS-PAGE and AP-conjugated HisDetector Nickel for immunoblotting. Marker used was the Precision Plus Protein™ All Blue Standards (Bio-Rad Laboratories, Hercules, CA, USA).

HA1/L/AcmA, HA1/AcmA and HA1 recombinant proteins determined using the Gel Pro Analyzer 4.0 was approximately 85%, 90% and 99%, respectively. Based on Micro BCA protein assay, the yield of the recombinant proteins was estimated to be at least 20 mg/l, 10 mg/l and 10 mg/l bacterial culture, respectively.

4.5.5 Protein identification

The identity of the HA1/L/AcmA (Table 4.2a), HA1/AcmA (Table 4.2b) and HA1 (Table 4.2c) recombinant proteins was confirmed by mass spectrometry. The recombinant protein band of a lower mass was identified as the HA1/L/AcmA (Table 4.2d). The mowse score for all the recombinant proteins was greater than 41, therefore, the results were considered as significant ($p<0.05$). For HA1/L/AcmA recombinant protein, the peptide mass fingerprinting spectra matched to both *L. lactis* subsp. c*remoris* AcmA and influenza A virus (A/New Zealand: South Canterbury/35/2000 H1N1) HA. The specific peptides that matched were K.SGDTLWGISQR.Y and R.YGISVAQIQSANNLK.S for the AcmA and R.EQLSSVSSFER.F for the HA. Peptide mass fingerprinting spectra of HA1/AcmA also gave matched to both *L. lactis* subsp. c*remoris* AcmA and influenza A virus (A/New Zealand: South Canterbury/35/2000 H1N1) HA. The specific peptides that matched were similar to the HA1/L/AcmA recombinant protein with an additional third peptide K.STIIYIGQK.L that matched for AcmA. Peptide mass fingerprinting spectra for HA1 and HA1/L/AcmA (lower molecular mass) recombinant protein matched to the influenza A virus (A/New Zealand: South Canterbury/35/2000 H1N1) HA with R.EQLSSVSSFER.F as the peptide that matched. The MASCOT search results for all four recombinant proteins were presented in Appendix E.

Table 4.2: Identification of HA1/L/AcmA, HA1/AcmA, HA1 and HA1/L/AcmA band of a lower molecular mass recombinant proteins.

The identity of (a) HA1/L/AcmA, (b) HA1/AcmA, (c) HA1 and (d) HA1/L/AcmA (lower molecular mass) recombinant proteins was confirmed by peptide mass fingerprinting and MALDI-TOF/TOF MS/MS analysis.

(a)

Identified protein	Mowse score[a]	Peptide sequence	Queries matched	Expected value
Probable N-acetylmuramidase OS=*Lactococcus lactis* subsp. *Cremoris* GN=acmA PE=3 SV=1 [AcmA_LACLC]	109	K.SGDTLWGISQR.Y	40	9.8e-005
		R.YGISVAQIQSANNLK.S	65	0.087
Hemagglutinin OS=Influenza A virus (strain A/New Zealand: South Canterbury/35/2000 H1N1) GN=HA PE=3 SV=1 [HEMA_I00A1]	70	R.EQLSSVSSFER.F	50	6.5e-005

[a] Mowse scores >41 were considered significant ($p<0.05$).

Table 4.2: Continued.

(b)

Identified protein	Mowse score[a]	Peptide sequence	Queries matched	Expected value
Probable N-acetylmuramidase OS=*Lactococcus lactis* subsp. *Cremoris* GN=acmA PE=3 SV=1 [AcmA_LACLC]	193	K.STIIYIGQK.L	28	1.5
		K.SGDTLWGISQR.Y	39	1.1e-006
		R.YGISVAQIQSANNLK.S	68	1.8e-005
Hemagglutinin OS=Influenza A virus (strain A/New Zealand: South Canterbury/35/2000 H1N1) GN=HA PE=3 SV=1 [HEMA_I00A1]	98	R.EQLSSVSSFER.F	51	1e-007

[a] Mowse scores >41 were considered significant ($p<0.05$).

Table 4.2: Continued.

(c)

Identified protein	Mowse score[a]	Peptide sequence	Queries matched	Expected value
Hemagglutinin OS=Influenza A virus (strain A/New Zealand: South Canterbury/35/2000 H1N1) GN=HA PE=3 SV=1 [HEMA_I00A1]	63	R.EQLSSVSSFER.F	52	0.00039

(d)

Identified protein	Mowse score[a]	Peptide sequence	Queries matched	Expected value
Hemagglutinin OS=Influenza A virus (strain A/New Zealand: South Canterbury/35/2000 H1N1) GN=HA PE=3 SV=1 [HEMA_I00A1]	96	R.EQLSSVSSFER.F	29	2e-007

[a] Mowse scores >41 were considered significant ($p<0.05$).

4.6 Hemagglutination activity of HA1/L/AcmA, HA1/AcmA and HA1 recombinant proteins

Functional activities of HA1 in the HA1/L/AcmA, HA1/AcmA and HA1 recombinant proteins were assessed by performing the hemagglutination assay. Hemagglutination assay was assessed by the formation of a lattice when recombinant proteins were incubated with guinea pig RBCs. The HA1/L/AcmA, HA1/AcmA and HA1 recombinant proteins completely agglutinated RBCs at comparable amount of protein, which was a minimum of 15 µg (Figure 4.18). No hemagglutination was observed when only protein buffer was used. The results obtained here suggested that the hemagglutinating activity of HA1 in HA1/L/AcmA, HA1/AcmA and HA1 recombinant proteins was retained and comparable. Although an additional protein band of a lower molecular mass was observed in the purified HA1/L/AcmA recombinant protein, hemagglutinating activity of HA1 in HA1/L/AcmA recombinant proteins was still comparable to that of HA1/AcmA and HA1. This suggested that the degradation in HA1/L/AcmA recombinant protein did not affect its hemagglutination activity and the degradation was not in the HA1 region.

4.7 Binding of HA1/L/AcmA, HA1/AcmA and HA1 recombinant proteins to *L. lactis*

4.7.1 Flow cytometry analysis

An *in vitro* binding assay was performed and the recombinant proteins bound to the cell surface of *L. lactis* were confirmed by flow cytometry analysis. *L. lactis* surface displaying recombinant proteins that immunofluorescence-labeled with Alexa Fluor 488 were represented by the right shift of the cell population in the flow cytometrical histogram (Figure 4.19a). Fluorescence signal was detected for the *L. lactis* samples that were incubated with HA1/L/AcmA or HA1/AcmA, indicating that HA1/L/AcmA

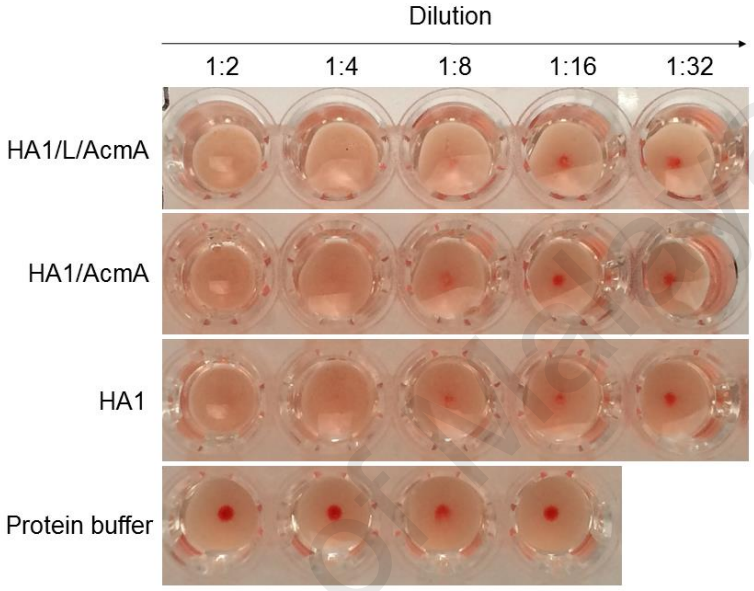

Figure 4.18: Hemagglutination assay results of HA1/L/AcmA, HA1/AcmA and HA1 recombinant proteins.

A total of 30 µg refolded HA1/L/AcmA, HA1/AcmA and HA1 recombinant proteins in two-fold serial dilutions were added to guinea pig RBCs suspension. Hemagglutination assay was assessed by the formation of a lattice when recombinant proteins were incubated with guinea pig RBCs.

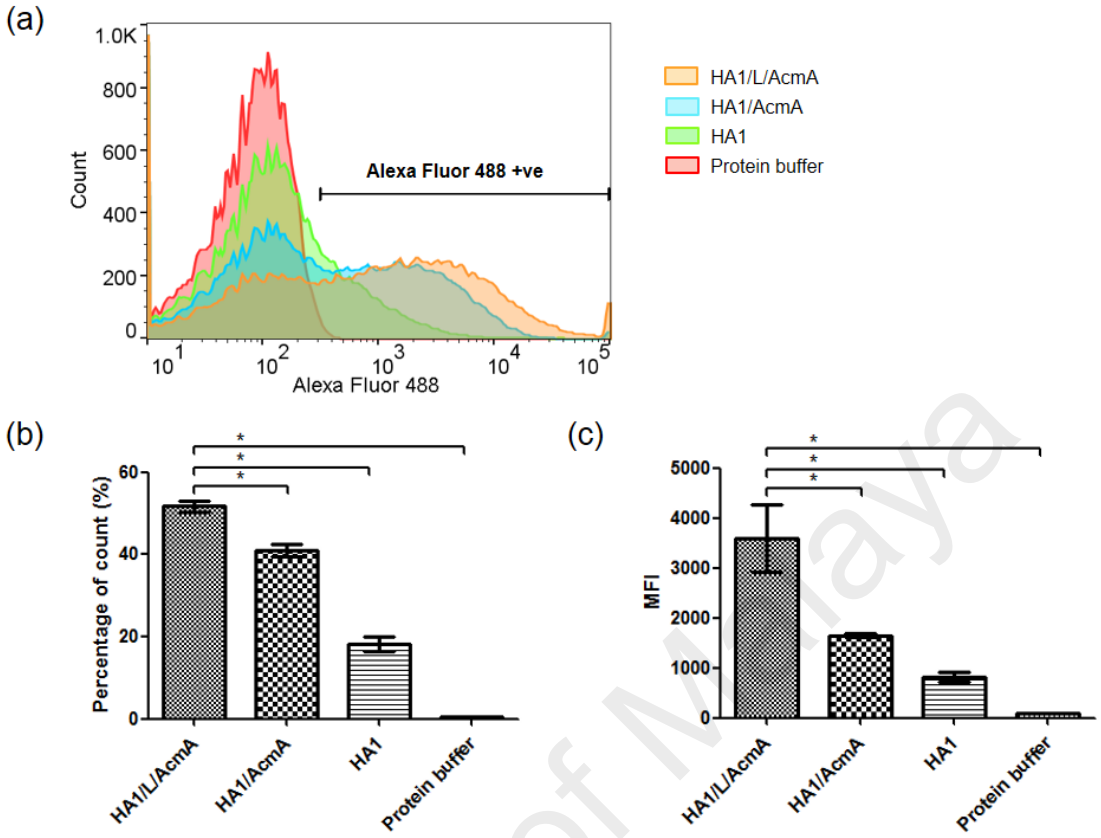

Figure 4.19: Flow cytometry analysis of HA1/L/AcmA, HA1/AcmA, HA1 recombinant proteins bound to *L. lactis*.

(a) A representative histogram of *L. lactis* after incubation with HA1/L/AcmA, HA1/AcmA, HA1 recombinant proteins and protein buffer from two biological replicates. (b) The percentages of count for Alexa Fluor 488-positive *L. lactis* after incubation with HA1/L/AcmA, HA1/AcmA, HA1 recombinant proteins or protein buffer. (c) The MFI value of *L. lactis* after incubation with HA1/L/AcmA, HA1/AcmA, HA1 recombinant proteins or protein buffer. The data represents mean ± standard deviation. Asterisks indicate statistically significant differences between groups ($P<0.05$). Representative data from two biological replicates with three technical replicates each are depicted.

and HA1/AcmA were successfully displayed on the cell wall of *L. lactis*. The Alexa Fluor 488-positive *L. lactis* population was observed to be higher for cells incubated with HA1/L/AcmA in comparison to those of HA1/AcmA. This increase was clearly demonstrated by the significantly higher percentage of Alexa Fluor 488-positive gated cells (Figure 4.19b) for *L. lactis* surface displaying HA1/L/AcmA (51.7±1.4%) as compared to *L. lactis* cells incubated with HA1/AcmA recombinant protein (41.1±1.5%). The percentages of Alexa Fluor 488-positive gated cells for the controls, *L. lactis* after incubation with HA1 recombinant protein and *L. lactis* after incubation with protein buffer were significantly lower at 18.2±1.7% and 0.5±0.2%, respectively. Moreover, the MFI value (Figure 4.19c) of *L. lactis* after incubation with HA1/L/AcmA recombinant protein (3594.0±675.9) was significantly higher in comparison to *L. lactis* after incubation with HA1/AcmA recombinant protein (1652.0±34.1). The lowest MFI values were noted for *L. lactis* incubated with HA1 recombinant protein and *L. lactis* incubated with protein buffer (820.0±103.1 and 94.0±7.6, respectively). These differences in percentages of Alexa Fluor 488-positive cells and MFI value, particularly between the *L. lactis* surface displaying HA1/L/AcmA and HA1/AcmA recombinant proteins, suggested that there were more *L. lactis* surface displaying the HA1/L/AcmA recombinant protein and a higher amount of HA1/L/AcmA recombinant proteins could be loaded onto the surface of a single *L. lactis* cell. The scFv peptide linker present on the HA1/L/AcmA recombinant protein could plausibly contribute to the results observed here. The role of scFv peptide linker, however, was not specifically addressed in this study.

4.7.2 Protein band density analysis

Approximately 1.5×10^{10} CFU of *L. lactis* cells pre-mixed with the refolded HA1/L/AcmA, HA1/AcmA, HA1 and protein buffer were separated on 12.5% SDS-

PAGE, transferred to a nitrocellulose membrane and the recombinant proteins were detected using AP-conjugated HisDetector Nickel. Protein bands were detected (Figure 4.20a), indicating that HA1/L/AcmA and HA1/AcmA recombinant proteins were surface displayed on *L. lactis*. No protein bands were detected in the controls, *L. lactis* cell pre-mixed with the HA1 and protein buffer, indicating that these proteins were not displayed on *L. lactis*. The IOD of each standard band on the nitrocellulose membrane which was of known concentration was quantified using Gel Pro Analyzer 4.0 and a standard curve was generated based on the band IOD (Figure 4.20b). The IOD of HA1/L/AcmA and HA1/AcmA quantified using Gel Pro Analyzer 4.0 was determined to be 31.981 and 14.864, respectively. From the standard curve, it was estimated that approximately 36.6 µg and 13.8 µg of HA1/L/AcmA and HA1/AcmA recombinant proteins, respectively, was bound on 1.5×10^{10} CFU of *L. lactis* cells. Therefore, the amount of HA1/L/AcmA and HA1/AcmA recombinant proteins bound on *L. lactis* was approximately 2.9×10^{4} and 1.1×10^{4} molecules per cell, respectively, calculated based on the molecular mass of the recombinant proteins.

The binding of HA1/L/AcmA recombinant protein on *L. lactis* was also analyzed by immunoblotting, particularly to determine the effect of the lower molecular mass protein band on binding. The HA1/L/AcmA recombinant protein before binding, the unbound fraction (HA1/L/AcmA in the supernatant after binding) and the bound fraction (HA1/L/AcmA surface displayed on *L. lactis*) were separated on 12.5% SDS-PAGE and transferred to a nitrocellulose membrane. The recombinant proteins were then detected using AP-conjugated HisDetector Nickel. The protein band of lower molecular mass (<50 kDa) was detected in the unbound fraction of the sample after binding with *L. lactis* and not in the bound fraction (Figure 4.21). This suggested that the protein band of lower molecular mass or the minor degradation of HA1/L/AcmA did not bind to *L. lactis*. The observed result could explain that, the minor degradation of

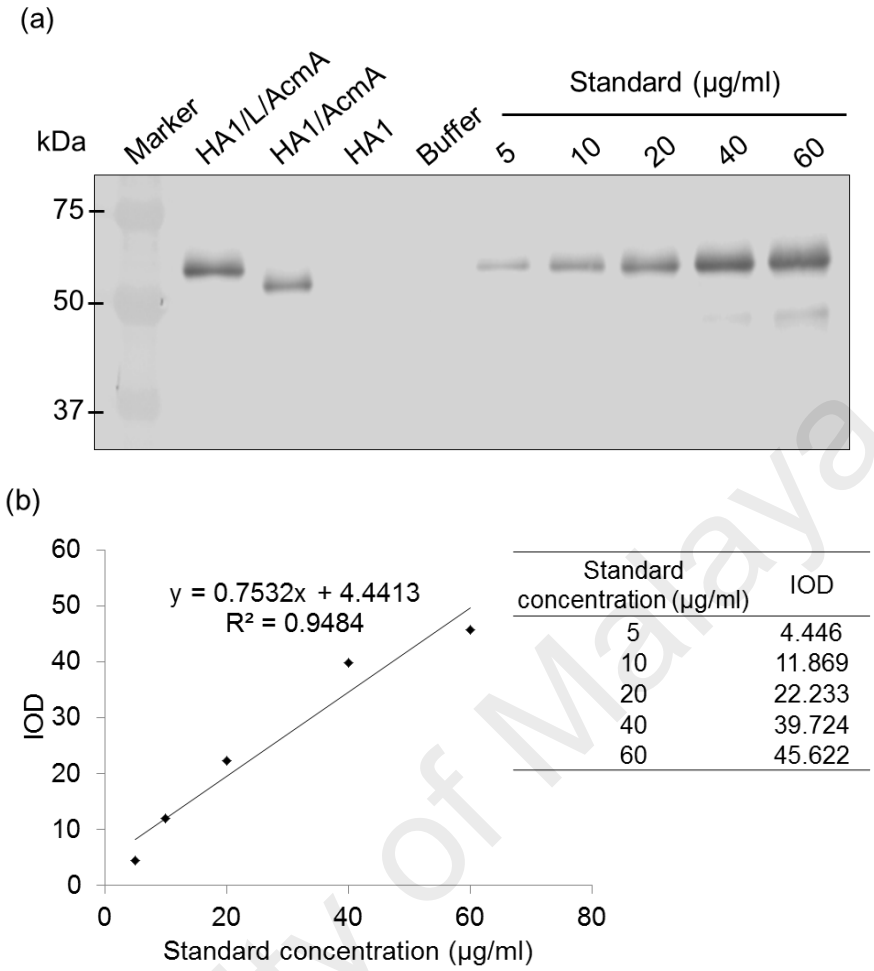

Standard concentration (µg/ml)	IOD
5	4.446
10	11.869
20	22.233
40	39.724
60	45.622

Figure 4.20: Protein band density analysis of *L. lactis* cells pre-mixed with the refolded HA1/L/AcmA, HA1/AcmA and HA1 recombinant proteins.

(a) *L. lactis* cells pre-mixed with the refolded HA1/L/AcmA, HA1/AcmA and HA1 recombinant proteins, control *L. lactis* cells and HA1/L/AcmA recombinant protein with previously determined concentrations were separated on 12.5% SDS-PAGE and transferred to a nitrocellulose membrane. Detection of the proteins was performed using AP-conjugated HisDetector Nickel. *L. lactis* cells pre-mixed with HA1 or protein buffer was used as the control. (b) The IOD of each standard band of HA1/L/AcmA recombinant protein on the nitrocellulose membrane was quantified and a standard curve was generated based on the band IOD. Marker used was Precision Plus Protein™ All Blue Standards (Bio-Rad Laboratories, Hercules, CA, USA).

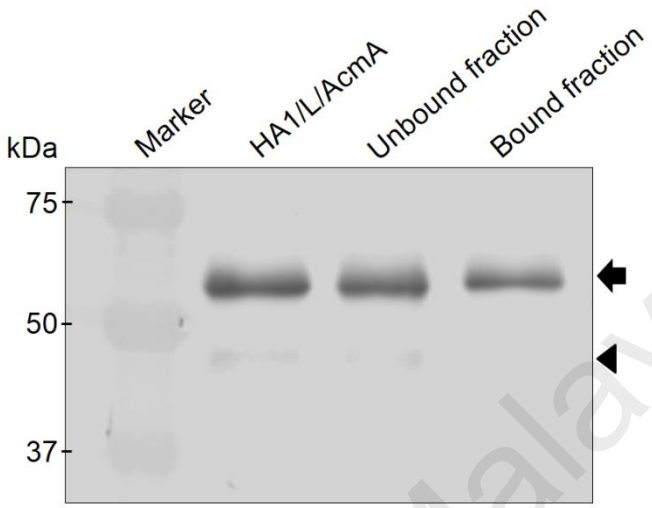

Figure 4.21: Immunoblotting analysis of the HA1/L/AcmA recombinant protein used in the binding to *L. lactis*.

The HA1/L/AcmA recombinant protein before binding, the unbound fraction (HA1/L/AcmA in the supernatant after binding) and the bound fraction (HA1/L/AcmA surface displayed on *L. lactis*) were separated on 12.5% SDS-PAGE and transferred to a nitrocellulose membrane. The membrane was probed with AP-conjugated HisDetector Nickel for detection. Marker used was Precision Plus Protein™ All Blue Standards (Bio-Rad Laboratories, Hercules, CA, USA). Arrow indicates the HA1/L/AcmA recombinant protein of the expected molecular mass at 50 kDa. Arrowhead indicates the HA1/L/AcmA recombinant protein of lower molecular mass (<50 kDa).

HA1/L/AcmA recombinant protein may occur in the AcmA region, which eventually affected its binding onto *L. lactis*. The recombinant protein displayed on *L. lactis* cells likely consist of only fully intact HA1/L/AcmA recombinant protein.

4.7.3 Structural modeling analysis

The 3D structures of HA1/L/AcmA and HA1/AcmA recombinant proteins were examined to determine if the presence of the scFv peptide linker helped to increase the binding capacity of recombinant proteins on *L. lactis*. There were three available structures of prokaryotes LysM in the PDB: the solution structure of AtlA-LysM2, MltD-LysM2 and *Bacillus subtilis* YkuD LysM (YkuD-LysM, PDB ID: 1Y7M). Amino acid sequence analysis of these available LysM of prokaryotes showed AtlA-LysM2, MltD-LysM2 and YkuD-LysM to have sequence identity of 42.6%, 30.6%, and 14.2%, with AcmA-LysM1, respectively (Figure 4.22a). As AtlA-LysM2 and MltD-LysM2 were noted to have higher amino acid sequence similarity to AcmA-LysM1, these two proteins were used as templates for the modeling. From the protein structure modeling analysis (representing one possible conformer), AcmA binding domain was noted to be immediately adjacent to the HA1 domain in the predicted structure of HA1/AcmA recombinant protein using AtlA-LysM1 and also in the predicted structure using MltD-LysM2 (Figure 4.22b). The AcmA binding domain in the predicted structures of HA1/L/AcmA recombinant protein using AtlA-LysM1 and MltD-LysM2, on the other hand, was separated by a distance from the HA1 domain. This longer distance was possibly attributed to the presence of the scFv peptide linker, which moved the AcmA binding domain away from the HA1 domain. With the locations of both domains (AcmA and HA1) at distal ends in HA1/L/AcmA, this recombinant protein would likely have lower steric hindrance in comparison to HA1/AcmA during its binding on *L. lactis* and therefore, have an improved binding capacity to *L. lactis* cells.

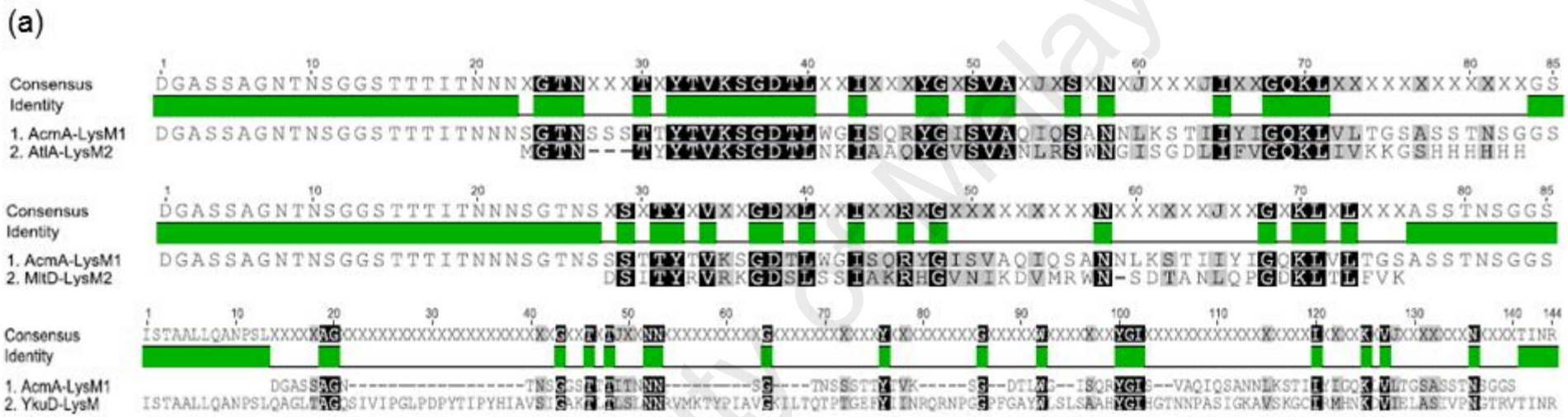

Figure 4.22: Amino acid sequence analysis and protein structure modeling of HA1/AcmA and HA1/L/AcmA recombinant proteins.

(a) The amino acid alignment of LysM motifs of *L. lactis* MG1363 AcmA-LysM1 with *E. faecalis* AtlA-LysM2, *E. coli* MltD LysM2 and *B. subtilis* YkuD-LysM, respectively. Amino acids are shaded in black for similarity and unshaded for amino acid difference. (b) The theoretical protein structures of HA1/AcmA and HA1/L/AcmA recombinant proteins when the solution structure of AtlA-LysM2 and MltD-LysM2 were used as the templates for modeling. The HA1 (green), scFv peptide linker (yellow) and AcmA (purple) are marked in respective colours for easier recognition.

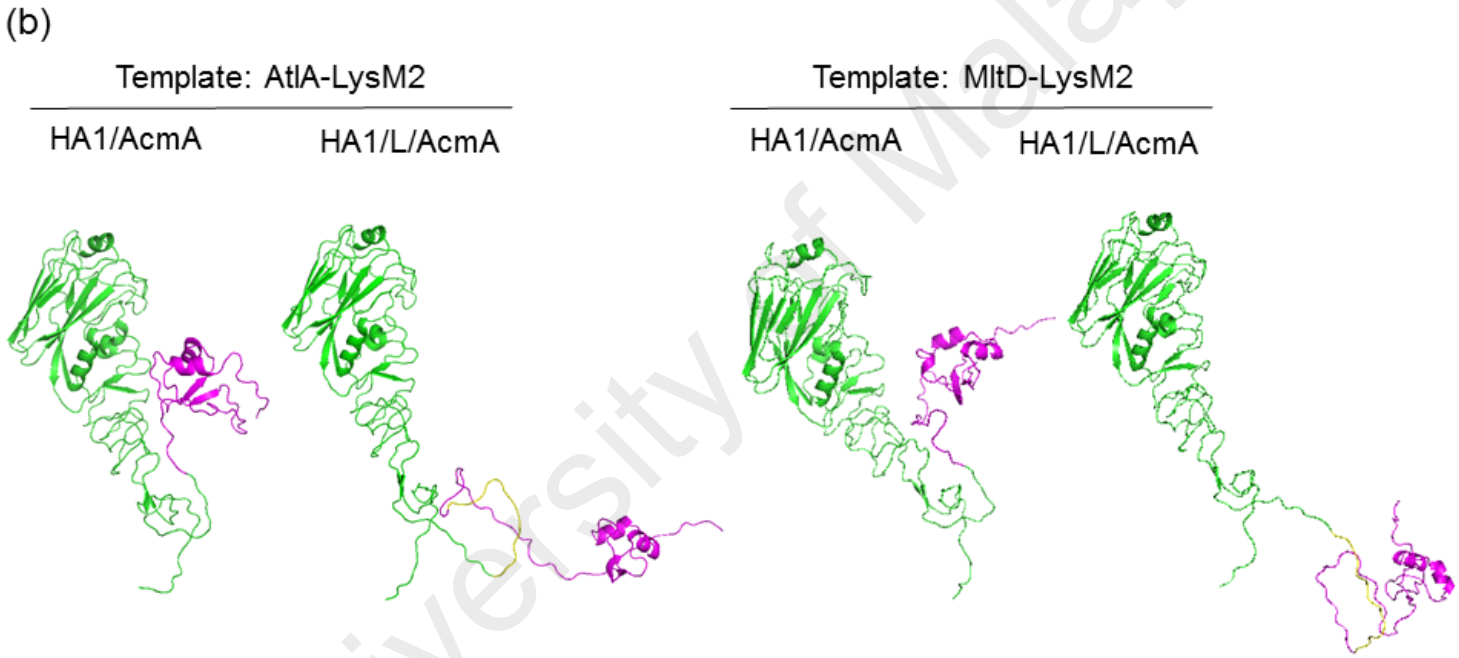

Figure 4.22: Continued.

4.8 Binding optimization and binding stability of HA1/L/AcmA recombinant protein to *L. lactis*

4.8.1 Optimization of *L. lactis* binding conditions

The HA1/L/AcmA recombinant protein was selected for further optimization of its binding activity onto *L. lactis*. *L. lactis* surface displaying HA1/L/AcmA recombinant protein was immunofluorescence-labeled with Alexa Fluor 488. The percentage of Alexa Fluor 488-positive gated cells (*L. lactis* surface displaying HA1/L/AcmA) increased steadily when increasing amount of HA1/L/AcmA recombinant protein was added to 1-3×10^9 CFU of *L. lactis* (Figure 4.23a). The percentage of Alexa Fluor 488-positive gated cells reached plateau when 20 µg of HA1/L/AcmA recombinant protein was used. The results suggested that the optimum amount of HA1/L/AcmA recombinant protein to be incubated with 1-3×10^9 CFU of *L. lactis* cells for surface display was 20 µg.

The percentage of *L. lactis* surface displaying HA1/L/AcmA recombinant protein following incubation of *L. lactis* with 20 µg of HA1/L/AcmA recombinant protein in GM17 for 1 h, 2 h, 3 h, and 4 h was examined. The percentage of Alexa Fluor 488-positive gated cells reached plateau when 20 µg of HA1/L/AcmA recombinant protein was incubated with *L. lactis* cells for 2 h, suggesting that incubation for 2 h was optimum for surface display of HA1/L/AcmA recombinant protein (Figure 4.23b). The binding of HA1/L/AcmA recombinant protein on *L. lactis* started to dissociate after incubation for 3 h.

The suitability of the buffer used for binding of HA1/L/AcmA recombinant protein to *L. lactis* was also evaluated. The percentage of *L. lactis* surface displaying HA1/L/AcmA recombinant protein after 2 h incubation with HA1/L/AcmA recombinant protein in GM17 and PBS was 53.8±0.9% and 52.3±5.5%, respectively, suggesting that the number of *L. lactis* cells detected to have HA1/L/AcmA on its cell

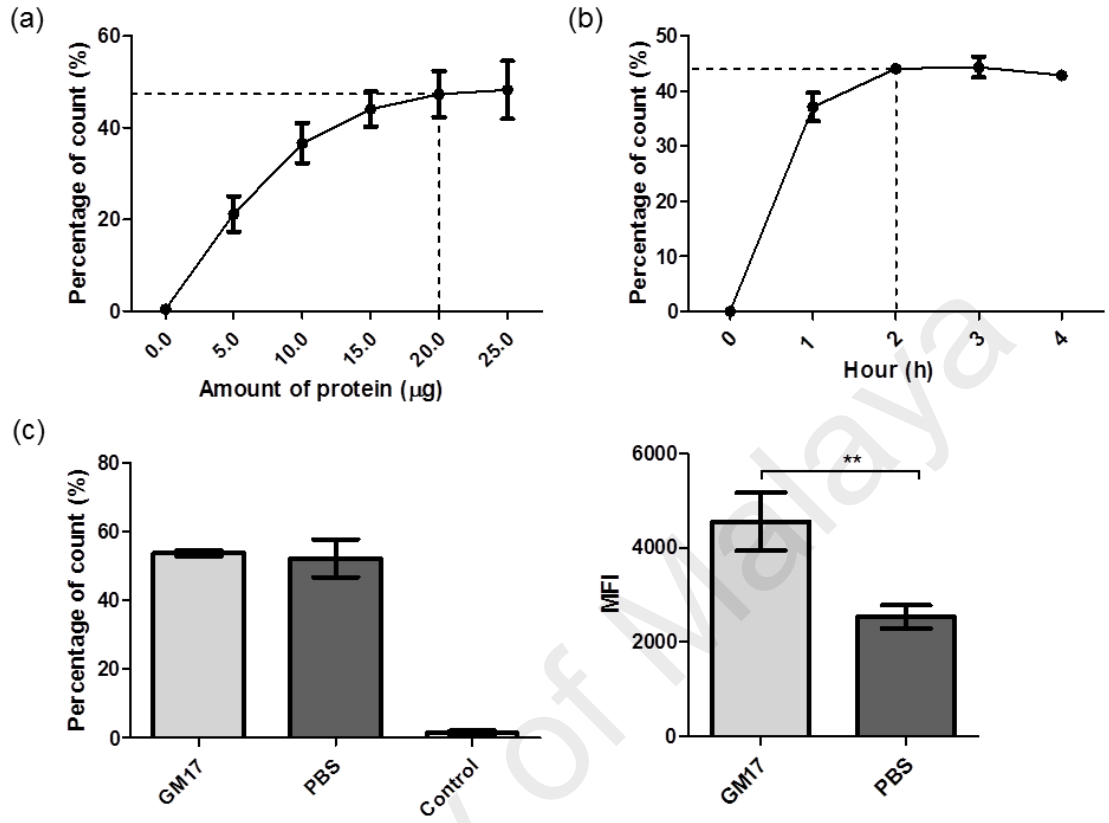

Figure 4.23: Binding optimization of HA1/L/AcmA recombinant protein to *L. lactis*. (a) The percentage of *L. lactis* surface displaying HA1/L/AcmA recombinant protein after incubation with different amount of HA1/L/AcmA recombinant protein. (b) The percentage of *L. lactis* surface displaying HA1/L/AcmA recombinant protein after incubation with HA1/L/AcmA recombinant protein for 1 h, 2 h, 3 h, and 4 h, respectively. (c) The percentage and MFI value of *L. lactis* surface displaying HA1/L/AcmA recombinant protein after incubation with HA1/L/AcmA recombinant protein in GM17 and PBS, respectively. The data represent mean ± standard deviation. Asterisk indicates statistically significant differences between groups (**P<0.01).

wall was similar in both buffers (Figure 4.23c). Therefore, the MFI value of *L. lactis* surface displaying HA1/L/AcmA recombinant protein was examined and the value for HA1/L/AcmA recombinant protein binding in GM17 (4552±614.9) was significantly higher in comparison to PBS (2538±243.4). This suggested that more recombinant proteins were bound per *L. lactis* cells in GM17 and hence, was a better buffer for the binding of the HA1/L/AcmA recombinant protein to *L. lactis*.

4.8.2 Binding stability of the recombinant protein on the *L. lactis*

The stability of *L. lactis* surface displaying HA1/L/AcmA recombinant protein stored in PBS at 4ºC was examined to evaluate the effect of storage duration at 4ºC on the binding. The *L. lactis* surface displaying HA1/L/AcmA recombinant protein was stored in PBS to prevent the continuos growth of the non-recombinant *L. lactis*. From the raw data, the percentage of *L. lactis* surface displaying HA1/L/AcmA recombinant protein was retained at 54.7±1.2%, 55.3±0.7%, 47.0±1.7% and 50.3±0.3% on day 1-4, respectively (Figure 4.24). The percentage of *L. lactis* surface displaying HA1/L/AcmA recombinant protein was reduced to 39.0±1.4% on day 5, followed by 27.8±1.0% and 32.7±2.8% on day 6 and 7, respectively. The percentage of *L. lactis* surface displaying HA1/L/AcmA recombinant protein was further reduced to 13.9±1.4% on day 8. From the best fit curve generated using the nonlinear regression analysis (R^2= 0.908), *L. lactis* surface displaying HA1/L/AcmA recombinant protein could retain at least 50% when stored in 4ºC for more than 3 days, as indicated by the dashed underline presented in Figure 4.24. The results suggested that the *L. lactis* surface displaying HA1/L/AcmA recombinant protein could be stably stored in 4ºC for at least 3 days.

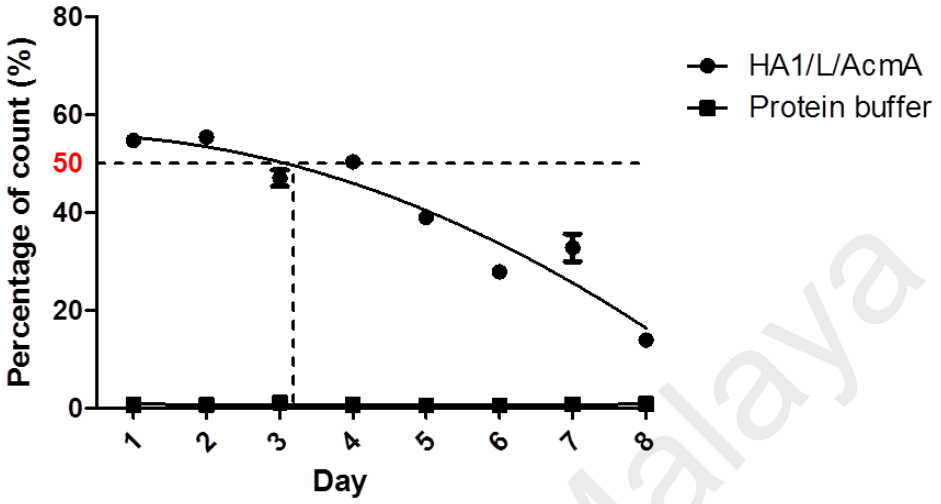

Figure 4.24: Stability analysis of the *L. lactis* surface displaying HA1/L/AcmA recombinant protein stored in 4°C.

L. lactis surface displaying the recombinant protein was prepared using the determined optimal conditions and stored in PBS at 4ºC. Samples were collected every day for 8 days and then stained for flow cytometry analysis to evaluate the effect of storage duration at 4ºC on the recombinant protein binding. The data points represent the mean ± standard deviation of the raw data, the percentage of *L. lactis* surface displaying HA1/L/AcmA recombinant protein. The solid curve represents the fit of raw data by the nonlinear regression analysis.

4.9 Immunogenicity studies of *L. lactis* surface displaying HA1/L/AcmA, LL-HA1/L/AcmA

4.9.1 MLD_{50} determination

Mice were inoculated intranasally with 10-fold serially diluted influenza virus to determine the MLD_{50} value. Body weight and survival of the mice were monitored daily. Mice showing weight loss of >20% were humanely sacrificed. Mice inoculated with A/Malaysia/2097724/2009(H1N1) influenza virus did not develop any signs of morbidity and body weight loss, suggesting the virus was avirulent in mice. However, mice inoculated with a mouse adapted influenza virus, A/TN/1-560/2009-MA2(H1N1) influenza virus, developed signs of morbidity such as hunched posture, ruffled fur and body weight loss up to 20% within 9 days after innoculation, suggesting this virus was virulent to mice. The survival rate of mice inoculated with 10-fold serially diluted A/TN/1-560/2009-MA2(H1N1) influenza virus was shown in the Figure 4.25. A total of 5/5, 2/5 and 2/5 mice inoculated with undiluted virus, 10-fold diluted virus and 100-fold diluted virus, respectively, showed weight loss up to 20% within 9 days and therefore, were humanely sacrificed. Mice inoculated with 1,000-fold diluted virus and PBS, respectively, did not show serious weight loss up to 20% and therefore, were not sacrificed. The MLD_{50} value of the A/TN/1-560/2009-MA2(H1N1) influenza virus was calculated using the Reed-Muench method and the calculation was presented in the Appendix F. The MLD_{50} of the A/TN/1-560/2009-MA2(H1N1) influenza virus was calculated to be at $10^{-1.22}$ dilution, which is approximately 3.10×10^{3} PFU of the virus.

4.9.2 Immune response induced by LL-HA1/L/AcmA

Study group A was a preliminary study to evaluate whether *L. lactis* surface displaying HA1/L/AcmA recombinant protein, LL-HA1/L/AcmA, could induce HA1 specific immune responses. Mice were administered orally with 1×10^{10} CFU of LL-

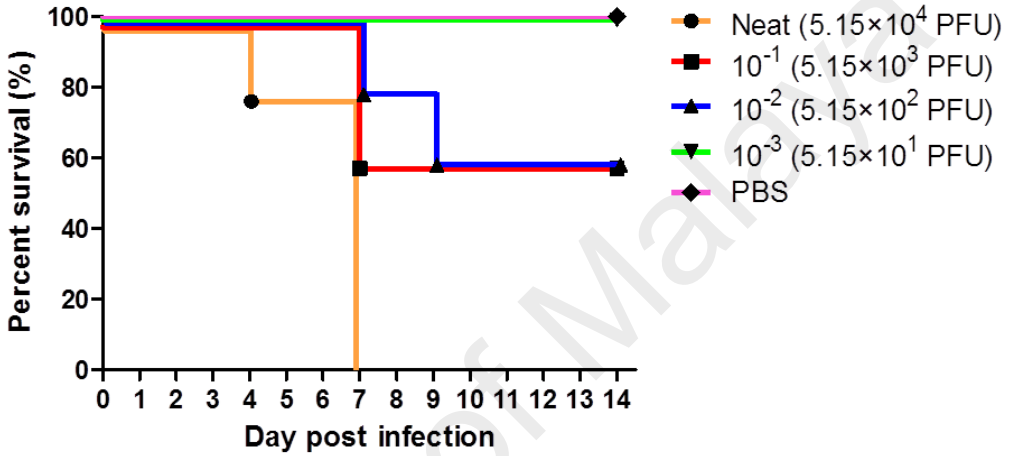

Figure 4.25: Fifty percent mouse lethal dose (MLD_{50}) determination.

Mice (n=5) were inoculated with 10-fold serially diluted A/TN/1-560/2009-MA2(H1N1) influenza virus intranasally in order to determine the MLD_{50}. Mice inoculated intranasally with PBS were used as the control. Survival rate of mice was monitored daily for 14 days and presented in Kaplan-Meier survival curve.

HA1/L/AcmA (25 µg/dosage) or PBS. Samples such as blood, faecal, small intestine, BAL fluid and nasal fluid were collected two weeks after the last immunization to evaluate the immune responses induced by LL-HA1/L/AcmA.

HA1/L/AcmA-specific serum IgG and IgA were measured as the main readout for systemic immunity. There were no differences in the HA1/L/AcmA-specific serum IgG (Figure 4.26a) and IgA (Figure 4.26b) in mice immunized with LL-HA1/L/AcmA (mean OD: 0.61±0.08 and 0.38±0.04, respectively) in comparison to the PBS-treated group (mean OD: 0.59±0.07 and 0.32±0.06, respectively). One significant outlier was detected in the data set for serum IgA of PBS-treated group using Grubbs' test ($p<0.05$) and therefore, was excluded in the statistical analysis. Overall, results suggested that there was no stimulation of serological immune responses, specifically HA1/L/AcmA-specific serum IgG and IgA, upon oral immunization of LL-HA1/L/AcmA in mice or the immune responses were below the detection limit of the assay.

Additionally, HA1/L/AcmA-specific sIgA in faecal extract, small intestine wash, BAL fluid and nasal fluid were measured as main readout of the mucosal immunity. The HA1/L/AcmA-specific sIgA in faecal sample (Figure 4.27a) was noted to be higher, but there was no statistically difference in mice immunized with LL-HA1/L/AcmA (mean OD: 0.59±0.11) in comparison to the PBS-treated group (mean OD: 0.36±0.09). In the data set for small intestine wash, one significant outlier was detected in PBS-treated group using Grubbs' test ($p<0.05$) and therefore, was removed from the statistical analysis. The HA1/L/AcmA-specific sIgA in small intestine wash (Figure 4.27b) of mice immunized with LL-HA1/L/AcmA (mean OD: 0.62±0.09) was detected to be significantly higher ($p<0.05$) in comparison to the PBS-treated group (mean OD: 0.40±0.05) after the removal of the outlier. Apart from that, one significant outlier was detected in both the data set for BAL and nasal fluid of mice immunized with LL-HA1/L/AcmA using Grubbs' test ($p<0.05$) and therefore, were excluded in the

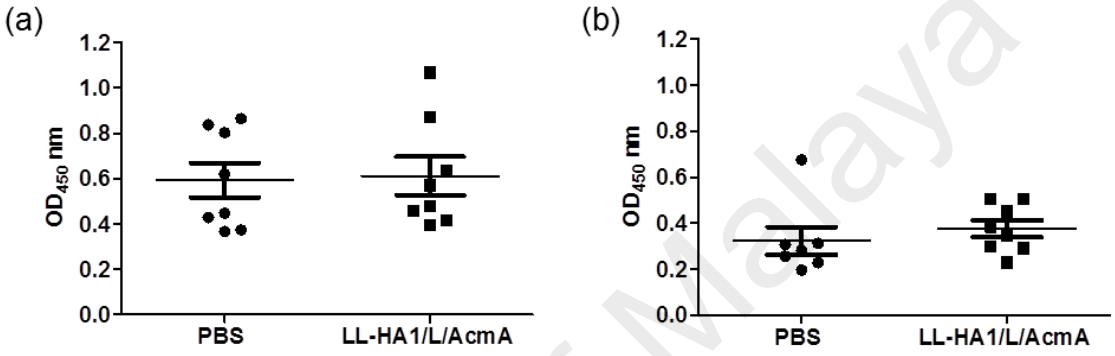

Figure 4.26: HA1/L/AcmA-specific serum IgG and IgA detected by ELISA.

Mice (8 mice/group) were orally immunized with PBS or LL-HA1/L/AcmA, and serum samples were collected two weeks after the last immunization. HA1/L/AcmA-specific (a) IgG and (b) IgA in serum at 1:10 dilution from individual mouse were detected by ELISA and the value was determined as the OD reading at 450 nm. One significant outlier was removed from the data set for serum IgA of PBS-treated group (Grubbs' test, $p<0.05$). Data are presented as mean ± standard error of the mean.

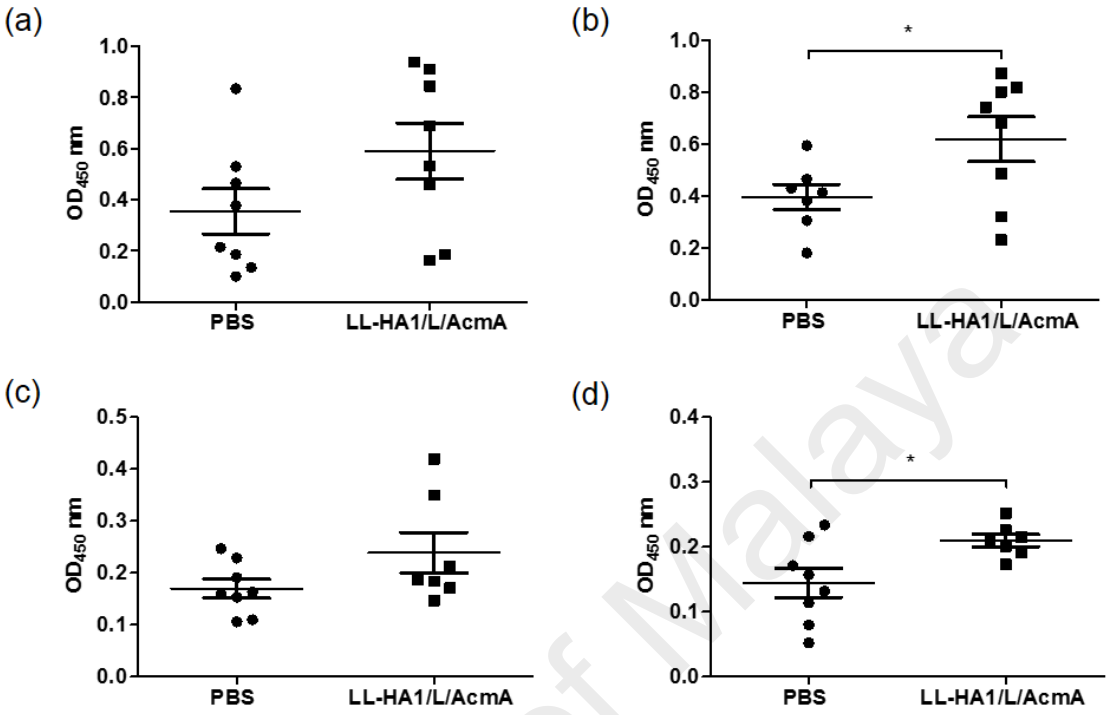

Figure 4.27: HA1/L/AcmA-specific IgA in faecal extract, small intestine wash, BAL fluid and nasal fluid detected by ELISA.

Mice (8 mice/group) were orally immunized with PBS or LL-HA1/L/AcmA, and samples were collected two weeks after the last immunization. HA1/L/AcmA-specific IgA in (a) faecal sample (1:5 dilution), (b) small intestine wash (neat), (c) BAL fluid (neat) and (d) nasal fluid (neat) from individual mouse was detected by ELISA and the value was determined as the OD reading at 450 nm. One significant outlier was removed from the data set for small intestine wash of PBS-treated group, as well as BAL and nasal fluid of LL-HA1/L/AcmA-treated group (Grubbs' test, $p<0.05$), respectively. Data are presented as mean ± standard error of the mean. Asterisks indicate statistically significant differences between the corresponding groups (*$p<0.05$).

statistical analysis. The HA1/L/AcmA-specific sIgA in BAL fluid (Figure 4.27c) was noted to be higher but not statistically different in mice immunized with LL-HA1/L/AcmA (mean OD: 0.24±0.03) in comparison to the PBS-treated group (mean OD: 0.17±0.01) after the removal of the outlier. In contrast, significantly higher HA1/L/AcmA-specific sIgA in nasal fluid (Figure 4.27d) ($p<0.05$) was detected in mice immunized with LL-HA1/L/AcmA (mean OD: 0.21±0.01) when compared to the PBS-treated group (mean OD: 0.14±0.02) after the removal of the outlier. Collectively, results suggested that oral immunization with LL-HA1/L/AcmA in mice stimulated a significant level of mucosal immunity in the gastrointestinal and respiratory tracts.

4.9.3 Immune response induced by higher dosage of LL-HA1/L/AcmA and protection against lethal H1N1 virus challenge

In study group B, mice were immunized orally with five-fold higher dosage of LL-HA1/L/AcmA which was 5×10^{10} CFU of LL-HA1/L/AcmA (125 µg/dosage) to determine if a higher dose would elicit a greater host immune response. For comparison, additional control groups of mice were included: mice orally administered with HA1/L/AcmA recombinant protein (125 µg/dosage) or PBS, and mice subcutaneously immunized with HA1/L/AcmA (50 µg/dosage) emulsified with Freund's adjuvant, HA1/L/AcmA-FA. Serum and faecal samples were collected two weeks after the last immunization to evaluate the specific immune responses.

There was no significant difference in the HA1/L/AcmA-specific serum IgG (Figure 4.28a) and IgA (Figure 4.28b) for mice orally immunized with LL-HA1/L/AcmA (mean OD: 0.49±0.13 and 0.24±0.07, respectively) or HA1/L/AcmA (mean OD: 0.45±0.06 and 0.12±0.01, respectively) in comparison to PBS-treated group (mean OD: 0.38±0.02 and 0.20±0.04, respectively). One significant outlier was detected in the data set for serum IgA of PBS-treated group using Grubbs' test ($p<0.05$) and was excluded in the

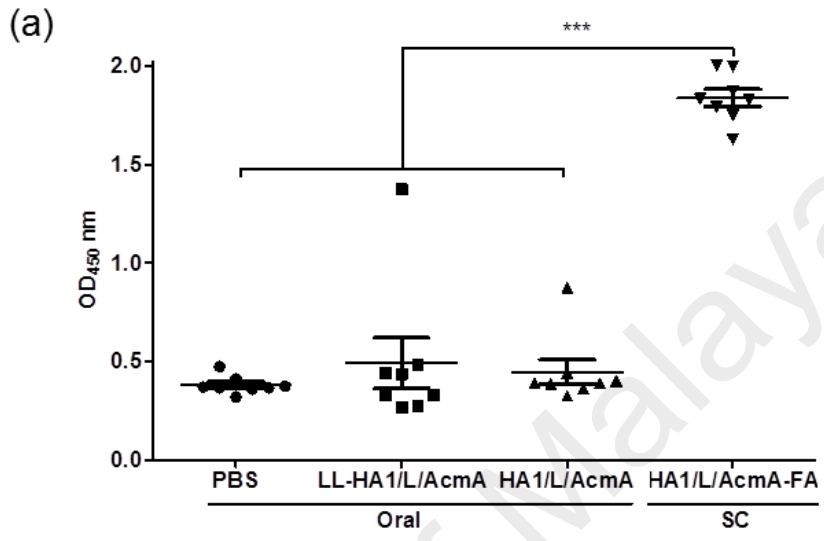

Figure 4.28: HA1/L/AcmA-specific serum IgG, serum IgA and faecal IgA detected by ELISA.

Mice (8 mice/group) were orally immunized with PBS, LL-HA1/L/AcmA or HA1/L/AcmA, or subcutaneously (SC) with HA1/L/AcmA-FA. Serum and faecal samples were collected two weeks after the last immunization. (a) HA1/L/AcmA-specific IgG and (b) IgA in serum (Oral: 1:10 dilution; SC: 1:1,000 dilution) and (c) HA1/L/AcmA-specific IgA in faecal sample (1:10 dilution) from individual mouse were measured by ELISA and the value was determined as the OD reading at 450 nm. Data are presented as mean ± standard error of the mean. Asterisks indicate statistically significant differences between the corresponding groups (**p<0.01; ***p<0.001).

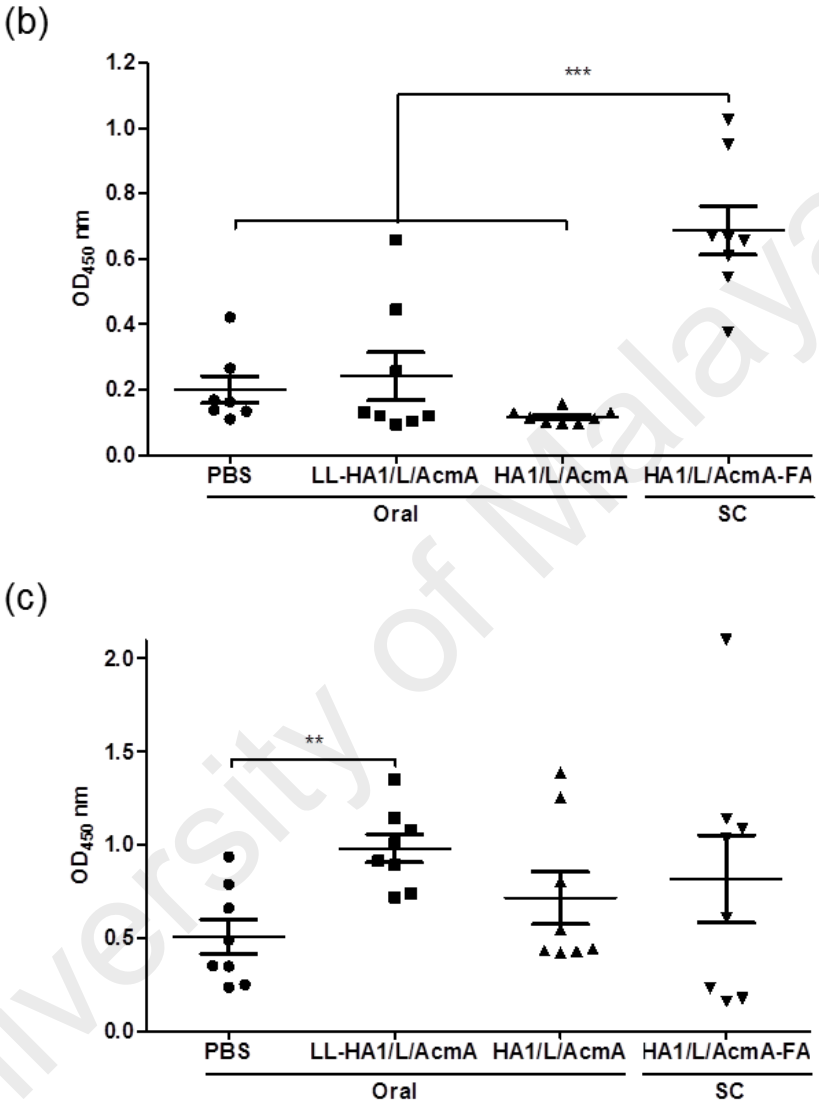

Figure 4.28: Continued.

statistical analysis. Another significant outlier was detected in the data set for serum IgG of mice immunized with LL-HA1/L/AcmA using Grubbs' test ($p<0.05$), but was not removed as an outlier because this mouse showed detectable HA1/L/AcmA-specific serum IgG and IgA response, which increased with each subsequent immunization. There was also no difference in the HA1/L/AcmA-specific serum IgG and IgA between mice immunized orally with LL-HA1/L/AcmA and HA1/L/AcmA. In contrast, significantly higher HA1/L/AcmA-specific serum IgG (Figure 4.28a) and IgA (Figure 4.28b) ($p<0.001$) were detected in the positive control group, which were mice immunized subcutaneously with HA1/L/AcmA-FA (mean OD: 1.84±0.04 and 0.69±0.07, respectively) in comparison to the other three groups. These results suggested that there was no stimulation of serological immune responses upon oral immunization of LL-HA1/L/AcmA or HA1/L/AcmA in mice. Alternatively, the responses were below the detection limit of the assay. Nonetheless, subcutaneous immunization of HA1/L/AcmA-FA in mice stimulated good serological immune responses, suggesting that HA1/L/AcmA was highly antigenic.

Significantly higher HA1/L/AcmA-specific sIgA (Figure 4.28c) ($p<0.01$) was detected in faecal sample of mice orally immunized with LL-HA1/L/AcmA (mean OD: 0.98±0.07) in comparison to the PBS-treated group (mean OD: 0.51±0.09). A higher dosage of LL-HA1/L/AcmA administered in mice effectively improved mucosal immune response, and this was indicated by the significant stimulation of sIgA detected in the faecal sample (Figures 4.27a and 4.28c). The HA1/L/AcmA-specific sIgA in faecal sample of mice orally immunized with LL-HA1/L/AcmA was also higher, but not statistically different in comparison to mice immunized with HA1/L/AcmA (mean OD: 0.72±0.14) or HA1/L/AcmA-FA (mean OD: 0.82±0.23) (Figure 4.28c). There was no significant difference in the detected HA1/L/AcmA-specific sIgA in faecal sample of mice orally immunized with HA1/L/AcmA as compared to the PBS-treated group,

suggesting HA1/L/AcmA without *L. lactis* as a carrier did not stimulate significant level of HA1/L/AcmA-specific sIgA. The same was noted for mice subcutaneously immunized with HA1/L/AcmA-FA as compared to the PBS-treated group. Although mice immunized subcutaneously with HA1/L/AcmA-FA stimulated good serological immune responses, however, it did not stimulate significant level of sIgA in the faecal sample. Taken together, these results suggested that LL-HA1/L/AcmA was a potent inducer of mucosal immunity in the gastrointestinal tract upon oral immunization of LL-HA1/L/AcmA in mice, and *L. lactis* delivery platform is capable in stimulating mucosal immunity in the gastrointestinal tract.

At 18 days following the last immunization, all mice in study group B were challenged intranasally with 10 MLD_{50} of A/TN/1-560/2009-MA2(H1N1) influenza virus to evaluate the protective efficiency of the immunization upon exposure to virulent influenza virus. Changes in body weight and survival of the mice were monitored daily as measure of disease severity. All the non-immunized mice were susceptible to influenza infection, showing sickness such as decreased activity and huddling by day 3 p.i. Severe sickness such as hunched posture, ruffled fur and increased body weight loss of up to 20% were observed within day 8 p.i. (Figure 4.29). The rate of body weight loss calculated by linear regression analysis was -2.7±0.1 and the maximum percentage change in body weight observed in individual mice over 14 days after lethal challenge with influenza virus was 20.6±0.1% (Table 4.3). In contrast, the body weight of mice in LL-HA1/L/AcmA-treated and HA1/L/AcmA-treated group decreased until day 6 and 7 p.i., respectively, after which mice in both groups continued to record an increase in their body weight till day 14 p.i. (Figure 4.29). A lower rate of body weight loss was observed in the LL-HA1/L/AcmA-treated (-0.3±0.1) and HA1/L/AcmA-treated group (-0.6±0.1), respectively, in comparison to the non-immunized mice (Table 4.3). In addition, significantly lower percentage change in body weight was observed in LL-

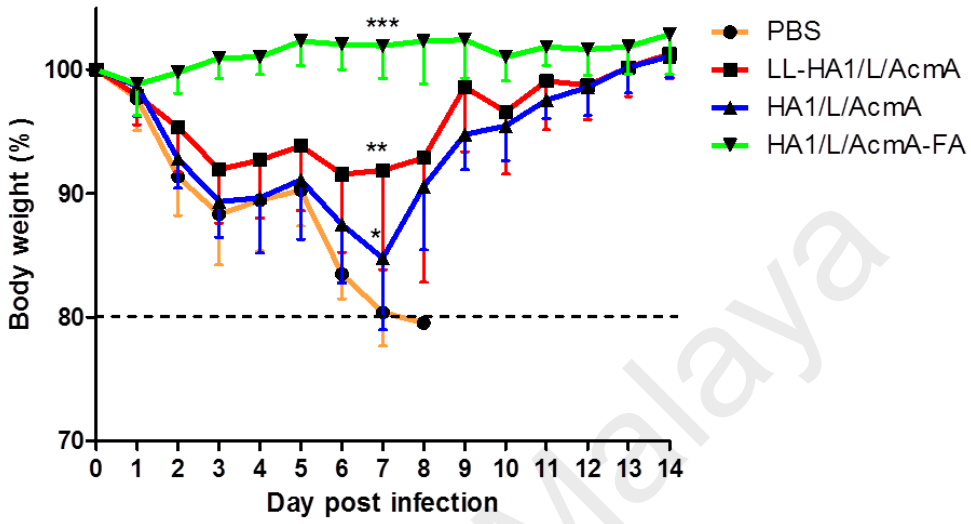

Figure 4.29: Body weight of mice following lethal challenge with H1N1/A/TN/1-560/2009-MA2 influenza virus.

At 18 days following the last immunization, all mice in study group B were intranasally challenged with 10 MLD_{50} of H1N1/A/TN/1-560/2009-MA2 virus. Body weight of mice immunized with PBS, LL-HA1/L/AcmA or HA1/L/AcmA orally, and HA1/L/AcmA-FA subcutaneously, following virus challenge was monitored daily for 14 days. The body weight of mice on the day of viral challenge was used as the baseline weight to determine the body weight changes post viral challenge. Asterisks indicate statistically significant differences in comparison to the PBS-treated group (*$p<0.05$; **$p<0.01$; ***$p<0.001$).

Table 4.3: Body weight and survival rate of immunized mice upon lethal challenge with H1N1/A/TN/1-560/2009-MA2 influenza virus.

Immunogen	Rate of body weight loss[a]	Rate of body weight recovery[b]	Body weight loss, %[c]	No. of survival (%)[d]	Mean day of death, p.i.[e]
PBS	-2.7±0.1	-	20.6±0.1	0/8 (0)	7.0±0.5
LL-HA1/L/AcmA	-0.3±0.1	0.3±0.1	11.6±2.5 **	7/8 (88) ***	8.0±0.0
HA1/L/AcmA	-0.6±0.1	0.3±0.1	15.7±1.8 *	6/8 (75) **	7.0±0.0
HA1/L/AcmA-FA	0.2±0.0	0.2±0.0	1.5±0.7 ***	8/8 (100) ***	>14.0

[a] Rate of body weight loss was calculated by linear regression analysis. Data are presented as mean ± standard deviation.

[b] Rate of body weight recovery was calculated by linear regression analysis. Data are presented as mean ± standard deviation.

[c] The maximum percentage change in body weight observed in individual mice over 14 days after lethal challenge with influenza virus. Data are presented as mean ± standard deviation.

[d] Total number of mice survived following lethal challenge with influenza virus. Percentage of mice survived following virus challenge is presented in parentheses.

[e] Day of death following lethal challenge with influenza virus. Data are presented as mean ± standard deviation.

Asterisks indicate statistically significant differences in comparison to the PBS-treated group (*$p<0.05$; **$p<0.01$; ***$p<0.001$).

HA1/L/AcmA-treated (11.6±2.5%) ($p<0.01$) and HA1/L/AcmA-treated group (15.7±1.8%) ($p<0.05$) in comparison to the non-immunized mice (Table 4.3). Collectively, these results suggested that oral immunization of LL-HA1/L/AcmA or HA1/L/AcmA in mice resulted significantly less morbidity upon exposure to virulent influenza virus in comparison to the non-immunized group. However, mice in the HA1/L/AcmA-treated group suffered more severe sickness as presented by higher rate of body weight loss and percentage change in body weight in comparison to the LL-HA1/L/AcmA-treated group. This suggested that oral immunization of LL-HA1/L/AcmA was superior in reducing morbidity upon exposure to influenza virus when compared to the HA1/L/AcmA without *L. lactis* as a carrier. Mice in the LL-HA1/L/AcmA-treated and HA1/L/AcmA-treated group, however, had similar rate of body weight recovery of 0.3±0.1 (Table 4.3). In contrast, the positive control group in which the mice were immunized with HA1/L/AcmA-FA subcutaneously did not show body weight loss upon exposure to influenza virus (Figure 4.29). The mice instead recorded rate of body weight gain of 0.2±0.0 (Table 4.3). In addition, there was significantly lower percentage change in body weight ($p<0.001$) in this HA1/L/AcmA-FA-treated group (1.5±0.7%) in comparison to the non-immunized group (Table 4.3). These results suggested that subcutaneous immunization of HA1/L/AcmA-FA in mice did not result in any morbidity upon exposure to virus.

The survival rate of the immunized mice upon exposure to virulent influenza virus is presented in Table 4.3 and Figure 4.30. All the non-immunized mice were not protected (0/8, 0%) upon exposure to influenza virus and the mean day of death was 7.0±0.5 p.i. Significantly higher survival rate of mice was observed in LL-HA1/L/AcmA-treated (7/8, 88%) ($p<0.001$) and HA1/L/AcmA-treated group (6/8, 75%) ($p<0.01$) in comparison to the non-immunized group. The mean day of death LL-HA1/L/AcmA-treated and HA1/L/AcmA-treated group was 8.0±0.0 p.i. and 7.0±0.0 p.i., respectively.

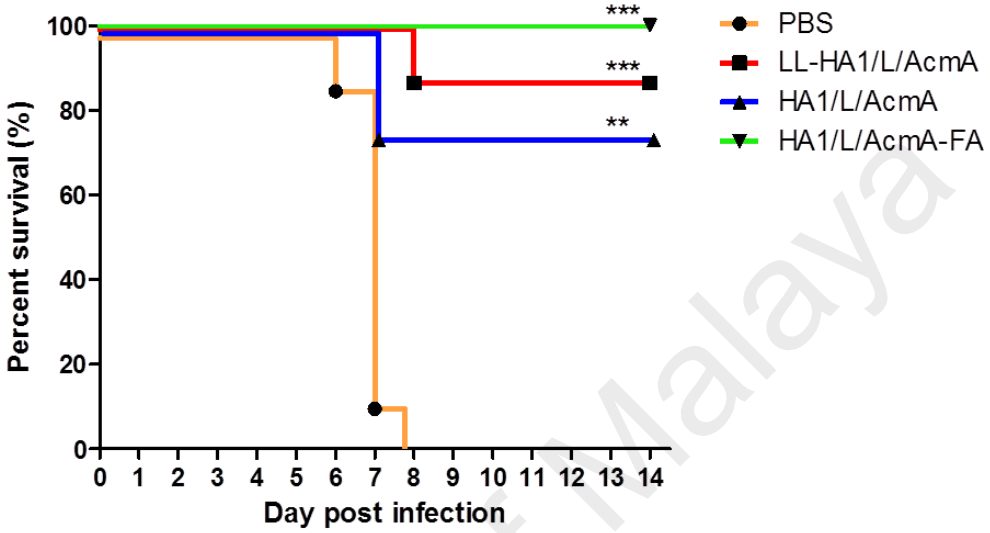

Figure 4.30: Survival rate of mice following lethal challenge with H1N1/A/TN/1-560/2009-MA2 influenza virus.

At 18 days following the last immunization, all mice in study group B were intranasally challenged with 10 MLD_{50} of H1N1/A/TN/1-560/2009-MA2 virus. Survival rate of mice immunized with PBS, LL-HA1/L/AcmA or HA1/L/AcmA orally, and HA1/L/AcmA-FA subcutaneously, following virus challenge was monitored daily for 14 days. Asterisks indicate statistically significant differences in comparison to the PBS-treated group (**$p<0.01$; ***$p<0.001$).

Nonetheless, all the mice immunized with HA1/L/AcmA-FA were fully protected (8/8, 100%) upon exposure to influenza virus and the survival rate ($p<0.001$) was significantly different from the non-immunized group. There was no difference in the survival between all the immunized groups. Taken together, the results suggested that oral immunization with LL-HA1/L/AcmA or HA1/L/AcmA, or subcutaneous immunization with HA1/L/AcmA-FA provided protection to mice against a lethal challenge with influenza virus.

CHAPTER 5: DISCUSSION

Influenza virus, a respiratory pathogen, contributes to a high rate of morbidity and mortality in humans globally. As such, while antiviral therapy has been available, vaccination is still the most effective strategy for the prevention and control of influenza. There is growing interest in mucosal vaccines due to their advantages over conventional injectable vaccines. Side effects associated with conventional vaccines, such as local reactions at the injection site are potentially reduced with implementation of mucosal vaccines. The need for needles during vaccine administration is also avoided thereby eliminating the possibility of blood transmissible infections (Levine, 2003; Hauri *et al.*, 2004). Moreover, mucosal vaccination can be easily administered without a trained personnel and is thus considered a more favorable approach for mass vaccination (Kim *et al.*, 2012), especially in remote regions where vaccination programs are difficult to implement. In the study, a method to develop a mucosal influenza candidate vaccine was described.

Surface display of heterologous protein on a Gram-positive bacterium using cell wall anchoring motif was first described in 1992 (Hansson *et al.*, 1992). Thereafter, this anchoring system has been widely used for many applications, especially in mucosal vaccine development. Of the various mucosal immunization approaches, *L. lactis* is being explored as an effective vaccine vehicle. A recombinant *L. lactis* displaying influenza HA1 was previously developed and the immunity elicited by this recombinant construct in mice was evaluated (Joan *et al.*, 2016). This recombinant *L. lactis* carried the HA1 gene that was genetically introduced into a vector containing an antibiotic resistance gene for selection purpose. The presence of this antibiotic resistance gene could eventually be a matter of great concern for vaccine delivery, particularly the transfer of its antibiotic resistance gene to another organism when *L. lactis* is released in

the field (Sybesma *et al.*, 2006). An approach utilizing a non-recombinant *L. lactis* will be advantageous as it is likely to overcome this concern, and hence be better accepted by the public. The present study is therefore to develop a non-recombinant *L. lactis* displaying influenza HA1 to target the stimulation of mucosal immunity.

Antigen delivery using *L. lactis* was mainly reported in membrane-anchored, intracellular or secreted forms. An earlier study demonstrated that the membrane-anchored form of TTFC on *L. lactis* was significantly more immunogenic than the intracellular and secreted forms (Norton *et al.*, 1996). In addition, Bermúdez-Humaran *et al.* (2004) showed that membrane-anchored form of E7 protein was more immunogenic compared to the intracellular and secreted forms. These earlier findings support the suggestion that the membrane-anchored form of antigen on *L. lactis* is likely a better route for antigen delivery.

In this study, a membrane-anchored form of influenza HA1 on non-recombinant *L. lactis* using the AcmA-LysM1 binding domain was described. LysM has a βααβ secondary structure with the two α-helices packing onto the same side of an antiparallel β-sheet. A shallow groove is formed by the two loops between α-helix and β-strand, and this shallow groove mediates the binding of LysM onto peptidoglycan in the bacterial cell wall (Bateman & Bycroft, 2000; Buist *et al.*, 2008; Visweswaran *et al.*, 2014). LysM has been shown to bind specifically to GluNAc residues in the peptidoglycan layer (Mesnage *et al.*, 2014; Visweswaran *et al.*, 2014), possibly modulated by the short peptide stem that cross-links GluNAc residues with the other alternating sugar residue, MurNAc (Mesnage *et al.*, 2014). It was previously reported that amino acid Asp11 in the highly conserved GDTL sequence of LysM likely interacted with GluNAc in the peptidoglycan layer (Bateman & Bycroft, 2000; Petrovic *et al.*, 2012). In this study, the highly conserved GDTL sequence is present in the

LysM1 domain in HA1/L/AcmA and HA1/AcmA recombinant proteins, hence, binding of these two recombinant proteins on *L. lactis* was predicted.

Although the entire surface of *L. lactis* is covered with peptidoglycan, the presence of LTA, which is associated with the peptidoglycan, can limit the surface display of heterologous protein on the *L. lactis* (Buist *et al.*, 2008; Visweswaran *et al.*, 2014). Increased amount of sugars in the LTAs can also obstruct binding of heterologous proteins on the bacterial cells (Steen *et al.*, 2008). In the study, it was shown for the first time that HA1/L/AcmA recombinant protein containing the scFv peptide linker had better binding to *L. lactis* compared to HA1/AcmA recombinant protein without the scFv peptide linker using flow cytometry and immunoblotting analysis. The presence of scFv peptide linker could have provided more flexibility to the recombinant protein, therefore reducing the steric hindrance effects during binding of recombinant protein onto *L. lactis* and allowed more recombinant protein to bind. LysM domains in AcmA are separated by a region rich in Ser, Thr and Asp or Pro residues (Buist *et al.*, 2008; Visweswaran *et al.*, 2014), providing flexibility between the LysM domains (Buist *et al.*, 2008). Although, this region has been included in the AcmA binding domain of HA1/L/AcmA and HA1/AcmA recombinant proteins, the insertion of the scFv peptide linker containing stretches of Gly residues could further enhance the flexibility of HA1/L/AcmA recombinant protein. The increase in binding of HA1/L/AcmA to *L. lactis* was further supported by the results from 3D structure analysis of HA1/L/AcmA and HA1/AcmA recombinant proteins as the protein structure modeling showed that scFv peptide linker kept the HA1 and AcmA binding domain separated at a distance.

To date, scFv peptide linker has been widely used in the construction of fusion protein, especially in the development of antibodies (Huston *et al.*, 1988; Chee & AbuBakar, 1998; Dimasi *et al.*, 2009; Ahmad *et al.*, 2012). Several studies showed that the linker length could affect the quaternary structure of the constructed fusion proteins

(Iliades *et al.*, 1997; Kortt *et al.*, 2001) and the overall performance of constructed fusion proteins (Iliades *et al.*, 1997; Kortt *et al.*, 1997; Atwell *et al.*, 1999; Shan *et al.*, 1999; Lu & Feng, 2008; Zhao *et al.*, 2008). For the fusion of β-glucanase and xylanase, a peptide linker with two repeats of GGGGS showed the highest performance (Lu & Feng, 2008). For the construction of the murine anti-human CD20 monoclonal antibody scFv, the construct with a shorter peptide linker had higher binding activity to CD20 expressing target cells compared to the construct with a longer peptide linker, and the binding activity was not improved if the construct had no peptide linker (Shan *et al.*, 1999). In this study, a peptide linker with three repeats of GGGGS was engineered in between the HA1 and AcmA binding domain to construct HA1/L/AcmA recombinant protein for surface displaying on *L. lactis*.

HA is the surface glycoprotein of influenza virus, which is responsible for viral attachment and entry. It has been well-known as a key antigen that is able to induce neutralizing antibodies (Virelizier, 1975; Okuno *et al.*, 1993). The HA monomer consists of a globular head, which is comprised of HA1, and the stalk, which is comprised of HA2 and part of HA1 subunit. The HA1 is more immunogenic compare to the full length HA in inducing neutralizing antibodies and it provides better protection against influenza virus challenge because HA1 contains the receptor binding site which is the most potent determinant recognized by virus neutralizing antibodies (Zhang *et al.*, 2015). Hence, the HA1 presents as an ideal candidate for vaccine development against influenza.

The HA1 surface displayed on *L. lactis* opens a possibility in the development of influenza virus oral vaccine (Van Braeckel-Budimir *et al.*, 2013; Visweswaran *et al.*, 2014). In the present study, the recombinant proteins containing HA1 were produced using the *E. coli* expression system, hence, the produced recombinant proteins were not glycosylated. The lack of post-translational modification mechanism for protein

glycosylation in *E. coli* expression system can possibly affect the functionality and antigenicity of the recombinant proteins. An earlier study, however, had demonstrated that HA1 produced using the bacterial expression system retained the functional ability to agglutinate RBC (Khurana *et al.*, 2010). Here, this study also showed that the HA1/L/AcmA, HA1/AcmA and HA1 recombinant proteins completely agglutinated RBCs at comparable amount of protein. These results suggested that the renatured bifunctional recombinant proteins regained their three-dimensional conformation of its HA1 domains, as well as retained its biological activity. Insertion of the scFv peptide linker and AcmA binding domain in the HA1/L/AcmA recombinant protein and insertion of AcmA binding domain in the HA1/AcmA recombinant protein obviously did not adversely affect the hemagglutination property of the recombinant HA. In addition, the predicted 3D structure of HA1/L/AcmA and HA1/AcmA recombinant proteins also suggested that the insertions did not potentially change the conformation of the HA.

Results from the flow cytometry analysis confirmed the surface display of influenza HA1 recombinant proteins (HA1/L/AcmA and HA1/AcmA) to *L. lactis*. Only a low percentage of Alexa Fluor 488-positive gated cells was detected for *L. lactis* incubated with HA1 recombinant protein without the AcmA binding domain (18.2±1.7%). *Lactococcus* strains are noted to be highly electronegative (Habimana *et al.*, 2007; Giaouris *et al.*, 2009) due to the presence of thick peptidoglycan, LTA and polysaccharides on the bacteria cell wall that could influence its physicochemical properties. In the presence of high electronegativity, an interaction between the *L. lactis* cell surface and a protein which carries charge could occur, resulting in the observed high background reading for *L. lactis* after incubation with AcmA-deficient HA1 recombinant protein, as well as with at least one other recombinant protein

(*Burkholderia pseudomallei* hypothetical protein lipoprotein) that has no AcmA binding domain (data not shown).

After purification and refolding of HA1/L/AcmA recombinant protein, a lower molecular mass of recombinant protein was noted in addition to the distinctive protein band at the predicted mass. The protein band was identified to be influenza virus HA by mass spectrometry analysis and it could be a minor degradation of the recombinant protein. This minor degradation of the recombinant protein could have a negative effect on protein binding to *L. lactis*, such as the degraded recombinant protein without the presence of AcmA binding domain could not bind to *L. lactis* and the degraded recombinant protein without HA1 could block the binding sites on *L. lactis*. In flow cytometry analysis, the antibody used was to detect the His-tag located at the N-terminal of the recombinant protein, while the AcmA binding domain which allows binding onto *L. lactis* was present at the C-terminus. The results obtained from the flow cytometry analysis detected recombinant proteins bound to *L. lactis* that were fully intact and not degraded. This was further supported by immunoblotting analysis which showed that no minor recombinant protein band was recovered in the bound fraction, hence, suggesting the minor degradation of HA1/L/AcmA recombinant protein may occur in the AcmA region.

While several studies have described the binding of heterologous protein to *L. lactis* (Norton *et al.*, 1996; Audouy *et al.*, 2007; Lim *et al.*, 2010), relatively little is known about the possible amount of protein to be surface-displayed on the *L. lactis*. Raha *et al.* (2005) showed that at least 10.0 µg of AcmA' fusion protein (15 kDa) bound to 2.0×10^9 *L. lactis* cells (Table 5.1), suggesting ~2.0×10^5 AcmA' molecules were displayed per cell. Bosma *et al.* (2006) showed that 150.0 µg of PA3 fusion protein (28 kDa) bound to 2.5×10^9 *L. lactis* GEM particles (Table 5.1), implying at least 1.3×10^6 PA3 molecules were displayed per cell. Ramasamy *et al.* (2006) further showed that 0.6 µg of

Table 5.1: Summary of recombinant protein amount surface-displayed on the *L. lactis*.

Recombinant protein	Molecular mass (kDa)	Amount of protein displayed on *L. lactis* (µg)	Amount of *L. lactis* cells (CFU)	Amount of molecules displayed per cell	Sources of references
AcmA'	15	10.0	2.0×10^{9}	2.0×10^{5}	(Raha *et al.*, 2005)
PA3	28	150.0	2.5×10^{9}	1.3×10^{6}	(Bosma *et al.*, 2006)
MSA2-Cov	65	0.6	5.0×10^{8}	10^{4}	(Ramasamy *et al.*, 2006)
HA1/L/AcmA	50	36.6	$\sim1.5\times10^{10}$	$\sim2.9\times10^{4}$	This work

MSA2-Cov fusion protein (65 kDa) bound to 5.0×10^8 *L. lactis* GEM particles (Table 5.1), suggesting 10^4 MSA-Cov molecules were displayed per cell. In the present study, 36.6 µg of HA1/L/AcmA recombinant protein (50 kDa) was estimated to bind to ~1.5×10^{10} *L. lactis* cells (Table 5.1), suggesting at least ~2.9×10^4 HA1/L/AcmA molecules were surface displayed per cell. The amount of the fusion protein molecules displayed on a *L. lactis* cell obviously varies with different fusion proteins. The amount of HA1/L/AcmA molecules bound per cell was less than AcmA' and PA3 fusion proteins. This could possibly due to the relatively larger mass of the HA1/L/AcmA. The result, however, is in agreement with the suggestion of Lim *et al.* (2010), where it was suggested that the binding capacity of the protein reduced as the protein size increases.

Most pathogens, including influenza viruses, initiate infection by entering human body through mucosal surfaces. Mucosal vaccination stimulates this natural infection and can provide local immune protection by stimulating sIgA at the mucosal surfaces. sIgA is the most abundant immunoglobulin isotype present in human secretions and it is a protease resistance immunoglobulin isotype due to its dimerization and high degree of glycosylation (Neutra & Kozlowski, 2006). sIgA has been shown to be effective in according protection against influenza virus infection (Asahi-Ozaki *et al.*, 2004). It has been reported to be more important than IgG in the protection of upper respiratory tract, specifically the nose and trachea (Renegar *et al.*, 2004), primarily by reducing virus attachment and preventing internalization of the virus at the mucosal surfaces, thereby preventing the initial infection (Taylor & Dimmock, 1985; Renegar *et al.*, 2004). In addition, sIgA provides cross-protection against other subtypes of influenza virus (Liew *et al.*, 1984; Tamura *et al.*, 1990; Tamura *et al.*, 1991; Asahi-Ozaki *et al.*, 2004). Cross-protection is particularly desirable due to the frequent antigenic changes that influenza viruses constantly undergo. The importance of IgA in virus clearance and protection

from re-infection was also clearly demonstrated in other viruses such as rotavirus (Blutt *et al.*, 2012).

In the present study, the findings of HA1/L/AcmA-specific sIgA in faecal extract, small intestine wash, BAL fluid and nasal fluid suggested that oral immunization with LL-HA1/L/AcmA in mice elicited significant level of mucosal immunity in the gastrointestinal tract and the respiratory tract. The result is consistent with previous studies showing that oral immunization with *L. lactis* displaying antigens induced sIgA at sites other than the gastrointestinal tract (Wang *et al.*, 2012b; Shi *et al.*, 2014; Gao *et al.*, 2015; Lei *et al.*, 2015a; Lei *et al.*, 2015c). The results of sIgA at other mucosal sites could be due to intestinally derived IgA plasma cells expressing CCR10 homing receptor that migrated towards CCL28 cytokine, which is secreted by mucosal epithelial tissues present at sites such as large intestine, stomach, trachea, bronchi, mammary glands and salivary glands (Kunkel & Butcher, 2003). These migrated intestinal IgA plasma cells then populate the mucosal sites, and secrete HA1/L/AcmA-specific sIgA. Therefore, oral immunization could lead to presence of antigen specific IgA in both intestinal and non-intestinal mucosal tissues (Czerkinsky *et al.*, 1991; VanCott *et al.*, 1994).

In study group B, higher dosage of LL-HA1/L/AcmA significantly increased the specific sIgA response in faecal sample compared to the non-immunized group. The results suggested that the immune response, specifically sIgA response, elicited by LL-HA1/L/AcmA could be improved in a dose-dependent manner with increasing dosage of LL-HA1/L/AcmA. The observed specific sIgA response upon oral immunization with non-recombinant LL-HA1/L/AcmA was consistent with previously reported findings in which specific sIgA was detected upon oral immunization with recombinant *L. lactis* expressing HA1 (Joan *et al.*, 2016).

HA1/L/AcmA-specific serum IgG and IgA were almost absence following immunization with LL-HA1/L/AcmA, with the exception of one mouse (1/8) that elicited detectable serum IgG and IgA upon administration with a higher dosage of LL-HA1/L/AcmA. The result obtained was in contrast with several studies that had demonstrated oral immunization of antigen using *L. lactis* elicited specific IgG in serum in addition to specific sIgA in faecal extract (Xin *et al.*, 2003; Lei *et al.*, 2010; Lei *et al.*, 2011; Marelli *et al.*, 2011; Wang *et al.*, 2012a; Ahmed *et al.*, 2014). The observed result in the present study might be due to no expression of CD62L homing receptor (L-selectin) on antibody secreting cell (ASC). The ASC expressing CD62L receptor binds to addressin, an endothelial cell carbohydrate antigen on high endothelial venules of peripheral lymph nodes (PLN) (Quiding-Järbrink *et al.*, 1997) and mediates the homing to PLN (Quiding-Järbrink *et al.*, 1997; Pasetti *et al.*, 2011). Earlier studies reported that CD62L was expressed on smaller fraction of ASC particularly upon oral immunization (Quiding-Järbrink *et al.*, 1997; Kantele *et al.*, 1999). Several efforts to develop effective influenza oral-based vaccine candidate using *L. lactis* targeting on the stimulation of both peripheral and mucosal immunity have been established. An earlier study reported that oral immunization with recombinant *L. lactis* pgsA-HA1 adjuvanted with cholera toxin subunit B (CTB) significantly increased specific serum IgG and fecal IgA in mice (Lei *et al.*, 2011). Similarly, mice immunized with *L. lactis* displaying NPadjuvanted with CTB also elicited significant humoral and mucosal immune responses (Lei *et al.*, 2015a).

Although mice immunized orally with LL-HA1/L/AcmA elicited significant mucosal immune response only, and not systemic immune response, more importantly, it was demonstrated that LL-HA1/L/AcmA could provide up to 88% protection in mice against a lethal challenge with influenza virus. All mice experienced body weight loss after a lethal challenge but gradually recovered after 6 days post viral challenge. All

mice in PBS-treated group died within 6-8 days after the viral challenge. An earlier study on mice immunized orally with recombinant *L. lactis* expressing HA of influenza H5N1 showed significant specific serum IgG and intestinal IgA, but IgA was not detected in tracheal mucosal and only 30% mice were protected upon viral challenge (Wang *et al.*, 2012a). Therefore, in this study, the protection in mice was likely due to the presence of sIgA specific against HA1 in the respiratory tract, which was possibly activated upon oral immunization, however, the possibility of other protective mechanisms cannot be excluded. Nonetheless, the findings obtained highlighted the importance of mucosal immunity in the respiratory tract in according protection against influenza virus challenge.

The protection of LL-HA1/L/AcmA immunized mice was not as good as the mice immunized subcutaneously with HA1/L/AcmA emulsified with Freund's adjuvant, HA1/L/AcmA-FA, which accorded 100% protection upon influenza virus challenge. This could be due to poor stimulation of serum IgG and IgA in LL-HA1/L/AcmA immunized mice. However, the role of peripheral immunity in according protection against influenza virus challenge cannot be concluded, as a previous study had reported that only 80% protection was observed although significant specific IgG in serum, IgA in intestinal and upper respiratory washes were detected after immunization with recombinant *L. lactis* displaying antigen (Lei *et al.*, 2015c).

In the present study, T cell-mediated immunity was not evaluated. T cell-mediated immunity was reported to be primarily directed against epitopes of internal and highly conserved antigens of influenza virus such as M, NP, PA and PB (van Els *et al.*, 2014). Therefore, T cell-mediated immunity plays a protective role, not by preventing infection (Lee *et al.*, 2014), but by clearing the established infection and reducing disease severity (van Els *et al.*, 2014). The protection has been associated to the cytotoxic $CD8^+$ and helper $CD4^+$ T cells (McMichael *et al.*, 1983; Sridhar *et al.*, 2013). $CD8^+$ T cells

recognize epitopes generated from proteasomal degradation of cytosolic viral proteins and presented by major histocompatibility complex (MHC) class I molecules (van Els *et al.*, 2014). $CD8^+$ T cells secrete antiviral cytokines and perforin which initiate apoptosis of the infected cell. On the other hand, $CD4^+$ T cells recognize epitopes processed by antigen presenting cells via endo-lysosomal pathway and presented by MHC class II molecules. $CD4^+$ T cells coordinate the $CD8^+$ T cells and B cells responses by secreting Th1, Th2, Th17, Tfh or other regulatory cytokines, in addition to directly kill the infected cells. The T cell-mediated immunity elicited upon oral immunization with LL-HA1/L/AcmA in mice and its protective role upon viral challenge was not examined, therefore, merits further investigation.

In comparing the importance of *L. lactis* as an antigen carrier, mice immunized orally with LL-HA1/L/AcmA showed markedly improved immune response than HA1/L/AcmA recombinant protein only, without the *L. lactis* attached. Mice immunized with LL-HA1/L/AcmA also suffered less sickness and body weight loss upon the lethal challenge with influenza virus. These results were in agreement with several earlier studies showing that oral immunization with *L. lactis* displaying antigen is more efficient than a simple antigen alone oral immunization (Pei *et al.*, 2005; Ahmed *et al.*, 2014). In addition, bacterium-like particles (BLPs) derived from *L. lactis* has been shown to be able to improve both systemic and mucosal immunity, and provide full protection upon homologous and heterologous infection with influenza (de Haan *et al.*, 2012). These results suggested the potential adjuvant effects of using *L. lactis* in oral immunization, as well as further support the potential application of *L. lactis* as a platform for vaccine delivery. The potential adjuvant effects of using *L. lactis* in oral immunization could be attributed to the presence of bacterial components that can stimulate innate immunity, which is a prerequisite for eliciting adaptive immunity (Mbow *et al.*, 2010). In addition, *L. lactis* presenting heterologous antigen as

a particle to the immune system is more superior to soluble antigen presented on its own, particularly if the vaccine is to be delivered orally (Visweswaran *et al.*, 2014).

In recent years, gut microbiota has gained increasing attention due to its profound impacts on the efficacy of oral vaccines. The microbiota has the potential to influence the development and maturation of immune tissues in the gastrointestinal tract (Lee & Mazmanian, 2010; Valdez *et al.*, 2014). The significance of the influence of microbiota was demonstrated in germ-free mice which showed defective organization of mucosal immune tissues in the gastrointestinal tract (Lee & Mazmanian, 2010), such as smaller and fewer Payer's patches and mesenteric lymph nodes (Falk *et al.*, 1998; Macpherson & Harris, 2004). Defective organization of the immune tissues may compromise its functions and result in impaired oral vaccine efficacy. The impaired efficacy of oral vaccines, particularly rotavirus (Goveia *et al.*, 2010; Jiang *et al.*, 2010; Lopman *et al.*, 2012), poliovirus (John, 1993) and cholera vaccines (Levine, 2010) have been shown in developing countries with poor sanitation. Likewise, children in poorer regions of northern India developed lower mucosal immunity to polio vaccine when compared to children in other parts of India (Grassly *et al.*, 2009). This observation is likely due to dysbiosis, malnutrition and overexposure to microorganisms (Valdez *et al.*, 2014). Years of clinical data on the efficacy of oral cholera vaccines were reviewed and it is concluded that the increased exposure to fecal-oral bacteria reduced immune responses and efficacy of the vaccine (Levine, 2010). Thus, studies on oral vaccine, especially for those involving bacteria as a carrier, should also assess microbiota composition as it is now known to correlate well with vaccine efficacy. In this study, the *L. lactis* strain used does not colonize oral and intestinal cavities (Nouaille *et al.*, 2003). In addition, it does not belong to the human microflora and has a short survival time of 24 hours in the human gastrointestinal tract (Martin *et al.*, 2013). Thus, the non-colonizing *L. lactis* is possibly a good candidate for formulating a mucosal vaccine when compared to other

colonizing microorganisms which could lead to tolerance towards the antigen. Nonetheless, it is worth exploring further the effect of the gut microbiota on the efficacy of LL-HA1/L/AcmA.

In addition to the efficacy of the vaccine, its stability is also another concern in vaccine development. The shelf life of commercially available influenza vaccines is about one year if stored refrigerated (Soema *et al.*, 2015). In this study, *L. lactis* surface displaying HA1/L/AcmA recombinant protein could be stably stored at 4°C for at least 3 days, and a drastic reduction in the stability of this construct was noted on day 5. This presents an additional challenge that should be overcome if it is to be further developed as a vaccine. The instability of *L. lactis* surface displaying HA1/L/AcmA recombinant protein could possibly be due to the poor stability of the HA1/L/AcmA recombinant protein as protein-based vaccines are generally restricted by their low stability (Wang *et al.*, 2015). Several attempts have been made to overcome the instability of protein-based vaccines. One of the techniques to improve protein-based vaccines stability is the conversion of liquid form protein-based vaccine into a dry formulation (Soema *et al.*, 2015). This approach has been successfully applied to *L. lactis* GEM particles displaying PA3 protein (van Roosmalen *et al.*, 2006). The *L. lactis* GEM particles displaying PA3 protein in freeze-dried formulation can be stably stored for at least one year at room temperature without any signs of degradation. In some circumstances, an excipient such as sugar is added to stabilize the antigen by providing a physical barrier during the freeze-drying process (Soema *et al.*, 2015). Furthermore, the stability of protein-based vaccine can also be achieved by encapsulating them using synthetic polymeric materials such as poly (lactic-co-glycolic acid), poly (lactic acid) and poly (ethylene glycol) (Wang *et al.*, 2015). Consequently, each of the mentioned techniques can be applied in future studies to further improve the stability of *L. lactis* surface displaying HA1/L/AcmA recombinant protein.

The present study is limited by focusing only on the protection of LL-HA1/L/AcmA in mice against homologous influenza virus challenge. Heterologous influenza virus challenge should be considered for future investigation. Another potential future investigation could involve the administration of candidate vaccine composed of antigens from multiple influenza subtypes surface displayed on a single *L. lactis* cell, to render protection against a broad range of influenza subtypes. In addition to that, co-administration of LL-HA1/L/AcmA and *L. lactis* secreting IL-2 can be considered for future investigation, as an earlier study had demonstrated that co-administration of antigen and *L. lactis* secreting IL-2 successfully enhanced antigen specific immune responses (Bermúdez-Humaran *et al.*, 2003). Notwithstanding the limitation of the study, findings from the study suggested potential application of *L. lactis* as a platform for vaccine delivery and the importance of mucosal immunity in according protection against lethal challenge with influenza virus.

Over the years, a number of studies have been done in attempt to develop an effective oral-based vaccine, considering oral vaccine is a more favorable approach among the mucosal vaccines due to the ease and lower cost of vaccine administration. Despite the great promise in preclinical studies using animal models, most of them have not been successful in human clinical trials (Pasetti *et al.*, 2011). Although greater amount of lymphoid tissues are present in the intestine, oral immunization presents significant challenges as gastrointestinal tract has low pH environment, digestive enzymes and most importantly often induce tolerance. Hence, development of an effective oral-based vaccine remains a major challenge. Moreover, the mechanisms that underlie the generation of protective immunity upon oral immunization are complex. More intensive studies are essential in future to elucidate the followings: i) better understanding of the innate and adaptive immunity towards the candidate vaccine, ii) the process of lymphocyte homing to mucosal effector sites, iii) approaches to elicite

persistent and robust immunological memory and perhaps iv) an effective yet safe mucosal adjuvants to be used with the oral vaccines.

CHAPTER 6: CONCLUSION

In summary, the binding activity of HA1 onto *L. lactis* was improved when scFv peptide linker was used to link the HA1 and AcmA binding domain in the construction of HA1/L/AcmA recombinant protein. Hence, this supports the hypothesis that surface display of HA1 can be improved by the inclusion of scFv peptide linker in the recombinant protein. Findings obtained from the animal study suggested that oral immunization of the non-recombinant *L. lactis* surface displaying influenza A (H1N1) HA1, LL-HA1/L/AcmA, in mice elicited mucosal immunity in both the gastrointestinal tract and the respiratory tract. The immunization accorded protection of immunized mice upon lethal challenge with virulent influenza virus, hence, supports the hypothesis that this delivery platform will accord protection against lethal challenge with influenza virus in mice. The mechanism of protection was possibly mediated through the stimulation of sIgA responses in mucosal surfaces.

However, the protection of LL-HA1/L/AcmA immunized mice was less effective than the subcutaneous immunization of HA1/L/AcmA-FA, which eventually accorded 100% protection upon lethal challenge with virulent influenza virus. The observed results could be due to poor stimulation of serological immune responses, the serum IgG and IgA, in mice immunized with LL-HA1/L/AcmA. Future work could therefore, focus on the improvement in the stimulation of serological immune responses in addition to the mucosal immune responses.

The findings here have implications for effective design of a potential mucosal candidate vaccine and also highlighted the importance of mucosal immunity in according protection against lethal challenge with influenza virus.

REFERENCES

Adar, Y., Singer, Y., Levi, R., Tzehoval, E., Perk, S., Banet-Noach, C., . . . Ben-Yedidia, T. (2009). A universal epitope-based influenza vaccine and its efficacy against H5N1. *Vaccine, 27*(15), 2099-2107.

Ahmad, Z. A., Yeap, S. K., Ali, A. M., Ho, W. Y., Alitheen, N. B., & Hamid, M. (2012). scFv antibody: principles and clinical application. *Clinical and Developmental Immunology, 2012*, 980250.

Ahmed, B., Loos, M., Vanrompay, D., & Cox, E. (2014). Oral immunization with *Lactococcus lactis*-expressing EspB induces protective immune responses against *Escherichia coli* O157:H7 in a murine model of colonization. *Vaccine, 32*(31), 3909-3916.

Amet, N., Lee, H. F., & Shen, W. C. (2009). Insertion of the designed helical linker led to increased expression of tf-based fusion proteins. *Pharmaceutical Research, 26*(3), 523-528.

Ammor, M. S., & Mayo, B. (2007). Selection criteria for lactic acid bacteria to be used as functional starter cultures in dry sausage production: An update. *Meat Science, 76*(1), 138-146.

Andre, G., Leenhouts, K., Hols, P., & Dufrene, Y. F. (2008). Detection and localization of single LysM-peptidoglycan interactions. *Journal of Bacteriology, 190*(21), 7079-7086.

Arai, R., Ueda, H., Kitayama, A., Kamiya, N., & Nagamune, T. (2001). Design of the linkers which effectively separate domains of a bifunctional fusion protein. *Protein Engineering, 14*(8), 529-532.

Arulanandam, B. P., O'Toole, M., & Metzger, D. W. (1999). Intranasal interleukin-12 is a powerful adjuvant for protective mucosal immunity. *The Journal of Infectious Diseases, 180*(4), 940-949.

Asahi-Ozaki, Y., Yoshikawa, T., Iwakura, Y., Suzuki, Y., Tamura, S., Kurata, T., & Sata, T. (2004). Secretory IgA antibodies provide cross-protection against infection with different strains of influenza B virus. *Journal of Medical Virology, 74*(2), 328-335.

Asahi, Y., Yoshikawa, T., Watanabe, I., Iwasaki, T., Hasegawa, H., Sato, Y., . . . Tamura, S. (2002). Protection against influenza virus infection in polymeric Ig

receptor knockout mice immunized intranasally with adjuvant-combined vaccines. *Journal of Immunology, 168*(6), 2930-2938.

Atwell, J. L., Breheney, K. A., Lawrence, L. J., McCoy, A. J., Kortt, A. A., & Hudson, P. J. (1999). scFv multimers of the anti-neuraminidase antibody NC10: length of the linker between VH and VL domains dictates precisely the transition between diabodies and triabodies. *Protein Engineering, 12*(7), 597-604.

Audouy, S. A., van Selm, S., van Roosmalen, M. L., Post, E., Kanninga, R., Neef, J., . . . Hermans, P. W. (2007). Development of lactococcal GEM-based pneumococcal vaccines. *Vaccine, 25*(13), 2497-2506.

Ayob, A., Selviendran, N., Hampson, A. W., Barr, I. G., Kumarasamy, V., & Chua, K. B. (2006). Outbreak of influenza amongst residential school students in Malaysia. *The Medical Journal of Malaysia, 61*(2), 168-172.

Bai, Y., & Shen, W. C. (2006). Improving the oral efficacy of recombinant granulocyte colony-stimulating factor and transferrin fusion protein by spacer optimization. *Pharmaceutical Research, 23*(9), 2116-2121.

Bateman, A., & Bycroft, M. (2000). The structure of a LysM domain from *E. coli* membrane-bound lytic murein transglycosylase D (MltD). *Journal of Molecular Biology, 299*(4), 1113-1119.

Béliveau, C., Potvin, C., Trudel, J., Asselin, A., & Bellemare, G. (1991). Cloning, sequencing, and expression in *Escherichia coli* of a *Streptococcus faecalis* autolysin. *Jounal of Bacteriology, 173*(18), 5619-5623.

Belshe, R. B., Edwards, K. M., Vesikari, T., Black, S. V., Walker, R. E., Hultquist, M., . . . Group, Caiv- T. Comparative Efficacy Study. (2007). Live attenuated versus inactivated influenza vaccine in infants and young children. *The New England Journal of Medicine, 356*(7), 685-696.

Berlec, A., Malovrh, T., Zadravec, P., Steyer, A., Ravnikar, M., Sabotič, J., . . . Štrukelj, B. (2013). Expression of a hepatitis A virus antigen in *Lactococcus lactis* and *Escherichia coli* and evaluation of its immunogenicity. *Applied Microbiology and Biotechnology, 97*(10), 4333-4342.

Bermúdez-Humarán, L. G. (2009). *Lactococcus lactis* as a live vector for mucosal delivery of therapeutic proteins. *Human Vaccines, 5*(4), 264-267.

Bermúdez-Humarán, L. G., Cortes-Perez, N. G., Le Loir, Y., Alcocer-Gonzalez, J. M., Tamez-Guerra, R. S., de Oca-Luna, R. M., & Langella, P. (2004). An inducible surface presentation system improves cellular immunity against human papillomavirus type 16 E7 antigen in mice after nasal administration with recombinant lactococci. *Journal of Medical Microbiology, 53*(Pt 5), 427-433.

Bermúdez-Humarán, L. G., Langella, P., Cortes-Perez, N. G., Gruss, A., Tamez-Guerra, R. S., Oliveira, S. C., . . . Le Loir, Y. (2003). Intranasal immunization with recombinant *Lactococcus lactis* secreting murine interleukin-12 enhances antigen-specific Th1 cytokine production. *Infection and Immunity, 71*(4), 1887-1896.

Blutt, S. E., Miller, A. D., Salmon, S. L., Metzger, D. W., & Conner, M. E. (2012). IgA is important for clearance and critical for protection from rotavirus infection. *Mucosal Immunology, 5*(6), 712-719.

Bosma, T., Kanninga, R., Neef, J., Audouy, S. A., van Roosmalen, M. L., Steen, A., . . . Leenhouts, K. (2006). Novel surface display system for proteins on non-genetically modified gram-positive bacteria. *Applied and Environmental Microbiology, 72*(1), 880-889.

Bouloy, M., Plotch, S. J., & Krug, R. M. (1978). Globin mRNAs are primers for the transcription of influenza viral RNA *in vitro*. *Proceedings of the National Academy of Sciences of the United States of America, 75*(10), 4886-4890.

Braakman, I., Hoover-Litty, H., Wagner, K. R., & Helenius, A. (1991). Folding of influenza hemagglutinin in the endoplasmic reticulum. *The Journal of Cell Biology, 114*(3), 401-411.

Brandtzaeg, P. (2003). Role of secretory antibodies in the defence against infections. *International Journal of Medical Microbiology, 293*(1), 3-15.

Buccato, S., Maione, D., Rinaudo, C. D., Volpini, G., Taddei, A. R., Rosini, R., . . . Margarit, I. (2006). Use of *Lactococcus lactis* expressing pili from group B *Streptococcus* as a broad-coverage vaccine against streptococcal disease. *The Journal of Infectious Diseases, 194*(3), 331-340.

Buist, G., Karsens, H., Nauta, A., van Sinderen, D., Venema, G., & Kok, J. (1997). Autolysis of *Lactococcus lactis* caused by induced overproduction of its major autolysin, AcmA. *Applied and Environmental Microbiology, 63*(7), 2722-2728.

Buist, G., Kok, J., Leenhouts, K. J., Dabrowska, M., Venema, G., & Haandrikman, A. J. (1995). Molecular cloning and nucleotide sequence of the gene encoding the

major peptidoglycan hydrolase of *Lactococcus lactis*, a muramidase needed for cell separation. *Journal of Bacteriology*, *177*(6), 1554-1563.

Buist, G., Steen, A., Kok, J., & Kuipers, O. P. (2008). LysM, a widely distributed protein motif for binding to (peptido)glycans. *Molecular Microbiology*, *68*(4), 838-847.

Carrat, F., & Flahault, A. (2007). Influenza vaccine: the challenge of antigenic drift. *Vaccine*, *25*(39-40), 6852-6862.

Carter, N. J., & Curran, M. P. (2011). Live attenuated influenza vaccine (FluMist(R); Fluenz): a review of its use in the prevention of seasonal influenza in children and adults. *Drugs*, *71*(12), 1591-1622.

CDC. (2010). Morbidity and Mortality Weekly Report (MMWR). Retrieved from http://www.cdc.gov/mmwr/preview/mmwrhtml/mm5933a1.htm?s_cid=mm5933a1_w

CDC. (2016a). ACIP votes down use of LAIV for 2016-2017 flu season. Retrieved from https://www.cdc.gov/media/releases/2016/s0622-laiv-flu.html

CDC. (2016b). Cell-based flu vaccines. Retrieved from http://www.cdc.gov/flu/protect/vaccine/cell-based.htm

CDC. (2016c). Flublok seasonal influenza (flu) vaccine. Retrieved from http://www.cdc.gov/flu/protect/vaccine/qa_flublok-vaccine.htm

CDC. (2016d). Influenza vaccines — United States, 2016–17 influenza season. Retrieved from http://www.cdc.gov/flu/protect/vaccine/vaccines.htm

CDC. (2016e). New flu information for 2016-2017. Retrieved from http://www.cdc.gov/flu/about/season/flu-season-2016-2017.htm

CDC. (2016f). Types of influenza viruses. Retrieved from http://www.cdc.gov/flu/about/viruses/types.htm

CDC. (2018). How the flu virus can change: "drift" and "shift". Retrieved from https://www.cdc.gov/flu/about/viruses/change.htm

Chapot-Chartier, M. P. (2014). Interactions of the cell-wall glycopolymers of lactic acid bacteria with their bacteriophages. *Frontiers in Microbiology, 5*, 236.

Chapot-Chartier, M. P., & Kulakauskas, S. (2014). Cell wall structure and function in lactic acid bacteria. *Microbial Cell Factories, 13 Suppl 1*, S9.

Chee, H. Y., & AbuBakar, S. (1998). Construction of a single chain variable fragment (ScFv) antibody recognizing the dengue 2 virus envelope protein. *Asia-Pacific Journal of Molecular Biology and Biotechnology, 6*(2), 79-87.

Chen, J., Huang, D., Chen, W., Guo, C., Wei, B., Wu, C., . . . Xiong, S. (2014). Linker-extended native cyanovirin-N facilitates PEGylation and potently inhibits HIV-1 by targeting the glycan ligand. *PLoS One, 9*(1), e86455.

Chen, M. W., Cheng, T. J., Huang, Y., Jan, J. T., Ma, S. H., Yu, A. L., . . . Ho, D. D. (2008). A consensus-hemagglutinin-based DNA vaccine that protects mice against divergent H5N1 influenza viruses. *Proceedings of the National Academy of Sciences of the United States of America, 105*(36), 13538-13543.

Chen, X., Zaro, J. L., & Shen, W. C. (2013). Fusion protein linkers: property, design and functionality. *Advanced Drug Delivery Reviews, 65*(10), 1357-1369.

Cho, H. J., Shin, H. J., Han, I. K., Jung, W. W., Kim, Y. B., Sul, D., & Oh, Y. K. (2007). Induction of mucosal and systemic immune responses following oral immunization of mice with *Lactococcus lactis* expressing human papillomavirus type 16 L1. *Vaccine, 25*(47), 8049-8057.

Cox, M. M., & Hashimoto, Y. (2011). A fast track influenza virus vaccine produced in insect cells. *Journal of Invertebrate Pathology, 107 Suppl*, S31-41.

Cox, M. M., Patriarca, P. A., & Treanor, J. (2008). FluBlok, a recombinant hemagglutinin influenza vaccine. *Influenza and Other Respiratory Viruses, 2*(6), 211-219.

Cox, N. J., & Subbarao, K. (2000). Global epidemiology of influenza: past and present. *Annual Review of Medicine, 51*, 407-421.

Cox, R. J., Brokstad, K. A., & Ogra, P. (2004). Influenza virus: immunity and vaccination strategies. Comparison of the immune response to inactivated and live, attenuated influenza vaccines. *Scandinavian Journal of Immunology, 59*(1), 1-15.

Cunliffe, S. L., Wyer, J. R., Sutton, J. K., Lucas, M., Harcourt, G., Klenerman, P., . . . Kelleher, A. D. (2002). Optimization of peptide linker length in production of MHC class II/peptide tetrameric complexes increases yield and stability, and allows identification of antigen-specific $CD4^{+}T$ cells in peripheral blood mononuclear cells. *European Journal of Immunology, 32*(12), 3366-3375.

Czerkinsky, C., Svennerholm, A. M., Quiding, M., Jonsson, R., & Holmgren, J. (1991). Antibody-producing cells in peripheral blood and salivary glands after oral cholera vaccination of humans. *Infection and Immunity, 59*(3), 996-1001.

Dang, J., Jing, L., Shi, W., Qin, P., Li, Y., & Diao, A. (2015). Expression and purification of active recombinant human bone morphogenetic 7-2 dimer fusion protein. *Protein Expression and Purification, 115*, 61-68.

de Ambrosini, V. M., Gonzalez, S., Perdigon, G., de Ruiz Holgado, A. P., & Oliver, G. (1996). Chemical composition of the cell wall of lactic acid bacteria and related species. *Chemical and Pharmaceutical Bulletin (Tokyo), 44*(12), 2263-2267.

de Haan, A., Haijema, B. J., Voorn, P., Meijerhof, T., van Roosmalen, M. L., & Leenhouts, K. (2012). Bacterium-like particles supplemented with inactivated influenza antigen induce cross-protective influenza-specific antibody responses through intranasal administration. *Vaccine, 30*(32), 4884-4891.

De Magistris, M. T. (2006). Mucosal delivery of vaccine antigens and its advantages in pediatrics. *Advanced Drug Delivery Reviews, 58*(1), 52-67.

Dimasi, N., Gao, C., Fleming, R., Woods, R. M., Yao, X. T., Shirinian, L., . . . Wu, H. (2009). The design and characterization of oligospecific antibodies for simultaneous targeting of multiple disease mediators. *Journal of Molecular Biology, 393*(3), 672-692.

DiNapoli, J. M., Nayak, B., Yang, L., Finneyfrock, B. W., Cook, A., Andersen, H., . . . Bukreyev, A. (2010). Newcastle disease virus-vectored vaccines expressing the hemagglutinin or neuraminidase protein of H5N1 highly pathogenic avian influenza virus protect against virus challenge in monkeys. *Journal of Virology, 84*(3), 1489-1503.

Dunkle, L.M., Izikson, R., Post, P., & Cox, M. M. (2015). Introducing Modern Recombinant Technology to the Realm of Seasonal Influenza Vaccine: Flublok® For Prevention of Influenza in Adults. *EC Microbiology, 2*(1), 224-234.

Endo, A., Tanaka, N., Oikawa, Y., Okada, S., & Dicks, L. (2014). Fructophilic characteristics of *Fructobacillus* spp. may be due to the absence of an alcohol/acetaldehyde dehydrogenase gene (*adhE*). *Current Microbiology, 68*(4), 531-535.

Endo, A., Tanizawa, Y., Tanaka, N., Maeno, S., Kumar, H., Shiwa, Y., . . . Arita, M. (2015). Comparative genomics of *Fructobacillus* spp. and *Leuconostoc* spp. reveals niche-specific evolution of *Fructobacillus* spp. *BMC Genomics, 16*, 1117.

Engelhardt, O. G., & Fodor, E. (2006). Functional association between viral and cellular transcription during influenza virus infection. *Reviews in Medical Virology, 16*(5), 329-345.

Falk, P. G., Hooper, L. V., Midtvedt, T., & Gordon, J. I. (1998). Creating and maintaining the gastrointestinal ecosystem: what we know and need to know from gnotobiology. *Microbiology and Molecular Biology Reviews, 62*(4), 1157-1170.

FDA. (2016). FDA information regarding FluMist Quadrivalent vaccine. Retrieved fromh ttp://www.fda.gov/BiologicsBloodVaccines/Vaccines/ApprovedProducts/ucm508761.htm

Freund, C., Ross, A., Guth, B., Pluckthun, A., & Holak, T. A. (1993). Characterization of the linker peptide of the single-chain Fv fragment of an antibody by NMR spectroscopy. *FEBS Letters, 320*(2), 97-100.

Gao, S., Li, D., Liu, Y., Zha, E., Zhou, T., & Yue, X. (2015). Oral immunization with recombinant hepatitis E virus antigen displayed on the *Lactococcus lactis* surface enhances ORF2-specific mucosal and systemic immune responses in mice. *International Immunopharmacology, 24*(1), 140-145.

Garvey, K. J., Saedi, M. S., & Ito, J. (1986). Nucleotide sequence of *Bacillus* phage Ø29 genes 14 and 15: homology of gene 15 with other phage lysozymes. *Nucleic Acids Research, 14*(24), 10001-10008.

Gianchecchi, Elena, Trombetta, Claudia, Piccirella, Simona, & Montomoli, Emanuele. (2016). Evaluating influenza vaccines: progress and perspectives. *Future Virology, 11*(5), 379-393.

Giaouris, E., Chapot-Chartier, M. P., & Briandet, R. (2009). Surface physicochemical analysis of natural *Lactococcus lactis* strains reveals the existence of

hydrophobic and low charged strains with altered adhesive properties. *International Journal of Food Microbiology, 131*(1), 2-9.

Gong, W., Zheng, Y., Chao, F., Li, Y., Xu, Z., Huang, G., . . . He, F. (2010). The anti-inflammatory activity of HMGB1 A box is enhanced when fused with C-terminal acidic tail. *Journal of Biomedicine and Biotechnology, 2010*, 915234.

Goveia, M. G., Nelson, C. B., & Ciarlet, M. (2010). RotaTeq: Progress toward developing world access. *The Journal of Infectious Diseases, 202 Suppl*, S87-92.

Grassly, N. C., Jafari, H., Bahl, S., Durrani, S., Wenger, J., Sutter, R. W., & Aylward, R. B. (2009). Mucosal immunity after vaccination with monovalent and trivalent oral poliovirus vaccine in India. *The Journal of Infectious Diseases, 200*(5), 794-801.

Gu, X., Jia, X., Feng, J., Shen, B., Huang, Y., Geng, S., . . . Long, M. (2010). Molecular modeling and affinity determination of scFv antibody: proper linker peptide enhances its activity. *Annals of Biomedical Engineering, 38*(2), 537-549.

Gupta, V., Dawood, F. S., Muangchana, C., Lan, P. T., Xeuatvongsa, A., Sovann, L., . . . Olsen, S. J. (2012). Influenza vaccination guidelines and vaccine sales in southeast Asia: 2008-2011. *PLoS One, 7*(12), e52842.

Habimana, O., Le Goff, C., Juillard, V., Bellon-Fontaine, M. N., Buist, G., Kulakauskas, S., & Briandet, R. (2007). Positive role of cell wall anchored proteinase PrtP in adhesion of lactococci. *BMC Microbiology, 7*, 36.

Hancock, S., Whitney, D., & Andrews, T. J. (2008). The initial interactions underlying binocular rivalry require visual awareness. *Journal of Vision, 8*(1), 3 1-9.

Hansson, M, Ståhl, S, Nguyen, T N, Bächi, T, Robert, A, Binz, H, . . . Uhlén, M. (1992). Expression of recombinant proteins on the surface of the coagulase-negative bacterium *Staphylococcus xylosus*. *Journal of Bacteriology, 174*(13), 4239-4245.

Hauri, A. M., Armstrong, G. L., & Hutin, Y. J. (2004). The global burden of disease attributable to contaminated injections given in health care settings. *International Journal of STD and AIDS, 15*(1), 7-16.

Hinc, K., Iwanicki, A., & Obuchowski, M. (2013). New stable anchor protein and peptide linker suitable for successful spore surface display in *B. subtilis*. *Microbial Cell Factories, 12*, 22.

Hoedemaeker, F. J., Signorelli, T., Johns, K., Kuntz, D. A., & Rose, D. R. (1997). A single chain Fv fragment of P-glycoprotein-specific monoclonal antibody C219. Design, expression, and crystal structure at 2.4 A resolution. *Journal of Biological Chemistry*, *272*(47), 29784-29789.

Hoelscher, M. A., Garg, S., Bangari, D. S., Belser, J. A., Lu, X., Stephenson, I., . . . Sambhara, S. (2006). Development of adenoviral-vector-based pandemic influenza vaccine against antigenically distinct human H5N1 strains in mice. *The Lancet, 367*(9509), 475-481.

Holmgren, J., & Czerkinsky, C. (2005). Mucosal immunity and vaccines. *Nature Medicine, 11*(4 Suppl), S45-53.

Hong, S. H., Byun, Y. H., Nguyen, C. T., Kim, S. Y., Seong, B. L., Park, S., . . . Lee, S. E. (2012). Intranasal administration of a flagellin-adjuvanted inactivated influenza vaccine enhances mucosal immune responses to protect mice against lethal infection. *Vaccine, 30*(2), 466-474.

Huang, Z., Zhang, C., Chen, S., Ye, F., & Xing, X. H. (2013). Active inclusion bodies of acid phosphatase PhoC: aggregation induced by GFP fusion and activities modulated by linker flexibility. *Microbial Cell Factories, 12*, 25.

Huston, J. S., Levinson, D., Mudgett-Hunter, M., Tai, M. S., Novotny, J., Margolies, M. N., . . . et al. (1988). Protein engineering of antibody binding sites: recovery of specific activity in an anti-digoxin single-chain Fv analogue produced in *Escherichia coli*. *Proceedings of the National Academy of Sciences of the United States of America, 85*(16), 5879-5883.

Iliades, P., Kortt, A. A., & Hudson, P. J. (1997). Triabodies: single chain Fv fragments without a linker form trivalent trimers. *FEBS Letters, 409*(3), 437-441.

Ito, T., Couceiro, J. N., Kelm, S., Baum, L. G., Krauss, S., Castrucci, M. R., . . . Kawaoka, Y. (1998). Molecular basis for the generation in pigs of influenza A viruses with pandemic potential. *Journal of Virology, 72*(9), 7367-7373.

Jiang, V., Jiang, B., Tate, J., Parashar, U. D., & Patel, M. M. (2010). Performance of rotavirus vaccines in developed and developing countries. *Human Vaccines, 6*(7), 532-542.

Joan, S. S., Pui-Fong, J., Song, A. A., Chang, L. Y., Yusoff, K., AbuBakar, S., & Rahim, R. A. (2016). Oral vaccine of *Lactococcus lactis* harbouring pandemic H1N1 2009 haemagglutinin1 and nisP anchor fusion protein elevates anti-HA1 sIgA levels in mice. *Biotechnology Letters, 38*(5), 793-799.

Johnson, N. P., & Mueller, J. (2002). Updating the accounts: global mortality of the 1918-1920 "Spanish" influenza pandemic. *Bulletin of the History Medicine, 76*(1), 105-115.

John, T. J. (1993). Immunisation against polioviruses in developing countries. *Reviews in Medical Virology, 3*(3), 149-160.

Kantele, A., Westerholm, M., Kantele, J. M., Makela, P. H., & Savilahti, E. (1999). Homing potentials of circulating antibody-secreting cells after administration of oral or parenteral protein or polysaccharide vaccine in humans. *Vaccine, 17*(3), 229-236.

Khurana, S., Verma, S., Verma, N., Crevar, C. J., Carter, D. M., Manischewitz, J., . . . Golding, H. (2010). Properly folded bacterially expressed H1N1 hemagglutinin globular head and ectodomain vaccines protect ferrets against H1N1 pandemic influenza virus. *PLoS One, 5*(7), e11548.

Kim, J. H., & Jacob, J. (2009). DNA vaccines against influenza viruses. *Current Topics in Microbiology and Immunology, 333*, 197-210.

Kim, S. H., Lee, K. Y., & Jang, Y. S. (2012). Mucosal immune system and M cell-targeting strategies for oral mucosal vaccination. *Immune Network, 12*(5), 165-175.

Kim, Y. G., Cha, J., & Chandrasegaran, S. (1996). Hybrid restriction enzymes: zinc finger fusions to Fok I cleavage domain. *Proceedings of the National Academy of Sciences of the United States of America, 93*(3), 1156-1160.

Klein, J. S., Jiang, S., Galimidi, R. P., Keeffe, J. R., & Bjorkman, P. J. (2014). Design and characterization of structured protein linkers with differing flexibilities. *Protein Engineering Design and Selection, 27*(10), 325-330.

Klement, M., Liu, C., Loo, B. L., Choo, A. B., Ow, D. S., & Lee, D. Y. (2015). Effect of linker flexibility and length on the functionality of a cytotoxic engineered antibody fragment. *Journal of Biotechnology, 199*, 90-97.

Kortt, A. A., Dolezal, O., Power, B. E., & Hudson, P. J. (2001). Dimeric and trimeric antibodies: high avidity scFvs for cancer targeting. *Biomolecular Engineering, 18*(3), 95-108.

Kortt, A. A., Lah, M., Oddie, G. W., Gruen, C. L., Burns, J. E., Pearce, L. A., . . . Hudson, P. J. (1997). Single-chain Fv fragments of anti-neuraminidase antibody NC10 containing five- and ten-residue linkers form dimers and with zero-

residue linker a trimer. *Protein Engineering Design and Selection, 10*(4), 423-433.

Kunisawa, J., Kurashima, Y., & Kiyono, H. (2012). Gut-associated lymphoid tissues for the development of oral vaccines. *Advanced Drug Delivery Reviews, 64*(6), 523-530.

Kunkel, E. J., & Butcher, E. C. (2003). Plasma-cell homing. *Nature Reviews Immunology, 3*(10), 822-829.

Lacroix-Desmazes, S., Navarrete, A. M., André, S., Bayry, J., Kaveri, S. V., & Dasgupta, S. (2008). Dynamics of factor VIII interactions determine its immunologic fate in hemophilia A. *Blood, 112*(2), 240-249.

Laddy, D. J., Yan, J., Kutzler, M., Kobasa, D., Kobinger, G. P., Khan, A. S., . . . Weiner, D. B. (2008). Heterosubtypic protection against pathogenic human and avian influenza viruses via *in vivo* electroporation of synthetic consensus DNA antigens. *PLoS One, 3*(6), e2517.

Lambert, L. C., & Fauci, A. S. (2010). Influenza vaccines for the future. *The New England Journal of Medicine, 363*(21), 2036-2044.

Lee, M. H., Roussel, Y., Wilks, M., & Tabaqchali, S. (2001). Expression of *Helicobacter pylori* urease subunit B gene in *Lactococcus lactis* MG1363 and its use as a vaccine delivery system against *H. pylori* infection in mice. *Vaccine, 19*(28-29), 3927-3935.

Lee, Y. K., & Mazmanian, S. K. (2010). Has the microbiota played a critical role in the evolution of the adaptive immune system? *Science, 330*(6012), 1768-1773.

Lee, Y. T., Kim, K. H., Ko, E. J., Lee, Y. N., Kim, M. C., Kwon, Y. M., . . . Kang, S. M. (2014). New vaccines against influenza virus. *Clinical and Experimental Vaccine Research, 3*(1), 12-28.

Lei, H., Peng, X., Jiao, H., Zhao, D., & Ouyang, J. (2015a). Broadly protective immunity against divergent influenza viruses by oral co-administration of *Lactococcus lactis* expressing nucleoprotein adjuvanted with cholera toxin B subunit in mice. *Microbial Cell Factories, 14*, 111.

Lei, H., Peng, X., Zhao, D., Jiao, H., & Ouyang, J. (2015b). Cross-protection of *Lactococcus lactis*-displayed HA2 subunit against homologous and heterologous influenza A viruses in mice. *Archives of Virology, 160*(12), 3011-3019.

Lei, H., Peng, X., Zhao, D., Ouyang, J., Jiao, H., Shu, H., & Ge, X. (2015c). *Lactococcus lactis* displayed neuraminidase confers cross protective immunity against influenza A viruses in mice. *Virology, 476*, 189-195.

Lei, H., Sheng, Z., Ding, Q., Chen, J., Wei, X., Lam, D. M., & Xu, Y. (2011). Evaluation of oral immunization with recombinant avian influenza virus HA1 displayed on the *Lactococcus lactis* surface and combined with the mucosal adjuvant cholera toxin subunit B. *Clinical and Vaccine Immunology, 18*(7), 1046-1051.

Lei, H., Xu, Y., Chen, J., Wei, X., & Lam, D. M. (2010). Immunoprotection against influenza H5N1 virus by oral administration of enteric-coated recombinant *Lactococcus lactis* mini-capsules. *Virology, 407*(2), 319-324.

Levine, M. M. (2003). Can needle-free administration of vaccines become the norm in global immunization? *Nature Medicine, 9*(1), 99-103.

Levine, M. M. (2010). Immunogenicity and efficacy of oral vaccines in developing countries: lessons from a live cholera vaccine. *BMC Biology, 8*, 129.

Liew, F. Y., Russell, S. M., Appleyard, G., Brand, C. M., & Beale, J. (1984). Cross-protection in mice infected with influenza A virus by the respiratory route is correlated with local IgA antibody rather than serum antibody or cytotoxic T cell reactivity. *European Journal of Immunology, 14*(4), 350-356.

Lim, S. H., Jahanshiri, F., Rahim, R. A., Sekawi, Z., & Yusoff, K. (2010). Surface display of respiratory syncytial virus glycoproteins in *Lactococcus lactis* NZ9000. *Letters in Applied Microbiology, 51*(6), 658-664.

Liu, G., Tarbet, B., Song, L., Reiserova, L., Weaver, B., Chen, Y., . . . Tussey, L. (2011). Immunogenicity and efficacy of flagellin-fused vaccine candidates targeting 2009 pandemic H1N1 influenza in mice. *PLoS One, 6*(6), e20928.

Liu, W. H., Chuang, H. L., Huang, Y. T., Wu, C. C., Chou, G. T., Wang, S., & Tsai, Y. C. (2016a). Alteration of behavior and monoamine levels attributable to *Lactobacillus plantarum* PS128 in germ-free mice. *Behavioural Brain Research, 298*(Pt B), 202-209.

Liu, Y. W., Liu, W. H., Wu, C. C., Juan, Y. C., Wu, Y. C., Tsai, H. P., . . . Tsai, Y. C. (2016b). Psychotropic effects of *Lactobacillus plantarum* PS128 in early life-stressed and naive adult mice. *Brain Research, 1631*, 1-12.

Ljungh, A., & Wadström, T. (2006). Lactic acid bacteria as probiotics. *Current Issues in Intestinal Microbiology, 7*(2), 73-89.

Lopman, B. A., Pitzer, V. E., Sarkar, R., Gladstone, B., Patel, M., Glasser, J., . . . Parashar, U. D. (2012). Understanding reduced rotavirus vaccine efficacy in low socio-economic settings. *PLoS One, 7*(8), e41720.

Lu, B., Zhou, H., Ye, D., Kemble, G., & Jin, H. (2005). Improvement of influenza A/Fujian/411/02 (H3N2) virus growth in embryonated chicken eggs by balancing the hemagglutinin and neuraminidase activities, using reverse genetics. *Journal of Virology, 79*(11), 6763-6771.

Lu, P., & Feng, M. G. (2008). Bifunctional enhancement of a beta-glucanase-xylanase fusion enzyme by optimization of peptide linkers. *Applied Microbiology and Biotechnology, 79*(4), 579-587.

Macpherson, A. J., & Harris, N. L. (2004). Interactions between commensal intestinal bacteria and the immune system. *Nature Reviews Immunology, 4*(6), 478-485.

Marelli, B., Perez, A. R., Banchio, C., de Mendoza, D., & Magni, C. (2011). Oral immunization with live *Lactococcus lactis* expressing rotavirus VP8 subunit induces specific immune response in mice. *Journal of Virological Methods, 175*(1), 28-37.

Martin, R., Miquel, S., Ulmer, J., Kechaou, N., Langella, P., & Bermúdez-Humarán, L. G. (2013). Role of commensal and probiotic bacteria in human health: a focus on inflammatory bowel disease. *Microbial Cell Factories, 12*, 71.

Mbawuike, I. N., Pacheco, S., Acuna, C. L., Switzer, K. C., Zhang, Y., & Harriman, G. R. (1999). Mucosal immunity to influenza without IgA: an IgA knockout mouse model. *The Journal of Immunology, 162*(5), 2530-2537.

Mbow, M. L., De Gregorio, E., Valiante, N. M., & Rappuoli, R. (2010). New adjuvants for human vaccines. *Current Opinion in Immunology, 22*(3), 411-416.

McMichael, A. J., Gotch, F. M., Noble, G. R., & Beare, P. A. (1983). Cytotoxic T-cell immunity to influenza. *The New England Journal of Medicine, 309*(1), 13-17.

Mesnage, S., Dellarole, M., Baxter, N. J., Rouget, J. B., Dimitrov, J. D., Wang, N., . . . Williamson, M. P. (2014). Molecular basis for bacterial peptidoglycan recognition by LysM domains. *Nature Communications, 5*, 4269.

Michon, C., Langella, P., Eijsink, V. G., Mathiesen, G., & Chatel, J. M. (2016). Display of recombinant proteins at the surface of lactic acid bacteria: strategies and applications. *Microbial Cell Factories, 15*, 70.

Muhammad Ismail, H. I., Tan, K. K., Lee, Y. L., Pau, W. S., Razali, K. A., Mohamed, T., . . . Hanif, J. (2011). Characteristics of children hospitalized for pandemic (H1N1) 2009, Malaysia. *Emerging Infectious Diseases, 17*(4), 708-710.

Neutra, M. R., & Kozlowski, P. A. (2006). Mucosal vaccines: the promise and the challenge. *Nature Reviews Immunology, 6*(2), 148-158.

Noh, J. Y., & Kim, W. J. (2013). Influenza vaccines: unmet needs and recent developments. *Infection and Chemotherapy, 45*(4), 375-386.

Norton, P. M., Brown, H. W., Wells, J. M., Macpherson, A. M., Wilson, P. W., & Le Page, R. W. (1996). Factors affecting the immunogenicity of tetanus toxin fragment C expressed in *Lactococcus lactis*. *FEMS Immunology and Medical Microbiology, 14*(2-3), 167-177.

Nouaille, S., Ribeiro, L. A., Miyoshi, A., Pontes, D., Le Loir, Y., Oliveira, S. C., . . . Azevedo, V. (2003). Heterologous protein production and delivery systems for *Lactococcus lactis*. *Genetics and Molecular Research, 2*(1), 102-111.

Okuno, Y., Isegawa, Y., Sasao, F., & Ueda, S. (1993). A common neutralizing epitope conserved between the hemagglutinins of influenza A virus H1 and H2 strains. *Journal of Virology, 67*(5), 2552-2558.

Ong, M. P., Sam, I. C., Azwa, H., Mohd Zakaria, I. E., Kamarulzaman, A., Wong, M. H., . . . Hussain, S. H. (2010). High direct healthcare costs of patients hospitalised with pandemic (H1N1) 2009 influenza in Malaysia. *The Journal of Infection, 61*(5), 440-442.

Pasetti, M. F., Simon, J. K., Sztein, M. B., & Levine, M. M. (2011). Immunology of gut mucosal vaccines. *Immunological Reviews, 239*(1), 125-148.

Pei, H., Liu, J., Cheng, Y., Sun, C., Wang, C., Lu, Y., . . . Xiang, H. (2005). Expression of SARS-coronavirus nucleocapsid protein in *Escherichia coli* and *Lactococcus lactis* for serodiagnosis and mucosal vaccination. *Applied Microbiology and Biotechnology, 68*(2), 220-227.

Perez, C. A., Eichwald, C., Burrone, O., & Mendoza, D. (2005). Rotavirus vp7 antigen produced by *Lactococcus lactis* induces neutralizing antibodies in mice. *Journal of Applied Microbiology, 99*(5), 1158-1164.

Petrovic, D. M., Leenhouts, K., van Roosmalen, M. L., Kleinjan, F., & Broos, J. (2012). Monitoring lysin motif-ligand interactions via tryptophan analog fluorescence spectroscopy. *Analytical Biochemistry, 428*(2), 111-118.

Polo, V., Alberola, A., Andres, J., Anthony, J., & Pilkington, M. (2008). Towards understanding of magnetic interactions within a series of tetrathiafulvalene-π conjugated-verdazyl diradical cation system: a density functional theory study. *Physical Chemistry Chemical Physics, 10*(6), 857-864.

Pouwels, P. H., Leer, R. J., Shaw, M., Heijne den Bak-Glashouwer, M. J., Tielen, F. D., Smit, E., . . . Conway, P. L. (1998). Lactic acid bacteria as antigen delivery vehicles for oral immunization purposes. *International Journal of Food Microbiology, 41*(2), 155-167.

Powers, D. C., Smith, G. E., Anderson, E. L., Kennedy, D. J., Hackett, C. S., Wilkinson, B. E., . . . Treanor, J. J. (1995). Influenza A virus vaccines containing purified recombinant H3 hemagglutinin are well tolerated and induce protective immune responses in healthy adults. *The Journal of Infectious Diseases, 171*(6), 1595-1599.

Prabakaran, M., Madhan, S., Prabhu, N., Qiang, J., & Kwang, J. (2010). Gastrointestinal delivery of baculovirus displaying influenza virus hemagglutinin protects mice against heterologous H5N1 infection. *Journal of Virology, 84*(7), 3201-3209.

Quiding-Järbrink, M., Nordström, I., Granström, G., Kilander, A., Jertborn, M., Butcher, E. C., . . . Czerkinsky, C. (1997). Differential expression of tissue-specific adhesion molecules on human circulating antibody-forming cells after systemic, enteric, and nasal immunizations. A molecular basis for the compartmentalization of effector B cell responses. *The Journal of Clinical Investigation, 99*(6), 1281-1286.

Raha, A. R., Varma, N. R., Yusoff, K., Ross, E., & Foo, H. L. (2005). Cell surface display system for *Lactococcus lactis*: a novel development for oral vaccine. *Applied Microbiology and Biotechnology, 68*(1), 75-81.

Ramasamy, R., Yasawardena, S., Zomer, A., Venema, G., Kok, J., & Leenhouts, K. (2006). Immunogenicity of a malaria parasite antigen displayed by *Lactococcus lactis* in oral immunisations. *Vaccine, 24*(18), 3900-3908.

Reichmann, N. T., & Gründling, A. (2011). Location, synthesis and function of glycolipids and polyglycerolphosphate lipoteichoic acid in Gram-positive bacteria of the phylum *Firmicutes*. *FEMS Microbiology Letters, 319*(2), 97-105.

Renegar, K. B., Jackson, G. D., & Mestecky, J. (1998). In vitro comparison of the biologic activities of monoclonal monomeric IgA, polymeric IgA, and secretory IgA. *The Journal of Immunology, 160*(3), 1219-1223.

Renegar, K. B., & Small, P. A., Jr. (1991). Passive transfer of local immunity to influenza virus infection by IgA antibody. *The Journal of Immunology, 146*(6), 1972-1978.

Renegar, K. B., Small, P. A., Jr., Boykins, L. G., & Wright, P. F. (2004). Role of IgA versus IgG in the control of influenza viral infection in the murine respiratory tract. *The Journal of Immunology, 173*(3), 1978-1986.

Robinson, K., Chamberlain, L. M., Schofield, K. M., Wells, J. M., & Le Page, R. W. (1997). Oral vaccination of mice against tetanus with recombinant *Lactococcus lactis*. *Nature Biotechnology, 15*(7), 653-657.

Rota, P. A., De, B. K., Shaw, M. W., Black, R. A., Gamble, W. C., & Kendal, A. P. (1990). Comparison of inactivated, live and recombinant DNA vaccines against influenza virus in a mouse model. *Virus Research, 16*(1), 83-93.

Rouleau, N., Wang, J., Karras, L., Andrews, E., Bielefeld-Sevigny, M., & Chen, Y. (2008). Highly sensitive assays for SUMOylation and small ubiquitin-like modifier-dependent protein-protein interactions. *Analytical Biochemistry, 375*(2), 364-366.

Saat, Z., Abdul Rashid, T. R., Yusof, M. A., Kassim, F. M., Thayan, R., Kuen, L. S., . . . Saraswathy, T. S. (2010). Seasonal influenza virus strains circulating in Malaysia from 2005 to 2009. *Southeast Asian Journal of Tropical Medicine and Public Health, 41*(6), 1368-1373.

Sabourin, M., Tuzon, C. T., Fisher, T. S., & Zakian, V. A. (2007). A flexible protein linker improves the function of epitope-tagged proteins in *Saccharomyces cerevisiae*. *Yeast, 24*(1), 39-45.

Sakamoto, S., Taura, F., Putalun, W., Pongkitwitoon, B., Tsuchihashi, R., Morimoto, S., . . . Tanaka, H. (2009). Construction and expression of specificity-improved single-chain variable fragments against the bioactive naphthoquinone, plumbagin. *Biological Pharmaceutical Bulletin, 32*(3), 434-439.

Saluja, V., Amorij, J. P., van Roosmalen, M. L., Leenhouts, K., Huckriede, A., Hinrichs, W. L., & Frijlink, H. W. (2010). Intranasal delivery of influenza subunit vaccine formulated with GEM particles as an adjuvant. *The AAPS Journal, 12*(2), 109-116.

Sam, I. C., & Abu Bakar, S. (2009). Pandemic influenza A (H1N1) 2009 in Malaysia--the next phase. *The Medical Journal of Malaysia, 64*(2), 105-107.

Samji, T. (2009). Influenza A: understanding the viral life cycle. *Yale Journal of Biology and Medicine, 82*(4), 153-159.

Schwartz, J. A., Buonocore, L., Suguitan, A. L., Jr., Silaghi, A., Kobasa, D., Kobinger, G., . . . Rose, J. K. (2010). Potent vesicular stomatitis virus-based avian influenza vaccines provide long-term sterilizing immunity against heterologous challenge. *Journal of Virology, 84*(9), 4611-4618.

Shahidah, N., Merican, I., & Ismail, R. (2003). Influenza surveillance in Malaysia: 1997-2001. *Malaysian Journal of Public Health Medicine, 3*(1), 11-15.

Shakya, A. K., Chowdhury, M. Y., Tao, W., & Gill, H. S. (2016). Mucosal vaccine delivery: Current state and a pediatric perspective. *Journal of Controlled Release, 240*, 394-413.

Shan, D., Press, O. W., Tsu, T. T., Hayden, M. S., & Ledbetter, J. A. (1999). Characterization of scFv-Ig constructs generated from the anti-CD20 mAb 1F5 using linker peptides of varying lengths. *The Journal of Immunology, 162*(11), 6589-6595.

Shi, S. H., Yang, W. T., Yang, G. L., Cong, Y. L., Huang, H. B., Wang, Q., . . . Li, Y. (2014). Immunoprotection against influenza virus H9N2 by the oral administration of recombinant *Lactobacillus plantarum*NC8 expressing hemagglutinin in BALB/c mice. *Virology, 464-465*, 166-176.

Sim, A. C., Lin, W., Tan, G. K., Sim, M. S., Chow, V. T., & Alonso, S. (2008). Induction of neutralizing antibodies against dengue virus type 2 upon mucosal administration of a recombinant *Lactococcus lactis* strain expressing envelope domain III antigen. *Vaccine, 26*(9), 1145-1154.

Soema, P. C., Kompier, R., Amorij, J. P., & Kersten, G. F. (2015). Current and next generation influenza vaccines: Formulation and production strategies. *European Journal of Pharmaceutics and Biopharmaceutics, 94*, 251-263.

Song, J. M. (2016). Advances in novel influenza vaccines: a patent review. *Journal of Microbiology*, *54*(6), 403-412.

Song, L., Xiong, D., Kang, X., Yang, Y., Wang, J., Guo, Y., . . . Jiao, X. (2015). An avian influenza A (H7N9) virus vaccine candidate based on the fusion protein of hemagglutinin globular head and *Salmonella typhimurium* flagellin. *BMC Biotechnology*, *15*, 79.

Sridhar, S., Begom, S., Bermingham, A., Hoschler, K., Adamson, W., Carman, W., . . . Lalvani, A. (2013). Cellular immune correlates of protection against symptomatic pandemic influenza. *Nature Medicine*, *19*(10), 1305-1312.

Steen, A., Buist, G., Kramer, N. E., Jalving, R., Benus, G. F., Venema, G., . . . Kok, J. (2008). Reduced lysis upon growth of *Lactococcus lactis* on galactose is a consequence of decreased binding of the autolysin AcmA. *Applied and Environmental Microbiology*, *74*(15), 4671-4679.

Steen, A., Buist, G., Leenhouts, K. J., El Khattabi, M., Grijpstra, F., Zomer, A. L., . . . Kok, J. (2003). Cell wall attachment of a widely distributed peptidoglycan binding domain is hindered by cell wall constituents. *Journal of Biological Chemistry*, *278*(26), 23874-23881.

Steidler, L., Robinson, K., Chamberlain, L., Schofield, K. M., Remaut, E., Le Page, R. W., & Wells, J. M. (1998). Mucosal delivery of murine interleukin-2 (IL-2) and IL-6 by recombinant strains of *Lactococcus lactis* coexpressing antigen and cytokine. *Infection and Immunity*, *66*(7), 3183-3189.

Subbarao, K., Murphy, B. R., & Fauci, A. S. (2006). Development of effective vaccines against pandemic influenza. *Immunity*, *24*(1), 5-9.

Sybesma, W., Hugenholtz, J., de Vos, W. M., & Smid, E. J. (2006). Safe use of genetically modified lactic acid bacteria in food. Bridging the gap between consumers, green groups, and industry. *Electronic Journal of Biotechnology*, *9*(4), 424-448.

Tamura, S., Funato, H., Hirabayashi, Y., Kikuta, K., Suzuki, Y., Nagamine, T., . . . Kurata, T. (1990). Functional role of respiratory tract haemagglutinin-specific IgA antibodies in protection against influenza. *Vaccine*, *8*(5), 479-485.

Tamura, S., Funato, H., Hirabayashi, Y., Suzuki, Y., Nagamine, T., Aizawa, C., & Kurata, T. (1991). Cross-protection against influenza A virus infection by passively transferred respiratory tract IgA antibodies to different hemagglutinin molecules. *European Journal of Immunology*, *21*(6), 1337-1344.

Tang, D. C., Zhang, J., Toro, H., Shi, Z., & Van Kampen, K. R. (2009). Adenovirus as a carrier for the development of influenza virus-free avian influenza vaccines. *Expert Review of Vaccines, 8*(4), 469-481.

Taylor, H. P., & Dimmock, N. J. (1985). Mechanism of neutralization of influenza virus by secretory IgA is different from that of monomeric IgA or IgG. *The Journal of Experimental Medicine, 161*(1), 198-209.

Treanor, J. (2004). Influenza vaccine--outmaneuvering antigenic shift and drift. *The New England Journal of Medicine, 350*(3), 218-220.

Treanor, J. J., Schiff, G. M., Couch, R. B., Cate, T. R., Brady, R. C., Hay, C. M., . . . Cox, M. M. (2006). Dose-related safety and immunogenicity of a trivalent baculovirus-expressed influenza-virus hemagglutinin vaccine in elderly adults. *The Journal of Infectious Diseases, 193*(9), 1223-1228.

Tripathi, P., Beaussart, A., Andre, G., Rolain, T., Lebeer, S., Vanderleyden, J., . . . Dufrene, Y. F. (2012). Towards a nanoscale view of lactic acid bacteria. *Micron, 43*(12), 1323-1330.

Tussey, L., Strout, C., Davis, M., Johnson, C., Lucksinger, G., Umlauf, S., . . . White, C. J. (2016). Phase 1 safety and immunogenicity study of a quadrivalent seasonal flu vaccine comprising recombinant hemagglutinin-flagellin fusion proteins. *Open Forum Infectious Diseases, 3*(1), ofw015.

Valdez, Y., Brown, E. M., & Finlay, B. B. (2014). Influence of the microbiota on vaccine effectiveness. *Trends in Immunology, 35*(11), 526-537.

Van Braeckel-Budimir, N., Haijema, B. J., & Leenhouts, K. (2013). Bacterium-like particles for efficient immune stimulation of existing vaccines and new subunit vaccines in mucosal applications. *Frontiers in Immunology, 4*, 282.

van Els, C., Mjaaland, S., Naess, L., Sarkadi, J., Gonczol, E., Korsholm, K. S., . . . Oftung, F. (2014). Fast vaccine design and development based on correlates of protection (COPs). *Human Vaccines and Immunotherapeutics, 10*(7), 1935-1948.

van Riet, E., Ainai, A., Suzuki, T., & Hasegawa, H. (2012). Mucosal IgA responses in influenza virus infections; thoughts for vaccine design. *Vaccine, 30*(40), 5893-5900.

van Roosmalen, M. L., Kanninga, R., El Khattabi, M., Neef, J., Audouy, S., Bosma, T., . . . Leenhouts, K. (2006). Mucosal vaccine delivery of antigens tightly

bound to an adjuvant particle made from food-grade bacteria. *Methods, 38*(2), 144-149.

VanCott, J. L., Brim, T. A., Lunney, J. K., & Saif, L. J. (1994). Contribution of antibody-secreting cells induced in mucosal lymphoid tissues of pigs inoculated with respiratory or enteric strains of coronavirus to immunity against enteric coronavirus challenge. *The Journal of Immunology, 152*(8), 3980-3990.

Varma, N. R., Toosa, H., Foo, H. L., Alitheen, N. B., Nor Shamsudin, M., Arbab, A. S., . . . Abdul Rahim, R. (2013). Display of the viral epitopes on *Lactococcus lactis*: A model for food grade vaccine against EV71. *Biotechnology Research International, 2013,* 431315.

Virelizier, J. L. (1975). Host defenses against influenza virus: the role of anti-hemagglutinin antibody. *The Journal of Immunology, 115*(2), 434-439.

Visweswaran, G. R., Leenhouts, K., van Roosmalen, M., Kok, J., & Buist, G. (2014). Exploiting the peptidoglycan-binding motif, LysM, for medical and industrial applications. *Applied Microbiology and Biotechnology, 98*(10), 4331-4345.

Wang, S., Liu, H., Zhang, X., & Qian, F. (2015). Intranasal and oral vaccination with protein-based antigens: advantages, challenges and formulation strategies. *Protein and Cell, 6*(7), 480-503.

Wang, Z., Gao, J., Yu, Q., & Yang, Q. (2012a). Oral immunization with recombinant *Lactococcus lactis* expressing the hemagglutinin of the avian influenza virus induces mucosal and systemic immune responses. *Future Microbiology, 7*(8), 1003-1010.

Wang, Z., Yu, Q., Gao, J., & Yang, Q. (2012b). Mucosal and systemic immune responses induced by recombinant *Lactobacillus* spp. expressing the hemagglutinin of the avian influenza virus H5N1. *Clinical and Vaccine Immunology, 19*(2), 174-179.

Webster, R. G., Bean, W. J., Gorman, O. T., Chambers, T. M., & Kawaoka, Y. (1992). Evolution and ecology of influenza A viruses. *Microbiological Reviews, 56*(1), 152-179.

Wen, D., Foley, S. F., Hronowski, X. L., Gu, S., & Meier, W. (2013). Discovery and investigation of O-xylosylation in engineered proteins containing a (GGGGS)n linker. *Analytical Chemistry, 85*(9), 4805-4812.

Werner, S., Marillonnet, S., Hause, G., Klimyuk, V., & Gleba, Y. (2006). Immunoabsorbent nanoparticles based on a tobamovirus displaying protein A. *Proceedings of the National Academy of Sciences of the United States of America, 103*(47), 17678-17683.

WHO. (2009). Sequencing primers and protocol. Retrieved from http://www.who.int/csr/resources/publications/swineflu/sequencing_primers/en/

WHO. (2010a). Pandemic (H1N1) 2009 - update 112. Retrieved from http://www.who.int/csr/don/2010_08_06/en/

WHO. (2010b). WHO recommendations for the post-pandemic period. Retrieved from http://www.who.int/csr/disease/swineflu/notes/briefing_20100810/en/

WHO. (2011). *Manual for the laboratory diagnosis and virological surveillance of influenza*. Switzerland: WHO Press.

WHO. (2014). Influenza (Seasonal). Retrieved from http://www.who.int/mediacentre/factsheets/fs211/en/

Widjaja, L., Ilyushina, N., Webster, R. G., & Webby, R. J. (2006). Molecular changes associated with adaptation of human influenza A virus in embryonated chicken eggs. *Virology, 350*(1), 137-145.

Wong, S. S., & Webby, R. J. (2013). Traditional and new influenza vaccines. *Clinical Microbiology Reviews, 26*(3), 476-492.

Xin, K. Q., Hoshino, Y., Toda, Y., Igimi, S., Kojima, Y., Jounai, N., . . . Okuda, K. (2003). Immunogenicity and protective efficacy of orally administered recombinant *Lactococcus lactis* expressing surface-bound HIV Env. *Blood, 102*(1), 223-228.

Zadravec, P., Štrukelj, B., & Berlec, A. (2015). Improvement of LysM-mediated surface display of designed ankyrin repeat proteins (DARPins) in recombinant and nonrecombinant strains of *Lactococcus lactis* and *Lactobacillus* Species. *Applied Environmental Microbiology, 81*(6), 2098-2106.

Zhang, N., Zheng, B. J., Lu, L., Zhou, Y., Jiang, S., & Du, L. (2015). Advancements in the development of subunit influenza vaccines. *Microbes and Infection, 17*(2), 123-134.

Zhang, Q., Zhong, J., & Huan, L. (2011). Expression of hepatitis B virus surface antigen determinants in *Lactococcus lactis* for oral vaccination. *Microbiological Research, 166*(2), 111-120.

Zhang, X., Xu, C., Zhang, C., Liu, Y., Xie, Y., & Liu, X. (2014). Established a new double antibodies sandwich enzyme-linked immunosorbent assay for detecting *Bacillus thuringiensis* (Bt) Cry1Ab toxin based single-chain variable fragments from a naive mouse phage displayed library. *Toxicon, 81*, 13-22.

Zhang, X. Y., Huang, Z. H., Wang, L. X., & Liu, X. N. (2015). Construction of a single chain variable fragment antibody (scFv) against carbaryl and its interaction with carbaryl. *Biochemistry (Moscow), 80*(5), 640-646.

Zhao, H. L., Yao, X. Q., Xue, C., Wang, Y., Xiong, X. H., & Liu, Z. M. (2008). Increasing the homogeneity, stability and activity of human serum albumin and interferon-α2b fusion protein by linker engineering. *Protein Expression and Purification, 61*(1), 73-77.

Zheng, W., & Tao, Y. J. (2013). Structure and assembly of the influenza A virus ribonucleoprotein complex. *FEBS Letters, 587*(8), 1206-1214.

LIST OF PUBLICATIONS AND PAPERS PRESENTED

Research articles

Jee, P. F., Chen, F. S., Shu, M. H., Wong, W. F., Raha, A. R., AbuBakar, S., Chang, L. Y. (2017). Insertion of single-chain variable fragmet (scFv) peptide linker improves surface display of influenza hemagglutinin (HA1) on non-recombinant *Lactococcus lactis*. *Biotechnology progress*, *33*(1): 154-162.

Jee, P. F., Tiong, V., Shu, M. H., Khoo, J. J., Wong, W. F., Raha, A. R., AbuBakar, S., Chang, L. Y. (2017). Oral immunization of a non-recombinant *Lactococcus lactis* surface displaying influenza hemagglutinin 1 (HA1) induces mucosal immunity in mice. *Plos One*, DOI: 10.1371/journal.pone.0187718.

Proceedings

Jee, P. F., AbuBakar, S., Raha, A. R., Chang, L. Y. (2011). Surface display of influenza virus A antigenic protein, HA1 on *Lactococcus lactis* MG1363. The International Congress of the Malaysian Society for Microbiology, Penang, Malaysia, p. 298.

Chang, L. Y., Raha, A. R., **Jee, P. F.**, Siaw, X. J. S., Yusoff, K., AbuBakar, S. (2012). Development of a food-grade influenza virus vaccine using *Lactococcus lactis*. The 7th National Infectious Disease Seminar and Workshop, Selangor, Malaysia.

Jee, P. F., AbuBakar, S., Raha, A. R., Chang, L. Y. (2012). Refolded fusion protein consisting of anchor region of N-acetylmuramidase (AcmA) and influenza hemagglutinin (HA1) retains its binding activity. The 31st Symposium of the Malaysian Society for Microbiology, Sabah, Malaysia, p. 42.

Jee, P. F., AbuBakar, S., Raha, A. R., Chang, L. Y. (2013). Construction of a non-recombinant *Lactococcus lactis* surface displaying influenza hemagglutinin. Proceedings of the 4th Chula International Workshop on Protein Expression and Purification Strategies. Chulalongkorn, Bangkok, Thailand, p. 41.

Jee, P. F., AbuBakar, S., Raha, A. R., Chang, L. Y. (2013). Immunogenic characterization of influenza A (H1N1) hemagglutinin (HA1) fusion protein expressed in *Escherichia coli*. Proceedings of the International Congress of the Malaysian Society for Microbiology, Langkawi, Malaysia, p. 285.

Jee, P. F., AbuBakar, S., Wong, W. F., Raha, A. R., Chang, L. Y. (2014). Development of an influenza candidate vaccine using *Lactococcus lactis*. Proceedings of the 16th International Congress on Infectious Diseases, Cape Town, South Africa, p. 80.

Jee, P. F., Chen, F. S., Shu, M. H., Tiong, V., Khoo, J.J., Wong, W.F., Raha, A.R., AbuBakar, S., Chang, L. Y. (2016). Surface display of the HA1 on *Lactococcus lactis*: A potential candidate vaccine against influenza. Proceedings of the 5th Asian Federation of Societies for Lactic Acid Bacteria International Symposium, Taipei, Taiwan, p. 36.